SVENSKA GEOFYSISKA FÖRENINGEN

VOLUME 6, NUMBER 3 **Tellus** AUGUST 1954

A QUARTERLY JOURNAL OF GEOPHYSICS

V. W. EKMAN in memoriam

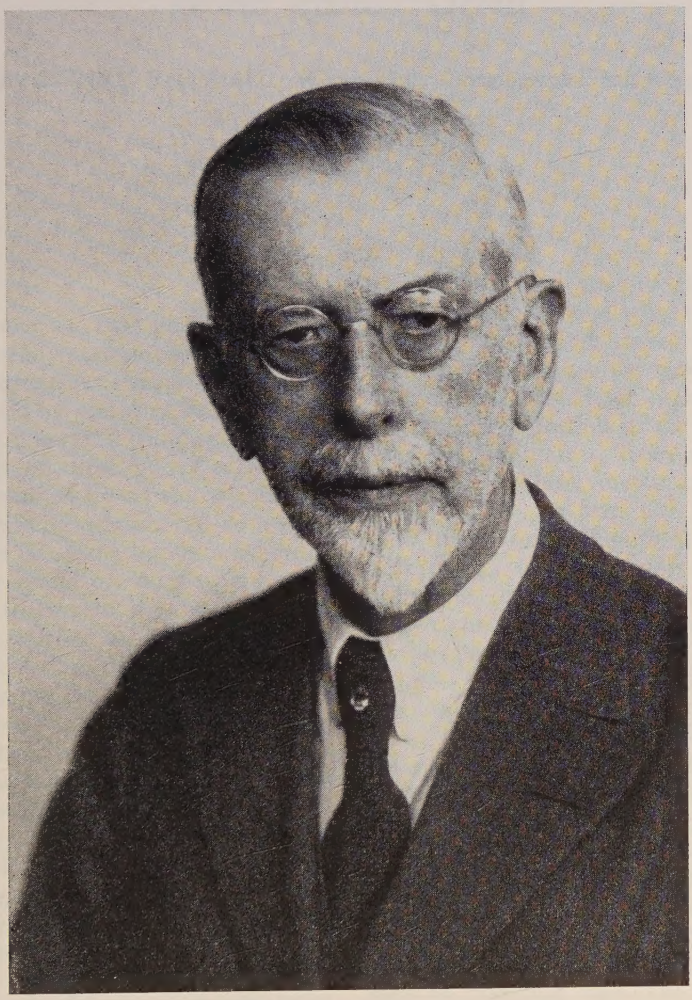

3/5 1874 — 9/3 1954

With Vagn Walfrid Ekman experimental and theoretical oceanography lost one of its great pioneers. Through this portrait the Swedish Geophysical Society and the Editorial Board of Tellus wish to honour a great scientist and a great humanitarian.

Digitized by the Internet Archive
in 2024

https://archive.org/details/tellus-series-a-dynamic-meteorology-and-oceanography_1954-08_6_3

Serial Observations of Drift Currents in the Central North Atlantic Ocean[1]

By HENRY STOMMEL, Woods Hole Oceanographic Institution,
Woods Hole, Massachusetts

(Manuscript received May 13, 1954)

1. Introduction

Between October 21, 1953 and February 9, 1954 a series of nearly continuous observations of wind-drift currents was made in the open ocean off Bermuda by means of drifting wireless-telemetering buoys. A rough plot of the position of each of these buoys relative to Bermuda was obtained by means of a mobile radio-direction-finding station. A composite plot of the tracks of all the buoys is exhibited in Figure 1. The island provides such a small base line for triangulation, especially for bearings to the northeast and southwest of the island, that reliable fixes of position could be obtained only during the time that the buoys were within about 20 miles of Bermuda. Because of the uncertainties in radio-direction-finding at 3 megacycles the information shown in Figure 1 cannot be used for measuring wind-drift of the buoys, but it does provide us with enough information to eliminate from the data those cases in which the buoys were within the 1000 fathom line. A total of 65 days of observations satisfying this criterion was obtained.

Figure 2 is a sketch of the buoy. A cylindrical steel can roughly 2 feet in diameter and 5 feet high surmounted by a 6 foot mast (which carried a 4 cup anemometer, wind vane, magnetic compass and whip type antenna) and carrying a 30 watt radio transmitter, telemetering equipment and batteries, is ballasted so as to float with about 5 inches of freeboard. To the lower portion of the can are attached two outrigger arms, from one of which is suspended a sheet metal drogue at depths from 120 to 530 feet. On the other arm a sheet metal rotor (Figure 3) is suspended as near to the surface as possible. Every three hours (in some cases every $1^1/_2$ hours) the buoy transmits by wireless the following data: (i) the number of revolutions of the rotor since the previous transmission; (ii) the number of revolutions of the anemometer since the previous transmission: (iii) the instantaneous magnetic heading of the buoy; (iv) the instantaneous bearing of the wind relative to the buoy. These wireless signals turn on the magnetic tape recording equipment in the land-based observatory so that the data is available for reduction in recorded form. The operation of the receiving station is entirely automatic except for occasional changing of reels of recording tape. The system in use at present works satisfactorily over distances up to 45 miles. Rough weather, even of moderate gale force, does not harm the buoys.

Calibration of the rotors was carried out in a tidal channel on the island. Because the buoys are free drifting they do not measure

[1] Contribution No. 713 from the Woods Hole Oceanographic Institution; under Contract with the Office of Naval Research. The work was done at the Bermuda Biological Station.

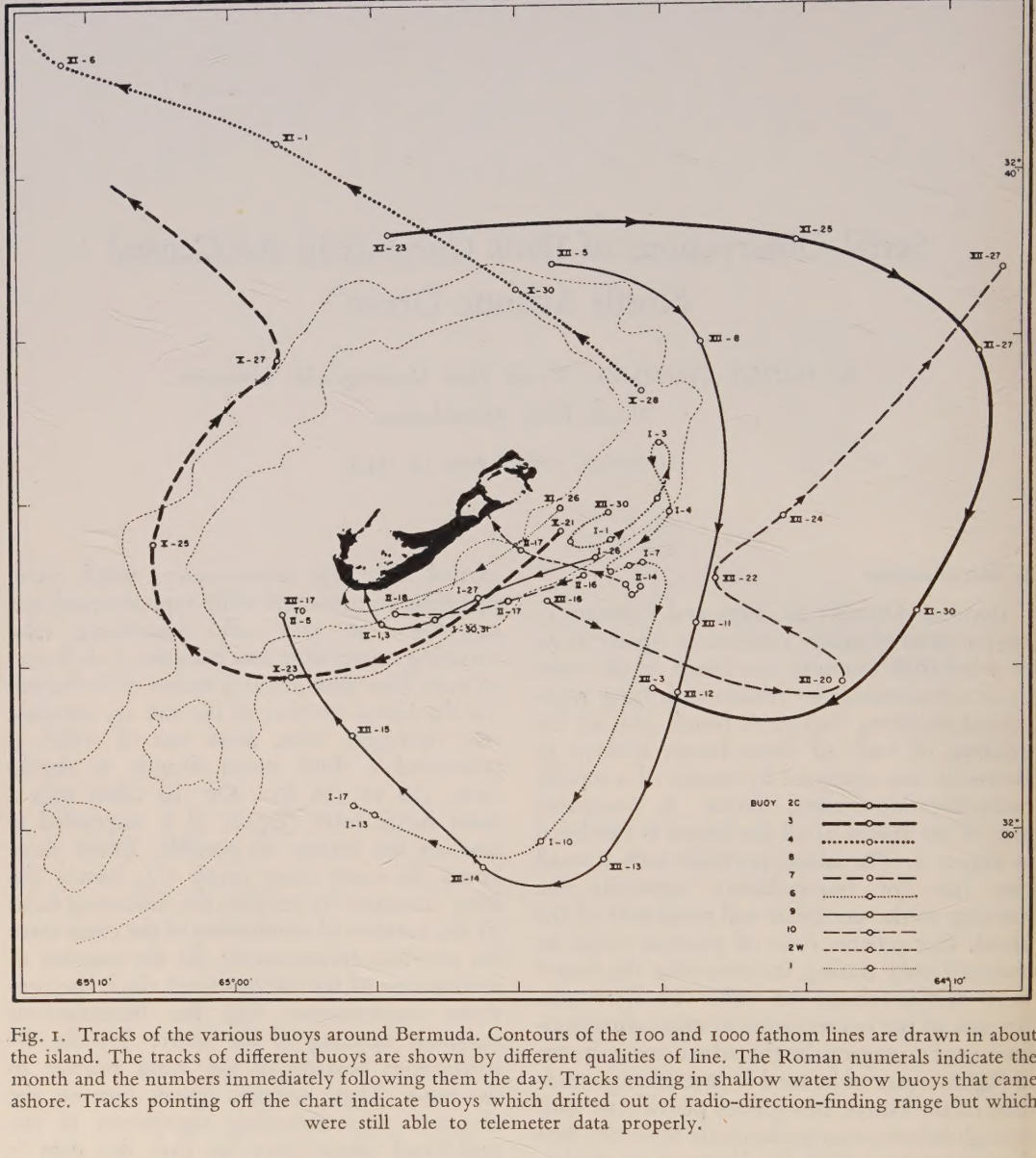

Fig. 1. Tracks of the various buoys around Bermuda. Contours of the 100 and 1000 fathom lines are drawn in about the island. The tracks of different buoys are shown by different qualities of line. The Roman numerals indicate the month and the numbers immediately following them the day. Tracks ending in shallow water show buoys that came ashore. Tracks pointing off the chart indicate buoys which drifted out of radio-direction-finding range but which were still able to telemeter data properly.

the velocity of the surface drift relative to the ocean bottom. They measure the vectorial difference of the surface velocity and the velocity at the depth of the drogue. The areas of the can and rotor together (in the surface water) and of the drogue (in the deep water) are nearly equal so that the actual speed of the vectorial difference is twice the speed past the surface rotor. The orientation of the buoy is determined by the direction of the vectorial difference. In this connection every effort has been made to reduce the area exposed to the wind. There is a small deflection (averaging 10°) of the orientation of the buoy from the direction of the vectorial difference of surface and deep velocities, due to Magnus effect of the rotor. A correction for this has been made on the basis of experiments made in a tidal

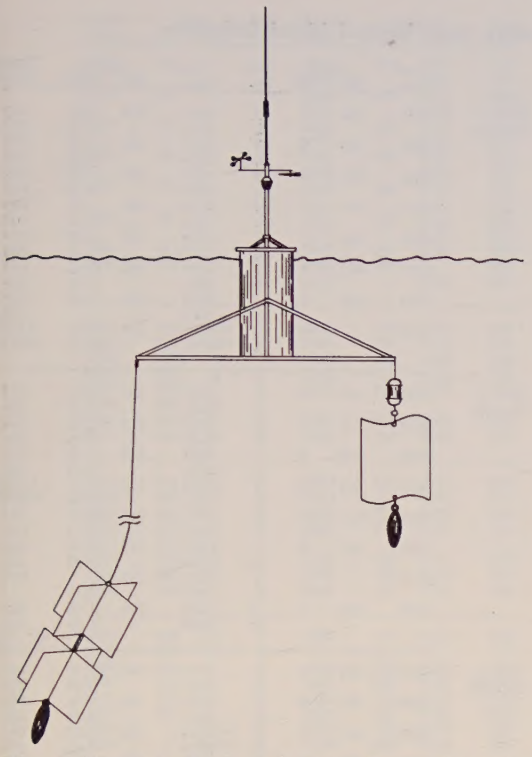

Fig. 2. Schematic sketch of the buoy showing the radio mast and meteorological instruments above water, the current and the deep drag each attached to ends of the outrigger arms.

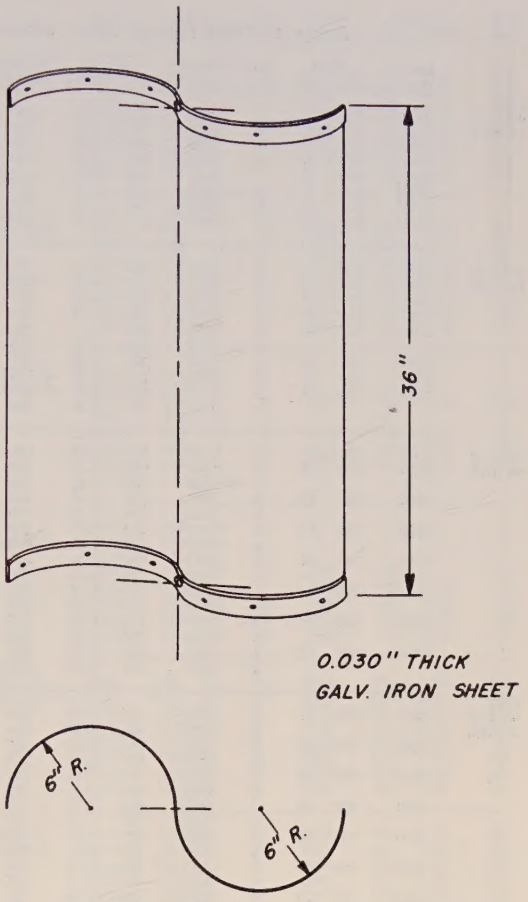

Fig. 3. Detailed sketch of the construction of the rotor.

channel; and the sense of rotation of the rotor was reversed in some of the later buoys in order to eliminate this possible source of error from the data.

The telemetering itself is done in the following manner: the various sensing elements operate variable electric resistances, which produce variable audio frequencies which in turn are transmitted as a modulation of the radio frequencies. It is believed that adequate precautions were taken to prevent possible errors in the telemetering system. Messrs. Robert G. Walden and Donald Parson, Jr. collaborated with me in the design and construction of the buoys.

II. Discussion of data

The original data from the buoys, including all cases where the buoys were not near to the shore of the island, is collected in Table I. Perhaps the most striking feature of this data

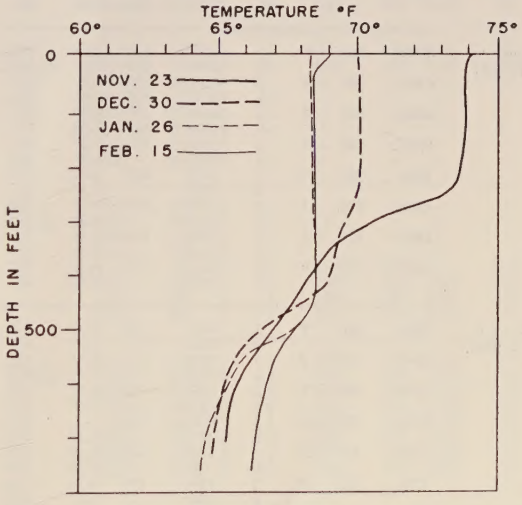

Fig. 4. Sample bathythermograph soundings showing the mixed water conditions prevailing through most of the period of measurements.

Table 1. Data for all cases where buoys were beyond island influence

	Local Time	Wind dir.	Wind mph	Buoy No.	Trans. Time	Current dir.	Current knots	Wind Vane
1953 Oct. 27 TM 0003	0000	200	1	3	0024	020	0.27	330
	0300	200	1	3	0325	035	0.85	240
	0600	200	1	3	0625	060	0.74	225
	0900	160	6	3	0922	105	0.10	160
	1200	180	8	3	1222	305	0.69	000
	1500	180	5	3	1522	020	0.61	000
	1800	190	3	3	1823	100	0.72	240
	2100	200	5	3	2123	195	0.69	130
Oct. 28 TM 0058	0000	200	7	3	0023	250	0.46	070
	0300	180	8	3	0323	310	0.61	030
	0600	170	8	3	0623	340	0.74	000
	0900	170	10	3	0923	340	0.54	320
	1200	180	15	3	1223	320	-	000
				4	1243	035	0.74	000
	1500	180	16	3	1522	000	0.50	350
	1800	180	15	4	1844	345	0.64	165
	2100	170	19	3	2122	000	0.51	310
				4	2145	080	0.34	340
Oct. 29 TM 0148	0000	180	23	3	0022	010	0.86	290
	0300	200	25	3	0321	035	0.48	290
				4	0346	080	0.75	350
	0600	190	23	3	0621	100	0.98	250
				4	0646	080	0.30	350
	0900	200	23	3	0922	100	0.98	270
				4	0949	000	0.28	030
	1200	200	25	3	1222	050	0.69	290
				4	1249	055	0.70	330
	1500	200	26	3	1522	055	0.77	240
				4	1549	070	0.90	000
	1800	200	25	3	1822	030	2.00	285
				4	1849	090	0.93	340
	2100	200	23	3	2122	050	2.64	300
				4	2149	045	0.05	000
1953 Oct. 30 TM 0234	0000	200	27	3	0022	105	0.54	260
				4	0050	055	0.58	000
	0300	200	26	3	0322	040	0.83	310
				4	0350	080	0.67	300
	0600	200	27	3	0622	070	0.90	300
				4	0650	060	1.01	355
	0900	200	26	3	0921	060	0.62	260
				4	0931	340	0.51	020
	1200	200	26	3	1221	035	0.83	330
				4	1252	010	0.21	020
	1500	200	26	3	1521	080	0.82	010
				4	1552	090	0.74	355
	1800	190	22	3	1821	200	1.01	340
				4	1854	070	0.88	340
	2100	270	5	3	2120	235	0.46	030
				4	2152	090	0.86	000
Oct. 31 TM 0317	0000	260	2	3	0020	290	0.80	270
				4	0100	090	0.08	000
	0300	000	14	3	0320	150	0.80	000
				4	0400	105	0.64	010
	0600	000	13	3	0620	125	0.80	000
				4	0700	145	0.69	350
	0900	100	11	3	0920	220	0.37	000
				4	1005	-	1.12	335
	1200	320	9	3	1220	170	0.70	290
				4	1308	-	0.32	145
	1500	270	3	3	1520	010	0.75	000
				4	1610	-	0.26	010
	1800	220	7	3	1820	035	0.98	315
				4	1912	-	0.74	110
	2100	220	9	3	2120	105	0.34	000
				4	2212	-	0.70	000
Nov. 1 TM 0357	0000	320	9	3	0020	105	0.77	000
				4	0114	-	0.92	215
	0300	320	7	3	0320	000	0.77	055
				4	0418	-	0.24	040
	0600	280	7	3	0620	070	0.67	020
				4	0718	-	0.30	245
	0900	270	11	3	0920	105	-	000
				4	1018	-	0.77	290
	1200	330	12	3	1220	070	0.48	350
				4	1317	-	0.90	000
	1500	320	12	3	1520	125	0.74	315
				4	1618	-	0.77	000
	1800	340	12	3	1819	150	0.75	270
				4	1918	-	0.03	000
	2100	350	7	3	2119	210	0.88	290
				4	2220	-	0.67	040
1953 Nov. 2 TM 0437	0000	340	3	3	0019	190	0.42	300
				4	0120	-	2.08	035
	0300	340	5	3	0319	180	0.67	290
				4	0420	-	2.48	060
	0600	000	6	3	0619	250	0.77	045
				4	0720	-	0.30	270
	0900	070	2	3	0920	230	0.88	280
				4	1023	-	0.27	000
	1200	040	6	3	1220	215	0.26	000
				4	1322	-	0.64	180
	1500	000	7	3	1520	180	0.61	000
				4	1623	-	1.76	090
	1800	040	6	3	1820	205	0.64	000
				4	1923	-	-	000
	2100	-	-	3	2119	260	0.67	310
				4	2224	-	0.19	210
Nov. 3 TM 0517	0000	045	8	3	0019	245	0.74	290
				4	0124	-	0.37	320
	0300	110	3	3	0319	210	0.51	300
				4	0424	-	0.74	280
	0600	060	5	3	0619	215	0.61	315
				4	0724	-	0.77	120
	0900	045	11	3	0920	210	0.67	000
				4	1024	-	0.88	350
	1200	045	10	3	1222	215	0.67	320
				4	1325	-	0.13	000
	1500	045	8	3	1522	215	0.30	340
				4	1626	-	0.32	340
	1800	-	-	3	1820	190	-	010
				4	1926	-	0.74	-
	2100	030	5	3	2123	220	0.54	310
				4	2226	-	0.62	210
Nov. 4 TM 0558	0000	045	3	3	0020	260	0.62	250
				4	0126	-	0.88	110
	0300	050	2	3	0320	320	0.54	260
				4	0420	-	0.29	135
	0600	045	3	3	0626	330	0.53	180
				4	0726	-	0.03	325
	0900	023	5	3	0926	350	0.56	130
				4	1027	-	0.57	335
	1200	010	5	3	1228	105	0.56	060
				4	1327	-	0.54	325
	1500	000	3	3	1500	330	0.54	210
				4	1600	-	0.69	270
	1800	005	3	3	1831	330	0.61	210
				4	1927	-	0.77	225
	2100	005	4	3	2133	330	0.43	110
1953 Nov. 5 TM 0640	0000	-	calm	3	0035	025	0.42	090
				4	0136	-	0.11	020
	0300	010	5	3	0300	050	0.58	060
				4	0436	-	0.56	305
	0600	015	3	3	0600	280	0.62	160
	0900	032	2	3	0941	270	0.69	215
	1200	055	3	3	1243	310	0.46	150
				4	1350	-	0.69	280
	1500	075	4	3	1545	310	0.69	085
				4	1654	-	0.10	000
	1800	075	5	3	1845	330	0.62	135
				4	1959	-	0.37	315
	2100	105	8	3	2146	010	0.61	280
				4	2303	-	0.54	000
Nov. 6 TM 0725	0000	110	7	3	0047	000	0.72	000
				4	0205	-	0.64	000
	0300	122	11	3	0347	300	0.19	310
				4	0505	-	0.90	000
	0600	120	5	3	0647	340	0.77	330
				4	0805	-	0.34	000
	0900	120	12	3	0946	010	0.72	340
				4	1109	-	0.14	340
	1200	120	14	3	1246	020	0.75	260
				4	1409	-	0.70	340
	1500	135	15	3	1547	340	0.48	280
				4	1710	-	0.67	325
	1800	135	13	3	1846	320	0.77	350
				4	2013	-	0.94	100
	2100	135	12	3	2146	340	0.72	300
				4	2317	-	0.18	355

(Cont.)

	Local Time	Wind dir.	Wind mph	Buoy No.	Trans. Time	Current dir.	Current knots	Wind Vane
Nov. 7 TM 0813	0000	140	-	3	0046	000	0.78	330
				4	0217	-	0.25	315
	0300	150	11	3	0346	020	0.51	290
				4	0519	-	0.69	350
	0600	180	-	3	0646	030	0.77	290
				4	0822	-	0.85	075
	0900	180	-	3	0946	010	0.83	315
				4	1123	-	0.80	005
	1200	220	-	3	1246	350	0.59	310
				4	1424	-	0.03	015
	1500	195	-	3	1545	035	0.43	340
				4	1727	-	0.51	010
	1800	123	7	3	1845	050	0.74	350
	2100	220	6	3	2145	290	-	000
				4	2333	-	0.83	025
1953 Nov. 8 TM 0905	0000	220	calm	3	0045	160	0.66	000
	0300	225	calm	3	0345	170	0.70	000
	0600	265	2	3	0645	215	0.48	340
	0900	050	4	3	0944	210	0.74	310
	1200	070	5	3	1244	230	0.82	280
	1500	050	6	-	-	-	-	-
	1800	050	5	3	1844	250	0.69	270
	2100	060	6	3	2144	240	0.75	270
Nov. 9 TM 0958	0000	015	6	3	0043	240	0.72	000
	0300	060	6	3	0343	225	0.64	290
	0600	080	3	3	0642	250	0.54	290
	0900	078	7	3	0942	230	0.67	320
	1200	120	7	-	-	-	-	-
	1500	070	3	3	1542	280	0.74	260
	1800	085	6	3	1841	305	0.43	240
	2100	080	6	3	2141	220	0.58	000
Nov. 10 TM 1053	0000	098	5	3	0041	220	0.59	010
	0300	098	3	-	-	-	-	-
	0600	090	3	3	0640	125	0.64	110
	0900	095	2	3	0940	000	0.27	270
	1200	090	3	3	1240	050	0.58	235
	1500	090	1	3	1539	060	0.64	240
	1800	-	calm	3	1839	035	0.58	270
	2100	-	calm	3	2138	000	0.69	340
Nov. 11 TM 1147	0000	-	calm	3	0037	030	0.18	350
	0300	240	3	3	0337	040	0.72	300
	0600	240	3	3	0637	105	0.64	260
	0900	220	7	-	-	-	-	-
	1200	190	10	3	1238	035	0.62	290
Nov. 25	0000	140	6	2	0048	010	0.72	280
	0300	140	7	2	0348	015	0.85	300
	0600	140	7	2	0648	010	0.37	310
	0900	150	8	2	0945	020	0.77	305
	1200	175	11	2	1236	055	0.67	295
	1500	175	11	2	1534	110	0.80	070
	1800	180	10	2	1830	090	0.37	290
	2100	180	8	2	2128	095	0.80	225
Nov. 26 TM 0027	0000	185	15	2	0025	315	0.70	030
	0300	185	11	-	-	-	-	-
	0600	190	14	2	0625	005	0.62	020
	0900	190	11	-	-	-	-	-
	1200	185	15	2	1216	060	0.59	350
	1500	185	18	2	1514	020	0.69	350
	1800	200	14	2	1812	035	0.80	330
	2100	195	23	2	2109	045	0.37	340
1953 Nov. 27 TM 0112	0000	210	12	2	0007	010	0.72	010
	0300	260	11	2	0305	080	0.70	350
	0600	295	14	2	0602	090	0.83	350
	0900	295	14	2	0900	145	0.37	305
	1200	295	10	2	1158	145	0.82	300
	1500	295	8	2	1456	190	0.70	235
	1800	285	3	2	1753	215	0.80	225
	2100	-	calm	2	2050	255	0.37	210

	Local Time	Wind dir.	Wind mph	Buoy No.	Trans. Time	Current dir.	Current knots	Wind Vane
Nov. 28 TM 0154	0000	-	calm	-	-	-	-	-
	0300	280	-	2	0245	305	0.67	010
	0600	280	-	2	0540	055	0.77	320
	0900	280	-	2	0842	070	0.54	305
	1200	190	6	2	1140	070	0.48	305
	1500	270	5	2	1437	090	0.77	290
	1800	225	3	2	1735	090	0.78	320
	2100	255	2	2	2033	090	0.74	330
Nov. 29 TM 0234	0000	255	3	-	-	-	-	-
	0300	255	6	2	0230	095	0.67	340
	0600	260	8	2	0528	125	0.59	325
	0900	340	12	2	0824	110	0.75	335
	1200	350	10	2	1122	110	0.48	000
	1500	000	9	2	1420	135	0.69	000
	1800	015	7	2	1717	180	0.69	335
	2100	050	6	2	2016	165	0.69	020
Nov. 30 TM 0314	0000	040	5	-	-	-	-	-
	0300	050	5	-	-	-	-	-
	0600	040	3	2	0510	090	0.88	105
	0900	065	5	-	-	-	-	-
	1200	095	6	2	1105	075	0.37	165
	1500	080	7	2	1404	010	0.26	240
	1800	070	4	2	1701	030	0.72	260
	2100	-	calm	-	-	-	-	-
Dec. 1 TM 0354	0000	100	10	-	-	-	-	-
	0300	120	10	-	-	-	-	-
	0600	125	11	-	-	-	-	-
	0900	110	15	2	1050	010	-	350
	1200	150	6	2	1348	035	0.70	350
	1500	230	24	2	1646	090	0.37	295
	1800	225	22	2	1944	080	0.86	275
	2100	270	15	2	2242	100	0.85	310
1953 Dec. 2 TM 0436	0000	270	12	2	0140	105	0.80	330
	0300	275	14	2	0439	100	0.61	295
	0600	280	22	2	0737	070	0.91	350
	0900	285	20	2	1035	115	0.93	020
	1200	285	20	2	1333	055	0.48	350
	1500	290	18	2	1631	100	0.91	350
	1800	320	19	2	1929	115	0.80	350
	2100	330	18	2	2228	120	0.90	325
Dec. 3 TM 0520	0000	330	15	2	0126	095	0.45	005
	0300	330	14	2	0424	145	0.85	335
	0600	330	15	2	0722	180	0.86	340
	0900	330	16	2	1022	215	0.59	345
	1200	335	15	2	1322	175	0.72	350
	1500	340	16	2	1620	140	0.82	350
	1800	000	12	2	1919	205	0.91	340
	2100	000	11	2	2118	260	0.40	335
Dec. 4 TM 0607	0000	015	7	2	0110	130	0.83	350
	0300	015	8	2	0410	350	0.75	210
	0600	025	6	-	-	-	-	-
	0900	030	7	-	-	-	-	-
	1200	055	7	-	-	-	-	-
	1500	075	8	-	-	-	-	-
	1800	070	6	-	-	-	-	-
	2100	095	9	-	-	-	-	-
Dec. 5 TM 0658	0000	095	6	-	-	-	-	-
	0300	095	5	-	-	-	-	-
	0600	100	4	-	-	-	-	-
	0900	120	4	-	-	-	-	-
	1200	020	2	8	1228	055	-	210
	1500	080	4	8	1528	025	0.06	220
	1800	080	4	8	1828	320	0.49	305
	2100	080	2	8	2128	195	0.34	040
Dec. 6 TM 0752	0000	075	3	8	0028	185	0.39	015
	0300	085	2	8	0328	230	0.43	325
	0600	080	4	8	0628	330	0.69	280
	0900	080	5	8	0929	010	0.36	250
	1200	060	4	8	1359	030	0.56	240
	1500	075	6	8	1659	080	0.60	230
	1800	080	5	8	1959	290	0.42	010
	2100	100	6	8	2127	305	0.34	000

(Cont.)

	Local Time	Wind dir.	Wind mph	Buoy No.	Trans. Time	Current dir.	Current knots	Wind Vane
1953 Dec. 7 TM 0847	0000	150	5	8	0027	000	0.00	315
	0300	180	10	8	0327	005	0.49	000
	0600	180	6	8	0627	350	0.59	350
	0900	220	8	8	0926	015	0.49	335
	1200	225	12	8	1224	080	0.43	315
	1500	230	12	8	1526	130	0.43	230
	1800	245	3	8	1825	210	0.00	210
	2100	260	2	8	2125	230	0.42	190
Dec. 8 TM 0943	0000	260	2	8	0025	230	0.56	185
	0300	260	2	8	0325	215	0.46	225
	0600	-	calm	8	0625	240	0.56	140
	0900	010	4	8	0925	215	0.13	295
	1200	035	5	8	1225	200	0.36	020
	1500	080	6	8	1525	260	0.56	350
	1800	125	3	8	1825	280	0.42	015
	2100	125	4	8	2125	285	0.46	245
Dec. 9 TM 1037	0000	125	4	8	0025	350	0.60	300
	0300	130	6	8	0325	330	0.07	320
	0600	130	7	8	0625	335	0.52	315
	0900	120	6	8	0925	305	0.49	330
	1200	100	8	8	1225	035	0.46	315
	1500	135	11	8	1525	030	0.52	300
	1800	120	11	8	1825	080	0.56	215
	2100	130	7	8	2125	200	0.13	080
Dec. 10 TM 1129	0000	120	7	8	0157	090	0.63	225
	0300	150	11	8	0325	080	0.49	245
	0600	180	14	8	0625	080	0.63	275
	0900	180	15	8	0923	080	0.39	280
	1200	200	18	8	1223	080	0.29	305
	1500	225	17	8	1521	080	0.83	285
	1800	225	15	8	1821	085	0.95	295
	2100	255	14	8	2121	095	0.53	260
Dec. 11 TM 1219	0000	-	calm	8	0021	130	0.70	260
	0300	240	4	8	0321	110	0.90	260
	0600	240	4	8	0621	150	0.63	300
	0900	230	6	8	0921	150	0.13	290
	1200	060	3	8	1221	195	0.83	115
	1500	080	10	8	1521	195	0.85	000
	1800	065	10	8	1821	200	0.70	010
	2100	090	11	8	2121	195	0.00	020
1953 Dec. 12 TM 1308	0000	090	12	8	0021	230	0.49	010
	0300	100	10	8	0321	190	0.62	030
	0600	110	10	8	0621	195	0.49	030
	0900	120	11	8	0921	190	0.34	100
	1200	150	11	8	1221	215	0.42	055
	1500	180	12	8	1521	205	0.17	080
	1800	200	14	8	1821	120	0.32	190
	2100	220	12	8	2121	100	0.40	225
Dec. 13 TM 1356	0000	220	15	8	0021	090	0.46	215
	0300	225	15	8	0321	180	0.46	185
	0600	225	14	8	0621	170	0.56	200
	0900	230	13	8	0921	120	0.07	235
	1200	240	17	8	1221	125	0.40	240
	1500	240	14	8	1521	120	0.60	235
	1800	220	11	8	1821	180	0.84	180
	2100	210	11	8	2121	185	0.07	135
Dec. 14 TM 1445	0000	220	13	8	0021	195	0.76	145
	0300	220	12	8	0321	120	0.73	215
	0600	210	13	8	0621	170	0.77	160
	0900	220	13	8	0918	160	0.39	160
	1200	220	15	8	1218	160	0.98	135
	1500	210	14	8	1521	195	0.70	140
	1800	210	14	8	1818	160	0.29	160
	2100	210	18	8	2117	185	0.87	130
Dec. 15 TM 1536	0000	210	15	8	0017	250	0.60	095
	0300	210	17	8	0317	280	0.49	035
	0600	210	16	8	0617	155	0.07	170
	0900	220	20	8	0917	150	-	220
	1200	210	23	-	-	-	-	-
	1500	270	10	-	-	-	-	-
	1800	330	12	-	-	-	-	-
	2100	350	16	-	-	-	-	-
Dec. 16 TM 1630	0000	350	12	-	-	-	-	-
	0300	345	9	-	-	-	-	-
	0600	015	7	-	-	-	-	-
	0900	045	3	-	-	-	-	-
	1200	030	3	-	-	-	-	-
	1500	350	4	7	1538	340	-	-
	1800	000	6	7	1838	310	0.53	-
	2100	000	5	7	2138	240	0.62	-
1953 Dec. 17 TM 1727	0000	330	3	7	0038	075	0.43	-
	0300	300	5	7	0338	175	0.07	-
	0600	280	10	7	0638	125	0.62	-
	0900	300	12	7	0938	170	0.52	-
	1200	320	14	7	1238	185	0.60	-
	1500	330	15	7	1537	270	0.55	-
	1800	330	19	7	1837	295	0.17	-
	2100	320	17	7	2137	150	0.60	-
Dec. 18 TM 1827	0000	320	14	7	0037	250	0.60	-
	0300	320	17	7	0337	215	0.45	-
	0600	320	14	7	0637	265	0.77	-
	0900	310	14	7	0937	220	0.00	-
	1200	310	9	7	1237	185	0.78	-
	1500	320	10	7	1537	190	0.81	-
	1800	320	18	7	1837	225	0.69	-
	2100	320	21	7	2137	235	0.00	-
Dec. 19 TM 1928	0000	320	23	7	0037	210	0.64	-
	0300	325	12	7	0337	255	0.70	-
	0600	325	18	7	0637	220	0.78	-
	0900	325	17	7	0937	225	0.31	-
	1200	320	18	7	1237	195	0.76	-
	1500	320	18	7	1537	235	0.70	-
	1800	320	18	7	1837	220	0.80	-
	2100	350	15	7	2137	190	0.18	-
Dec. 20 TM 2028	0000	350	11	7	0037	225	0.70	-
	0300	345	9	7	0337	190	0.70	-
	0600	340	6	7	0637	180	0.60	-
	0900	340	6	7	0936	250	0.45	-
	1200	340	6	7	1236	225	0.31	-
	1500	270	2	7	1536	210	0.62	-
	1800	270	2	7	1836	210	0.53	-
	2100	270	3	7	2136	240	0.55	-
Dec. 21 TM 2124	0000	270	7	7	0036	120	0.42	-
	0300	270	6	7	0336	145	0.07	-
	0600	-	calm	7	0636	115	0.62	-
	0900	270	2	7	0936	095	0.59	-
	1200	200	15	7	1236	095	0.46	-
	1500	195	18	7	1536	065	0.50	-
	1800	210	15	7	1836	065	0.28	-
	2100	210	16	7	2136	065	0.38	-
1953 Dec. 22 TM 2216	0000	210	22	7	0036	065	0.64	-
	0300	210	22	7	0336	065	0.70	-
	0600	210	22	7	0636	065	0.67	-
	0900	210	19	7	0935	095	0.15	-
	1200	210	22	7	1235	085	0.69	-
	1500	210	19	7	1535	075	0.64	-
	1800	210	16	7	1835	095	0.69	-
	2100	210	15	7	2135	110	0.25	-
Dec. 23 TM 2303	0000	230	9	7	0035	090	0.36	-
	0300	215	6	7	0335	110	0.73	-
	0600	-	-	7	0635	125	0.60	-
	0900	250	4	7	0935	135	0.52	-
	1200	260	6	7	1235	165	0.21	-
	1500	260	6	7	1534	105	0.13	-
	1800	250	6	-	-	-	-	-
	2100	250	9	7	2134	105	0.52	-
Dec. 24 TM 2348	0000	260	17	7	0034	230	0.52	-
	0300	260	20	7	0334	110	0.60	-
	0600	260	21	7	0634	120	0.13	-
	0900	260	23	7	0934	095	0.70	-
	1200	270	12	7	1234	130	0.70	-
	1500	030	8	7	1534	195	0.70	-
	1800	020	11	7	1834	345	0.34	-
	2100	000	10	7	2134	275	0.18	-

(Cont.)

	Local Time	Wind dir.	Wind mph	Buoy No.	Trans. Time	Current dir.	Current knots	Wind Vane
Dec. 25	0000	000	13	7	0034	250	0.73	-
	0300	020	10	7	0334	285	0.70	-
	0600	030	9	7	0634	270	0.66	-
	0900	045	5	7	0934	300	0.17	-
	1200	045	3	7	1234	315	0.43	-
	1500	120	3	7	1534	065	0.57	-
	1800	180	7	7	1834	065	0.53	-
	2100	210	12	7	2134	065	0.49	-
Dec. 26	0000	210	22	7	0034	065	0.41	-
TM 0029	0300	210	20	7	0334	130	0.20	-
	0600	210	32	7	0634	075	0.74	-
	0900	250	18	7	0932	105	0.71	-
	1200	320	12	7	1232	175	0.73	-
	1500	320	11	7	1532	190	0.07	-
1953 Dec. 30	0000	250	14	-	-	-	-	-
TM 0313	0300	270	9	-	-	-	-	-
	0600	270	8	-	-	-	-	-
	0900	260	7	-	-	-	-	-
	1200	270	9	6	1346	115	0.66	280
	1500	270	7	6	1527	130	0.46	280
				6	1646	150	0.07	225
	1800	250	6	6	1827	145	0.85	225
				6	1946	275	0.71	180
	2100	250	6	6	2127	255	0.59	175
				6	2246	255	0.71	175
Dec. 31	0000	250	12	6	0027	130	0.67	230
TM 0359				6	0146	090	0.57	230
	0300	250	8	6	0327	355	0.50	080
				6	0446	090	0.20	355
	0600	250	12	6	0627	090	0.27	355
				6	0746	065	0.77	000
	0900	250	18	6	0948	095	0.66	240
				6	1048	105	0.66	240
	1200	250	22	6	1228	115	0.70	240
				6	1348	105	0.90	255
	1500	250	22	6	1529	085	0.77	240
				6	1649	095	0.17	225
	1800	250	21	6	1828	105	0.69	145
				6	1949	095	0.78	025
	2100	330	27	6	2128	115	0.74	005
				6	2249	130	0.87	355
1954 Jan. 1	0000	330	25	6	0028	130	0.97	005
TM 0448				6	0149	150	0.80	015
	0300	330	24	6	0328	120	0.43	015
				6	0449	115	0.69	355
	0600	330	21	6	0628	120	0.87	035
				6	0749	160	0.71	335
	0900	330	18	6	0928	140	0.80	030
				6	1049	125	0.74	015
	1200	330	16	6	1228	130	0.71	025
				6	1351	120	0.08	025
	1500	310	13	6	1651	120	0.71	120
	1800	310	11	6	1830	115	0.59	030
				6	1951	105	0.55	355
	2100	310	10	6	2130	055	0.74	060
				6	2251	110	0.74	000
1954 Jan. 2	0000	326	13	6	0030	105	0.63	295
TM 0540				6	0151	120	0.11	355
	0300	330	13	6	0330	095	0.48	045
				6	0451	120	0.00	355
	0600	330	13	6	0630	120	0.59	025
				6	0751	120	0.63	355
	0900	340	11	6	0932	125	0.67	295
				6	1053	130	0.71	355
	1200	340	9	6	1232	140	0.70	030
				6	1353	140	0.21	295
	1500	030	7	6	1532	165	0.24	040
				6	1653	175	1.06	025
	1800	050	3	6	1832	205	0.70	000
				6	1953	185	0.63	040
	2100	-	calm	6	2132	195	0.70	045
				6	2253	145	0.77	125

	Local Time	Wind dir.	Wind mph	Buoy No.	Trans. Time	Current dir.	Current knots	Wind Vane
Jan. 3	0000	-	calm	6	0032	205	0.63	125
TM 0636				6	0153	165	0.15	170
	0300	-	calm	6	0332	285	0.35	115
				6	0453	220	0.60	100
	0600	060	1	6	0632	210	0.81	140
	0900	120	3	6	0934	270	0.71	055
				6	1054	310	0.85	020
	1200	180	12	6	1234	285	0.67	025
				6	1356	295	0.11	035
	1500	300	4	6	1534	285	0.67	060
				6	1656	305	0.66	025
	1800	210	20	6	1834	045	0.59	355
				6	1956	340	0.63	355
	2100	200	19	6	2134	320	0.70	015
				6	2256	025	0.85	185
Jan. 4	0000	210	19	6	0034	025	0.59	355
TM 0732				6	0156	030	0.14	355
	0300	210	22	6	0334	350	0.35	355
				6	0456	005	0.77	010
	0600	210	19	6	0634	340	0.67	025
				6	0756	055	0.77	060
	0900	210	20	6	0936	031	-	001
				6	1056	015	0.63	358
	1200	210	23	6	1236	022	0.77	356
				6	1356	030	0.08	-
	1500	210	19	6	1556	005	1.68	002
	1800	240	7	6	1836	-	0.13	-
				6	1956	102	1.67	356
	2100	000	9	6	2136	110	0.08	-
				6	2256	212	-	097
1954 Jan. 5	0000	020	8	6	0036	301	0.35	-
TM 0828				6	0156	212	0.20	-
	0300	035	4	6	0336	147	1.40	059
				6	0456	175	0.35	000
	0600	060	5	6	0636	298	0.85	041
				6	0756	297	0.77	042
	0900	038	4	6	0940	295	0.67	105
				6	1056	270	0.53	356
	1200	085	5	6	1240	212	0.63	048
				6	1356	212	0.00	059
	1500	063	5	6	1540	339	0.66	012
				6	1700	264	0.69	012
	1800	090	10	6	1842	264	0.13	042
	2100	120	14	6	2142	270	0.41	026
Jan. 6	0000	170	17	6	0042	270	0.11	031
TM 0923				6	0200	297	0.27	-
	0300	180	19	6	0342	311	-	000
				6	0500	330	0.62	356
	0600	185	19	6	0642	321	0.62	358
				6	0800	330	0.59	018
	0900	220	14	6	0942	005	0.74	352
				6	1100	201	0.83	000
	1200	225	9	6	1242	032	0.56	000
				6	1400	076	0.27	020
	1500	260	6	6	1542	076	0.66	338
				6	1700	060	0.62	-
	1800	260	8	6	1842	100	0.87	338
				6	2000	041	0.60	-
	2100	225	14	-	-	-	-	-
Jan. 7	0000	220	24	-	-	-	-	-
TM 1015	0300	215	26	-	-	-	-	-
	0600	210	20	-	-	-	-	-
	0900	200	16	6	0942	153	-	000
				6	1100	121	0.63	338
	1200	305	15	6	1242	119	0.21	000
				6	1400	152	-	338
	1500	305	15	6	1542	130	-	338
	1800	315	16	-	-	-	-	-
	2100	315	20	6	2142	092	-	000
				6	2300	066	0.27	-
1954 Jan. 8	0000	315	20	6	0042	085	0.88	338
TM 1105				6	0200	100	0.11	000
	0300	320	19	6	0342	110	0.43	000
				6	0500	169	0.88	301
	0600	330	20	6	0800	154	0.56	283
	0900	330	22	6	0944	160	-	275
				6	1100	122	0.10	000
	1200	330	20	6	1244	131	0.74	000
	1500	330	20	6	1545	103	0.77	000
				6	1700	155	0.90	000
	1800	335	22	6	1845	158	0.07	338
				6	2000	160	0.27	000
	2100	335	20	-	-	-	-	-

(Cont.)

	Local Time	Wind dir.	Wind mph	Buoy No.	Trans. Time	Current dir.	Current knots	Wind Vane
Jan. 9	0000	330	19	-	-	-	-	-
TM 1154	0300	330	13	6	0500	270	-	000
	0600	345	15	6	0642	192	0.43	000
	0900	000	10	6	1100	168	0.56	357
	1200	000	13	6	1242	211	0.83	338
				6	1400	202	0.85	000
	1500	000	7	6	1548	230	0.56	000
				6	1700	168	0.27	-
	1800	010	5	6	1848	239	0.64	224
	2100	-	calm	6	2128	097	0.56	085
Jan. 10	0000	-	calm	-	-	-	-	-
TM 1243	0300	-	calm	-	-	-	-	-
	0600	225	6	-	-	-	-	-
	0900	225	7	-	-	-	-	-
	1200	220	10	6	1249	330	-	356
				6	1400	329	0.55	356
	1500	190	12	6	1548	350	0.69	000
				6	1700	358	0.55	000
	1800	190	14	-	-	-	-	-
	2100	185	17	-	-	-	-	-
Jan. 11	0000	185	14	-	-	-	-	-
TM 1333	0300	195	20	-	-	-	-	-
	0600	220	21	-	-	-	-	-
	0900	225	17	6	0951	349	-	356
				6	1100	005	1.62	000
	1200	220	20	6	1413	357	0.15	000
	1500	210	21	6	1552	008	0.80	301
				6	1700	008	0.83	000
	1800	200	16	-	-	-	-	-
	2100	200	16	-	-	-	-	-
1954 Jan. 12	0000	190	21	-	-	-	-	-
TM 1425	0300	190	21	6	0342	026	-	000
				6	0500	006	0.77	000
	0600	240	26	6	0642	027	0.76	139
				6	0800	008	0.88	003
	0900	245	26	6	0953	041	0.11	352
				6	1141	103	0.83	008
	1200	270	8	6	1253	028	0.46	358
				6	1414	060	0.66	301
	1500	250	10	6	1553	078	0.88	150
	1800	245	8	6	2015	103	-	-
	2100	270	8	6	2153	121	0.21	353
				6	2315	-	1.16	007
Jan. 13	0000	300	11	6	0053	060	0.49	042
TM 1519	0300	300	12	6	0353	152	0.49	264
				6	0515	152	1.10	264
	0600	310	14	6	0653	121	0.84	000
				6	0815	010	0.15	000
	0900	335	21	6	0953	264	0.70	098
				6	1015	264	0.76	221
Jan. 26	0000	355	13	-	-	-	-	-
TM 0107	0300	030	11	-	-	-	-	-
	0600	030	7	-	-	-	-	-
	0900	040	6	-	-	-	-	-
	1200	065	7	9	1245	293	0.35	026
	1500	070	6	9	1545	-	0.56	332
	1800	095	4	9	1845	011	0.66	350
	2100	090	4	9	2145	031	0.71	305
Jan. 27	0000	090	5	9	0047	328	0.20	312
TM 0151	0300	090	4	9	0347	063	0.52	286
	0600	100	4	9	0647	048	0.57	287
	0900	105	5	9	0946	045	0.66	311
	1200	100	6	9	1246	005	0.49	260
	1500	090	3	9	1545	334	0.34	328
	1800	-	calm	9	1845	350	0.59	338
	2100	-	calm	9	2145	034	1.54	348
1954 Feb. 8	0000	280	10	-	-	-	-	-
TM 1221	0300	-	-	-	-	-	-	-
	0600	-	-	-	-	-	-	-
	0900	-	-	-	-	-	-	-
	1200	150	7	-	-	-	-	-
	1500	140	14	14	1637	307	-	000
	1800	180	17	14	1937	001	0.72	000
				14	2043	359	0.45	312
	2100	225	24	-	-	-	-	-
Feb. 9	0000	265	26	-	-	-	-	-
TM 1315	0300	270	50	-	-	-	-	-
	0600	260	43	-	-	-	-	-
	0900	265	30	14	1040	100	-	000
				14	1145	095	0.96	270
	1200	270	18	14	1340	096	1.08	280
	1500	280	18	14	1445	140	1.08	336
	1800	280	20	-	-	-	-	-
	2100	280	23	-	-	-	-	-

Notes on Table I.

Buoys 8, 9, and 14 were all rigged as shown in Figure 2; buoys 6 and 7 were rigged with the deep drag on a bridle directly beneath the can; buoys 2, 3 and 4 were rigged the same as Figure 2, but the deep drag was replaced by another rotor similar to that at the surface. The depth of the deep drag, of the surface rotor, and the Magnus correction applied in determining current direction from the rough data, were as follows:

Buoy No.	Depth of deep drag (or rotor) (feet)	Depth of surface rotor (feet)	Current direction correction
2	150	8	− 10°
3	200	8	− 10°
4	150	8	− 10°
6	170	8	unknown
7	120	8	− 25°
8	530	13	− 10°
9	150	8	+ 10°
14	300	10	+ 10°

It is probable that there is a systematic error in all angles measured by buoy 6.

The notation "TM" means the Bermuda Time (GMT − 4 hours) of Greenwich upper transit of the moon. The anemometers on the buoys were so unreliable (due to circuit troubles) that all of their data are omitted. Winds tabulated are those on a 50 foot mast at the observatory at Bermuda. The exposure was not ideal, there being several hills, and a large building in the neighborhood. Particularly, the anemometer is partly sheltered from west winds.

The notation 'Trans. Time" means the Bermuda time at which the buoy wireless transmission was received. The current direction is the instantaneous magnetic direction of the surface current (vectorial difference of surface and deep) with the above corrections applied. The current speed is an average for the previous three hours (in the case of buoy 6, 90 minutes).

The figures under "Wind Vane" are angle between the geographical orientation of the buoy and the wind direction measured by the vane on the buoy. Thus an angle of 000° means that the instantaneous wind and uncorrected current vector point in the same direction; an angle of 030° means the uncorrected current is 30° to the left of the wind; an angle of 320° means the uncorrected current is 40° to the right of the wind.

is the considerable irregularity of the currents even during days while the wind is fairly steady. In his discussion of the current measurements which he made on board the "Armauer Hansen" in 1930, EKMAN (1953) has called this irregular motion a kind of "macro-turbulence". As a result it is difficult to extract from the data definite statements about such things as: (i) the deviation of the surface current from the direction of the surface wind; and (ii) the ratio of current speed to the speed of the wind producing it. EKMAN (1953) attempted to analyze his data for "Armauer Hansen" anchor station D in order to find the answer to these questions and to delineate the drift current spiral as a function of depth. Because of the macro-turbulence the results of his analysis were disappointingly indefinite. The purpose of such an analysis, of course, was to verify in the deep ocean the results of his theory (EKMAN 1905).

Table 2. Total number of vane readings (cumulative) for each 10° angle of deviation of current from wind

Buoys 2, 3, 4, and 8

170 R	4	010 L	274
160 R	6	020 L	288
150 R	7	030 L	297
140 R	18	040 L	307
130 R	25	050 L	309
120 R	30	060 L	311
110 R	32	070 L	314
100 R	46	080 L	318
090 R	56	090 L	320
080 R	68	100 L	322
070 R	79	110 L	325
060 R	103	120 L	331
050 R	121	130 L	333
040 R	141	140 L	338
030 R	154	150 L	340
020 R	172*	160 L	341
010 R	192	170 L	345
000	223		

*Half the readings are on either side of this point.

The present buoy measurements are confined to the surface. They cover a longer period than those made on the "Armauer Hansen". It is therefore hopeful that certain features of drift currents may emerge more clearly from the confusion of the macro-turbulence.

In order to appreciate how serious an obstacle the macro-turbulence is to a simple analysis of the data, an analysis can be made of all the wind vane readings obtained from buoys 2, 3, 4, and 8 (Table II). The current direction correction due to the Magnus effect on the rotor has been applied. As can be seen, there is a very large scatter of the angle of deviation of the current from the wind; at one time or another every possible angle has occurred. On the average, however, there is a greater frequency of small angles of deviation showing that usually a current does not run against the wind. Moreover, there is a rather definite indication that currents to the right of the wind are more frequent than currents to the left of the wind. The mode of this frequency distribution lies at about 20° to the right of the wind, but it is obvious that this type of analysis of the data, including as it does all cases where the winds were rapidly varying, and all cases with pronounced irregular motions or possible inertial oscillations, gives at best a very diffuse and indefinite kind of answer to question (i). Similar objections can be raised to an attempt to make a gross average determining the ratio of current to wind velocity. A more rational approach is to study individual cases where the wind was observed to be steady. Of course the currents are not exactly steady during the same time. The question arises as to how long a time interval to employ for the study of individual cases. EKMAN (1905) indicated that after the onset of a wind the average of the current for the first 24 hours (at 30° N) is a very close approximation to the theoretical current produced by a wind of infinite duration. Thus, in attempting to find answers to questions such as (i) and (ii) (above), 24-hour vectorial averages of wind and current are formed for days of steady wind. The concept of a steady wind is subjective.

The data obtained from October 28—31 is a good sample of the relation between wind and current as it actually appears in nature (Figure 5). During October 28 the wind began to blow toward the north and by midnight was blowing about 23 knots; the currents, which were at first weak and variable, gradually veered to the right of the wind and grew stronger. Early on October 29 the wind itself veered until it blew toward NNE. The current veered, too, and executed a rotatory motion about a mean velocity about 42° to the right of the wind. During the afternoon of October 30, the wind dropped rapidly, and the current began to execute a rotatory (inertial) motion about a zero mean velocity. By October 31,

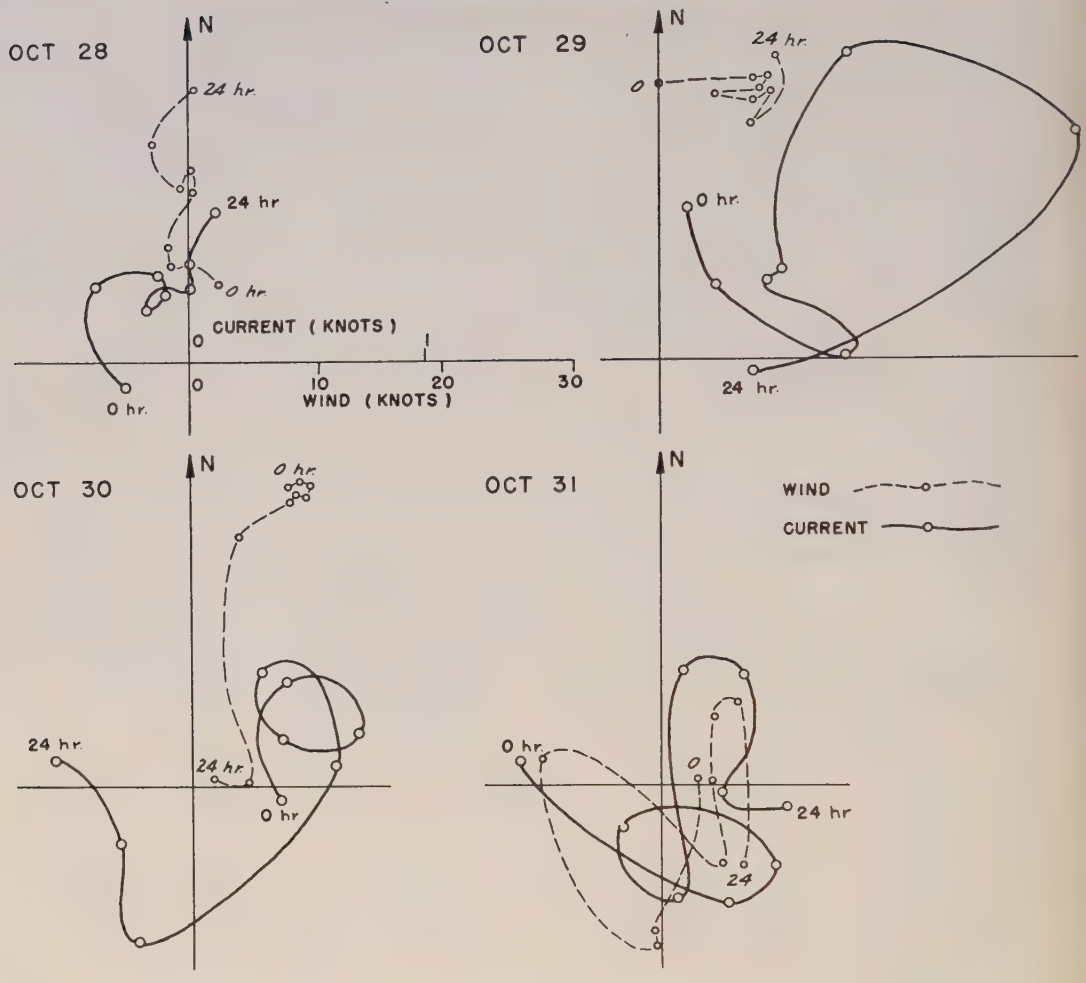

Fig. 5. Sample daily records of wind and current showing the response of the current to a strong wind and the after-effects following it.

the winds were light variable and the motions of the current were very irregular and confused. All evidence of a simple 24-hour inertial period was gone. During the winter of 1953—1954 the currents in the Northwestern Sargasso Sea are most often in a confused state such as depicted on October 31. It is only during days of steady strong winds, and immediately following them, that the theoretical features deduced by EKMAN (1905) are clearly defined. Table III contains means of wind and current for all days during which the wind was steady. It was prepared for the purpose of examining the data from the 24-hour mean "case history" point of view.

III. The angle between the wind and current

Two independent ways of measuring the angle between wind and current are possible. The angle may be determined by comparing the mean wind direction at the observatory with direction of the current given by the magnetic compass on the buoy (Method 1). The angle may also be determined directly from the wind vane on the buoy, which

Table 3. 24-hour vectorial means of current and winds for days with steady winds.

Day	Buoy	Wind blows toward	Wind speed (knots)	Current Direction	Speed (knots)	Angle of current relative to wind Method (1)	Method (2)
Oct. 29	3	018	20.0	060	1.09	042 R	070 R
29	4	018	20.0	070	0.70	052 R	000
Nov. 3	3	225	6.1	230	0.51	005 R	025 R
6	3	305	11.2	345	0.64	040 R	045 R
8	3	230	4.4	235	0.72	005 R	040 R
9	3	270	4.5	270	0.57	000	055 R
23(1)	2	285	11.2	315	0.45	030 R	010 R
24	2	335	6.0	335	0.56	000	005 L
26	2	015	13.0	030	0.57	015 R	005 R
Dec. 2-3	2	150	13.0	170	0.50	020 R	020 R
5	8	270	3.0	(2)	0.08	(2)	(2)
6	8	260	4.0	(2)	0.18	(2)	(2)
18	7	140	13.0	220	0.61	080 R	(5)
19	7	145	16.0	225	0.67	080 R	(5)
22	7	030	17.0	075	0.62	045 R	(5)
23	7	060	6.0	115	0.48	055 R	(5)
Jan. 1	6	150	18.0	(3)	0.70	(3)	(3)
3-4	6	030	17.0	(3)	0.50	(3)	(3)
8	6	150	18.0	(3)	0.68	(3)	(3)
11(4)	6	025	18.0	(3)	0.72	(3)	(3)
26-27	9	270	4.0	010	0.48	100 R	055 R
Feb. 9	14	270	23.0	(4)	1.45	(4)	045 R

(1) Current data not available for entire 24 hours, but winds blew steady for previous four days.

(2) Mean direction meaningless because of large oscillatory motions.

(3) Angles have unknown systematic errors due to faulty bridling of Buoy 6.

(4) Current data not available for entire 24 hours.

(5) Wind vane broken.

measures the instantaneous angle between wind and buoy orientation (Method 2). Although this latter method is direct, it is likely to be more erratic due to gustiness of the wind—the sampling of wind direction from wind vane measurements on the buoy is naturally much poorer than the continuous records available at the observatory.

By both methods it is seen that (in agreement with EKMAN, 1905) the current is to the right of the wind, by an angle varying between 30° and 60°. During weak winds there is a greater spread of angles, and on the average the angle appears to be less than for strong winds.

IV. The Ratio of current speed to wind speed

The ratios of current speed to wind speed cited in Table III are about twice what would be expected from Ekman's study. When plotted on a logarithmic scale (Figure 6) these data give some indication that the ratio is not independent of wind speed. There is enough scatter in the data to prevent certainty concerning this point. EKMAN (1905) discussed the case of a "quadratic" law of friction in the sea, and showed that in this case the current speed would be proportional to the three-halves power of the wind speed (rather than linearly proportional). The very limited data at hand suggests the reality of this law of friction, but of course does not prove it. The solid line in Figure 6 depicts the linear law; the dashed line, the three-halves law.

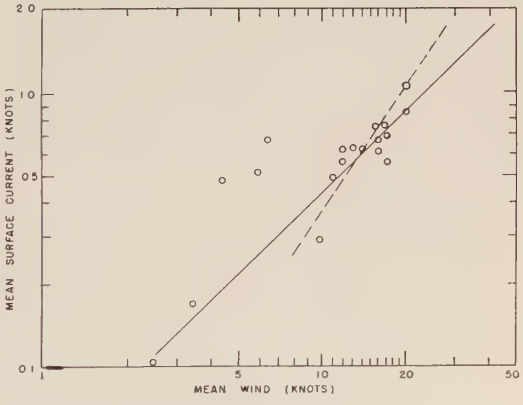

Fig. 6. Logarithmic graph of mean wind against mean surface current for days with steady wind. The solid line has slope of 1.0; the dashed line, slope of 1.5.

Table 4. Inertial amplitudes and phase for days showing 24-hour rotatory currents. All cases are cum sole.

Day	Buoy	Amplitude (knots)	Time of Maximum Northerly Flow	
			Local Mean Solar Time	Greenwich Lunar Time
Oct. 29	3	0.20	1500	1310
30	3	0.25	0800	0530
Nov. 1	3	0.13	0430	0030
5	3	0.10	2030	1400
9	3	0.10	1330	0330
25	2	0.06	0000	0030
27	2	0.25	0000	2230
Dec. 6	8	0.25	0730	2330
7	8	0.20	0630	2145
23	7	0.10	0900	1000
24	7	0.25	1300	1330
26	7	0.06	1100	1200
Jan. 4	6	0.20	0730	0000
6	6	0.20	0900	2330

V. The Presence of inertial oscillations

The design of the rig used on these buoys is not ideal for detecting or studying inertial oscillations because, as Fredholm (EKMAN, 1905) showed, the inertial motions penetrate quickly to layers below the depth of frictional influence, and hence the inertial, or quasi-periodic, term in the vectorial difference of velocity is likely to diminish quickly if the deep drag is not much below the depth of frictional influence. Very clear and distinct rotatory currents with 24-hour period were observed on 14 separate days (Table IV); they were quickly damped out (whether by vertical diffusion of momentum, or horizontal dispersion of energy in the form of gravity waves is uncertain). The sense of rotation in every case was *cum sole*. Comparison of phase, to time of transit of the moon results in a complete scatter, thus ruling out the likelihood that these 24-hour periods are lunar tidal currents. There is also no relation to time of day, thus ruling out solar tides.

REFERENCES

EKMAN, V. W., 1905: On the influence of the earth's rotation on ocean-currents. *Arkiv for Matematik, Astronomi o. Fysik*, **2**, No. 11: 1 – 52.

– 1953: Results of a cruise on board the "Armauer Hansen" in 1930 under the leadership of Bjørn Helland-Hansen. Studies on Ocean Currents. Pt. I. Text. Pt. II. Tables and Plates. *Geofys. Publ.*, **19** (1): 106 + 122 pp.

Origin and Accumulation of Aluminosilicates in the Ocean[1]

By GUSTAF ARRHENIUS, University of California, Scripps Institution of Oceanography
La Jolla, California

(Manuscript received April 20, 1954)

Abstract

The basic assumptions used by B. Kullenberg in his attempt to calculate the probable magnitude of the variations of the rate of accumulation of clay appear unrealistic in the light of present knowledge, and consequently the results are hardly applicable. His assumptions imply that the sizes of the clay particles now observed in samples from the ocean floor have remained essentially unchanged during transport and deposition. Most probably, however, the marine clays represent the end product of precipitation and coarsening processes, the initial particles partly being of ionic and molecular size. Changes in the rate of deposition of aluminosilicates in eupelagic areas are rather determined by physico-chemical properties of sea water than by changes in the influx to the ocean. Such changes are supposed to be practically equalled out in the neritic and hemipelagic environment.

In a recent paper (1953), B. KULLENBERG has made an interesting attempt to estimate the maximum concentration of inorganic particles suspended in the open ocean. Kullenberg's calculation is based on the assumption that the approximate size distribution of the suspended mineral matter can be derived from the size distribution of the pelagic clay sediments. Knowing the effect of size and concentration of suspended particles on the scattering of light, Kullenberg uses measurements of the latter property, and arrives at an oceanic maximum concentration of $56 \cdot 10^{-6}$ g of solid matter per liter, or $21 \cdot 10^{-3}$ g in a column of 1 cm^2 cross section at average oceanic depth. Pointing to the fact that this amount is deposited in less than 300 years over a surface of 1 cm^2 in the calcareous part of the eupelagic area of the East Equatorial Pacific, Kullenberg demonstrates in an elegant way, that, provided his assumptions are valid and complete, the amount of fine terrigenous matter present in the sea is probably insufficient to act as a buffer against variations of supply during a major climatic cycle. He further claims that these variations were probably considerable, and that consequently changes in the rate of accumulation of terrigenous matter during the Pleistocene cannot be neglected, even in pelagic areas far away from the source of supply and characterized by great regional uniformity of this rate. Therefore, it does not appear feasible to Kullenberg to base an estimate of geological time in pelagic sequences on the assumption of a constant rate of accumulation of clay in eupelagic areas.

These conclusions are contradictory to those which can be drawn from the composition of Pleistocene eupelagic clay sediments as a

[1] Contribution of the Scripps Institution of Oceanography, New Series No. 750.

function of time. The main constituents of these sediments are solid phases, formed in the ocean (marine hydrogenous matter, GOLDBERG 1954), further solids originating in the supramarine part of the hydrosphere and transported to the sea in suspension, and finally solid phases formed in the lithosphere (lithogenous matter, ibid.), and represented by igneous minerals such as finely divided quartz. Biogenous matter is of subordinate importance in the case of most pelagic clays.

If the rate of accumulation of any of the main constituents changes considerably, as supposed by Kullenberg, this will certainly be reflected by a corresponding change in their proportios in the sediment. The probability of simultaneous changes in the rates of accumulation of all phases, such that changes in the relative proportions were cancelled out, is exceedingly small. It ought therefore to be relatively easy to trace changes in the rate of accumulation of one phase or another by variation with time of the composition of the sediment. Such changes are, indeed, frequently recognized in shelf and hemipelagic deposits. Extensive rate changes in space and time also seem to be normal features of most pelagic sediment sequences in topographically irregular areas, and in environments with a considerable influx of turbidity currents (STETSON and SMITH 1938, PHLEGER 1951, ARRHENIUS 1952, ch. 2.39—2.48, RIEDEL 1952, CORRENS 1954). Under certain conditions, however, the changes in space and time of the rate of non-biogenous accumulation appear to be lowered to a small fraction of the rate value. These conditions seemingly are fulfilled in the eupelagic area of the East Equatorial Pacific (Arrhenius, l.c. fig. 1.0). Here the thickness of the Pleistocene strata (corrected for biogenous matter in the calcareous facies) is strikingly uniform, and the Pleistocene clay deposits so far investigated are characterized by considerable homogeneity with regard to the relative proportions of the inorganic components, thus indicating that no drastic changes in the rate of accumulation of single components took place in this area during Pleistocene time. A quantitative study of these conditions is being carried out at the present time, using the sediment cores collected from the East Equatorial Pacific during the Scripps Institution CAPRICORN Expedition of 1952—1953.

The relative uniformity of the rate of non-biogenous accumulation in the east eupelagic area of the Pacific Ocean may partly be explained by the large distance to the continents, the absence of islands, the smooth, rolling bottom topography, the low seismicity, and the presence further to the east of the East Pacific Rise, acting as a barrier to turbidity currents, released on the shelf slope. Even in the predominantly eupelagic parts of the East Equatorial Pacific, local depositional disturbances are found on topographic highs, where erosion sometimes occurs, and close to these localities, where the eroded material contributes to an abnormally high rate of accumulation (ARRHENIUS 1952, ch. 2.53). These effects appear, however, to be of only local importance, probably because the eroded, coagulated sediment in suspension forms aggregates which settle out again quickly enough to prevent transport over more than a few nautical miles.

The apparent disagreement between the observed evidence of low variability in Pleistocene time of the rate of non-biogenous accumulation in the east eupelagic area, on one hand, and Kullenberg's arguments on the other, still remains to be explained. To accomplish this we shall scrutinize the assumptions, on which Kullenberg has based his reasoning. The sedimentation model used by most earlier workers, including the present author (ARRHENIUS 1952) and KULLENBERG (1953) implies that the clay particles, observed in the eupelagic deposits, were transported to the site of deposition from the continental source without any essential changes in size and internal structure. Kullenberg, in accordance herewith, uses the grain size distribution of a recent pelagic clay to compute the size distribution of particles suspended in the ocean. A serious objection against this procedure arises from the fact that the mineral grains have to a large extent been cemented to aggregates, by hydrous oxides of manganese and iron. Many minerals further appear to have undergone secondary enlargement after deposition. This makes it highly doubtful whether the size distribution quoted by Kullenberg is in any way representative of the size distribution of the grains, even at the time when they crossed the water-sediment interface. Furthermore, the static model applied, which postulates an essentially unchanged size and internal structure

of the particles from the moment of suspension to the moment of arrival to the sediment interface appears to be unrealistic in the light of recent investigations. CORRENS and v. ENGELHARDT (1938) have demonstrated that weathering proceeds by the breakdown of the parent mineral to ionic solutions and that the secondary minerals are reaction products of such solutions. A large fraction of the aluminum and silica, dissolved from continental rocks, is precipitated in the continental part of the hydrosphere or in the coastal areas of the ocean, but considerable amounts are carried in solution, even in the open ocean, and must be taken into account as a source of pelagic clay minerals. Dissolved silica is present in the sea in comparatively high concentration, and provides a steady source of reactive silicate ions. Analyses of the aluminum of sea water range between 3 and $2400 \cdot 10^{-6}$ g/l, the very high values reported from coastal waters (THOMPSON and ROBINSON, 1932; HAENDLER and THOMPSON, 1939; KALLE, unpubl., quoted by WATTENBERG, 1943; ISHIBASHI and FUJINAGA, 1951; SIMONS, MONAGHAN and TAGGART, 1953). For the sake of discussion we shall adopt a tentative figure for the open Pacific, and choose the conservative value of $10 \cdot 10^{-6}$ g/l Al. In addition to the dissolved aluminum a certain amount is present in particulate form, presumably as aluminosilicates. This amount is probably several times the mass in ionic solution. A concentration of particulate aluminum three times the concentration of dissolved aluminum is certainly a conservative estimate. The total amount of aluminum may thus be of the order of $40 \cdot 10^{-6}$ g/l. Although this figure may be far off from the true concentration, it is probably not too high, and it may be justified to use it for minimum computations. The concentration value used corresponds to $18 \cdot 10^{-3}$ g Al or $35 \cdot 10^{-3}$ g Al_2O_3 in a column of 1 cm^2 cross section at average depth, 4600 m, in the equatorial east eupelagic area of the Pacific. The mean concentration of Al_2O_3 in the eupelagic clay is 19 % by weight at 110° C and 17 % at the temperature and moisture conditions adopted in the work of the Swedish Deep Sea Expedition. Thus $18 \cdot 10^{-3}$ g Al will ultimately produce $206 \cdot 10^{-3}$ g of clay, i.e. ten times more than Kullenberg's estimate. With a rate of accumulation of $73 \cdot 10^{-3}$ g of clay per cm^2 in 1000 years (ARRHENIUS 1952, § 1. 2. 10) the period of turnover is at least 3000 years.

The aluminum bearing particles presumably have a particle size range from a few units of 10^{-8} cm to the order of magnitude 10^{-4} cm. Below the particle size 10^{-5} cm (MECKLENBURG, 1915) or $8 \cdot 10^{-5}$ cm (BECHHOLD and HEBLER, 1922) the scattering entirely follows Rayleigh's law, and the intensity of the scattered light of the Tyndall beam is thus a function of the third power of the diameter of the particles, the mass concentration of the solid phase being kept constant. Tyndall measurements, used as a basis for the determination of mass concentration, thus give far too low values, if Kullenberg's above mentioned assumption is applied with regard to the size distribution of inorganic suspended particles.

In order to arrive at a maximum figure for the concentration of the solid phase, Kullenberg allows the entire scattering observed to be regarded as due to inorganic particles. Considering the probably very small dimensions of most of these particles and the resulting weakness of the Tyndall effect, however, only a small fraction of the total scattering needs to be ascribed to inorganic matter, the main part of the Tyndall effect probably being due to plankton and organic detritus.

The mechanism of precipitation of aluminum in the sea has not yet been experimentally studied, but as the concentration in the ocean appears to be far below the solubility of aluminum hydroxide, it is believed that the primary solid phase consists of an aluminosilicate sol, which is progressively turning coarser by condensation and coagulation, and thereby settles out.

The concept of a marine origin of clay minerals is not a new one, but as far as the present author is aware, it has not been previously published or discussed in detail. Dr Josef Eklund at the Geological Survey of Sweden mentioned the idea in the early 1940's and the possibility of similar processes has recently been pointed out also by Dr George Bien at the Scripps Institution of Oceanography. The concept is in agreement with the results of GRIM, DIETZ, and BRADLEY (1949) on the properties of Pacific clay minerals. The formation of clay minerals in the marine environment has been demonstrated by NORIN's (1953) finding of authigenic illitic

mica in sediments from the Tyrrhenian Sea. The mineral is confined to coarse-grained strata, where the water can circulate readily, and Norin points out that the authigenic illite is not derived from the detrital minerals, which are perfectly fresh, and that there is no relationship between the composition of the authigenic mineral and that of the surrounding detritus.

Even if the period of turnover of non-biogenous matter in the eupelagic area of the Pacific Ocean is 3000 years or a low number multiple of this value, instead of Kullenberg's value 300 years, this period is still short in comparison with a major climatic cycle. Following Kullenberg's reasoning there would under such circumstances be a close relationship between the rate of accumulation of clay in the eupelagic environment and the considerable changes, which he postulates in the rate of influx of source material of eupelagic clay. First, however, if the source material or a great part of it prevails in dissolved form, there is no need to assume large variations in the influx of such material to the ocean during the Pleistocene. Second, even large variations in the total influx of the reactive components may have a negligibly small effect on the concentration of these components in an advanced state of the reaction, i.e., after the lapse of such a time that the water mass in question has been transported far away from a coastal area. In a second order reaction, where, for the sake of simplicity, both reactants are regarded as identical, and enter the reaction in the concentration A_0, the concentration a′ found after a time t is expressed by

$$a' = \frac{A_0}{1+ktA_0},$$

where k under given conditions is a constant.

If the initial concentration were different from A_0 by a factor n, the concentration a'' at the time t would be

$$a'' = \frac{nA_0}{1+ktnA_0}$$

and thus the ratio between concentrations under these two conditions is:

$$\frac{a'}{a''} = \frac{\frac{1}{n}+ktA_0}{1+ktA_0} \qquad \lim_{t\to\infty}\frac{a'}{a''} = 1$$

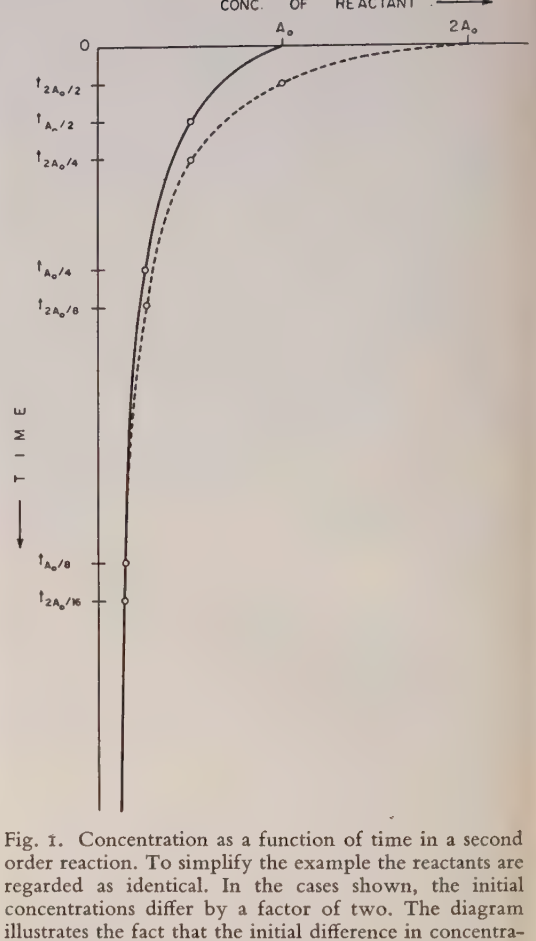

Fig. 1. Concentration as a function of time in a second order reaction. To simplify the example the reactants are regarded as identical. In the cases shown, the initial concentrations differ by a factor of two. The diagram illustrates the fact that the initial difference in concentration decreases rapidly with time, and that in an advanced state of the reaction the concentrations are practically equal in both cases. At a varying influx in the sea of suspended colloids or of dissolved thalassoxenic solids, large variations in the rate of precipitation can thus be expected in the coastal areas, close to river mouths, and negligible variations after a certain time of travel of the water mass containing the reacting system. Eupelagic conditions require that the uniformity of precipitation should be accompanied by uniformity of accumulation of the solid phase in question on the ocean floor.

$t_{A_0/2}$ indicates the first, $t_{A_0/4}$ the second, etc. half life of the reactants, in the case where the original concentration was A_0. $t_{2A_0/2}$, etc. are corresponding symbols for the case of the original concentration $2A_0$.

It is evident that the initial deviation of the ratio from unity is rapidly decreasing with increasing time and thus that differences in the initial concentration are practically eliminated in an early stage of the reaction. This is graphically illustrated in fig. 1. The rapidity

of the elimination of these differences is still greater if the reaction is of higher order, which may very well be the case.

Similar relationships hold true also for the coagulation of particulate matter, which has been demonstrated by v. SMOLUCHOWSKI (1917) to be a second order reaction. Even if a considerable amount of the eupelagic clay is of supramarine origin it is thus possible to account for eupelagic uniformity of the rate of accumulation of clay, occurring togetner with large variations in the influx to the ocean. The main factor determining the eupelagic rate of accumulation of aluminosilicates appears to be the magnitude k, which is determined by the physico-chemical properties of sea water, and therefore probably subject to comparatively small fluctuations during the Pleistocene period.

This kinetic model is a deliberately oversimplified representation of the real conditions. The precipitation, condensation, and coagulation reactions in the ocean are most certainly much more complicated and heterogeneous than a simple second order reaction. However, such a simplified model appears to be useful and significant as long as the discussion is restricted to the question whether a buffer mechanism for the pelagic rate of precipitation can or cannot exist in the ocean.

It should further be pointed out that iron, titanium and zirconium on one hand, and the aluminosilicates on the other, appear to have different cycles in the sea (LEWIS and GOLDBERG, 1954, ARRHENIUS and BLOMQVIST, 1954). Although the uniformity of the titanium content of the eupelagic clay furnishes additional evidence of uniformity of the rate of accumulation of these two components, the validity of the use of titanium for dating purposes is obviously not directly connected to the question of the rate of accumulation of clay minerals.

The estimation of geological time from accumulated mass involves the approximation of a constant rate of accumulation. The error of age determination may largely be determined by deviation of this approximation from true conditions. Our knowledge of the average magnitude and the variance of this error is at present limited to the order of magnitude, and further studies of these factors are needed. Keeping in mind actual limitations of the method, it can, however, be used for the approximation of time factors and rate processes in the area and time interval in question. Although far from perfected, the procedure appears more reliable than previously available dating methods for the Pleistocene, which place the duration of this period between the probable limits 0.6 and 2 million years.

As some confusion appears to have arisen (BROTZEN, 1953) with regard to the significance of the uniformity in space and time of the rate of non-biogenous accumulation, it should be stressed again that the conclusions drawn by the present author apply only to the area and the time-rock units, where the indicative observations have been made, i.e., to the Pleistocene strata of the east eupelagic area of the Equatorial Pacific, and in a strict sense only to the cores from which the observations in question were derived. Large areas have been investigated (ARRHENIUS, 1952) where no such uniformity was found. It is therefore erroneous to regard the concept of uniformity of the rate in question as suggested for the entire ocean bottom.

From what has been said above, it is concluded that the indications of Pleistocene uniformity of the rate of accumulation of non-biogenous matter, observed, and so far observed only in the equatorial east eupelagic area of the Pacific Ocean, are in agreement with what is so far known and what can safely be postulated with regard to the mechanism of formation of pelagic deposits. Kullenberg's criticism deals with an improbable model of petrogenesis and does not take into consideration the reaction kinetics of the process of formation of marine sediments. Although it is an interesting and elegant attempt to treat one aspect of marine sedimentation, it does not, for the reasons given, apply to the pelagic environment.

REFERENCES

Arrhenius, G., 1952: Sediment cores from the East Pacific. *Rep. Swed. Deep Sea Exp.*, **5**, fasc. 1.

Arrhenius, G., and Blomqvist, N., 1954: Proportions of sedimentary components in the calcareous eupelagic area of the East Equatorial Pacific. *Rep. Swed. Deep Sea Exp.*, **5**, fasc. 2 (in press).

Bechhold, H., and Hebler, F., 1922: The nephelometer effect of colloid systems of different particle sizes. *Kolloid Ztschr.*, **31**, 70.

Brotzen, F., 1953: G. *Arrhenius*; Sediment cores from the East Pacific. Review. *Geol. Fören. Stockholm Förhandl.*, **75**, 115.

Correns, C. W. 1954: Titan in Tiefseesedimenten. *Deep Sea Res.*, **1**.

Correns, C. W., and v. Engelhardt, W., 1938: Neue Untersuchungen über die Verwitterung des Kalifeldspates. *Chemie. d. Erde*, **12**.

Fischer, R. A., 1925 – 48: Statistical methods for research workers. London.

Goldberg, E. D., 1954: Marine geochemistry I. Chemical scavengers of the sea. *Jour. Geol.*, 62.

Goldschmidt, V. M., 1945: The geochemical background of minor-element distribution. *Soil. Sci.*, 60.

Grim, R. E., Dietz, R. S., and Bradley, W. F., 1949: Clay mineral composition of some sediments from the Pacific Ocean. *Bull. Geol. Soc. Am.*, 60, 1785.

Haendler, H. M., and Thompson, T. G., 1939: The determination and occurrence of aluminum in sea water. *Jour. Mar. Res.* 12.

Lewis, G. and Goldberg, E. D., 1954: Iron in marine waters. *Jour. Mar. Res.* 13.

Ishibashi, M., and Fujinaga, T., 1951: Polarography of aluminum. *Sbornik Mezinarod. Polarog. Sjezdu v. Praze*, Pt. 1.

Kullenberg, B., 1953: Absolute chronology of deep sea sediments and the deposition of clay on the ocean floor. *Tellus*, 5, 302.

Mecklenburg, W., 1915: The relation between the Tyndall effect and the size of the particles of colloidal solutions. *Kolloid Ztschr.*, 16, 97.

Norin, E. 1953. Occurrence of authigenous illitic mica in the sediments of the Central Tyrrhenian Sea. *Bull. Geol. Inst. Uppsala*, 34, 279.

Phleger, F., 1951: Displaced foraminifera faunas. *Soc. Econ. Paleont. and Mineralogi. Spec. Publ.* No. 2, 66 – 75.

Riedel, W. R. 1952. Tertiary Radiolaria in Western Pacific sediments. *Medd. Oc. Inst. Göteborg*, 19.

Simons, L. H., Monaghan, P. H., and Taggart, M. S., 1953: Determination and occurrence of aluminum and iron in sea water. *Analytical Chemistry*, 25.

von Smoluchowski, M., 1917: Versuch einer Mathematischen Theorie der Koagulationskinetik Kolloider Lösungen. *Ztschr. physik. Chem.*, 92, 129.

Stetson, H. C., and Smith, J. F., 1938: Behavior of suspension currents and mud slides on the continental slope. *Am. Jour. Sci.*, 35.

Thompson, T. G., and Robinson, R. J., 1932: *Physics of the Earth*, 5, Chapt. 5.

Wattenberg, H., 1943: Ergänzung zu der Mitteilung: Zur Chemie des Meerwassers. *Ztschr. anorg. u. allgem. Chemie*, 251, 86.

On the presence of sea water in the Baltic ice-lake

By B. KULLENBERG, Göteborg

(Manuscript received June 21, 1954)

Abstract

A discussion of the salinity of the interstitial water in five sediment cores from the Baltic containing mainly glacial deposits appears to prove that the Baltic ice-lake contained sea water during the early stage when only the South Baltic was laid free by the retreating ice.

The existing information regarding the complicated development of the Baltic since the first appearance of the Baltic ice-lake has been obtained by investigations above the present sea level, such as studies of shore lines, varves in glacial clay, and fossils. Fossils in the deposits have given information on the salinity of the water, and especially made it possible to decide during which periods the Baltic was a lake containing fresh water, or a sea with a more or less good connection with the ocean. In many cases observations above sea level necessitate an extrapolation beyond the shoreline, the results of which are inevitably doubtful. The development of the piston corer (KULLENBERG 1947) has made it possible to extend the investigations beyond the present shoreline by collecting sediment cores in the Baltic sufficiently long enough to reach down into the moraine, so the study of the cores should furnish information comprising the lateglacial and postglacial stages of the Baltic. An informal Danish-Swedish committee under the chairmanship of Dr HILMER ÖDUM, Director of the Danish Geological Survey, has therefore undertaken to study the bottom deposits in the Baltic by means of the piston corer with a view to extend the knowledge of the history of the Baltic. By the courtesy of the Swedish board of fisheries the research ship the "Skagerak" has repeatedly been put at the disposal of the committee, or the present writer, for these investigations. By the courtesy of Dr VEDEL-TÅNING the Danish research vessel the "Biologen" was put at the disposal of the committee on one occasion.

The committee has, among other things, tried to find evidences in the bottom deposits in the South Baltic that the present sea bottom has been raised above sea level during lateglacial or postglacial time, such as the occurrence of peat, stumps of trees, lacustrine sediments, or simply a very hard and dry crust. Finds of stumps of trees are reported by fishermen at about lat. N 55°15′, long. E 14°00′ at a depth of 40 m. So far, the present investigations have not verified the occurrence of anything indicating an up-heaval of the sea bottom south or east of Scania. In the area where the present water depth exceeds about 30 m a study of the sediment cores rather suggests that the area in question has been perpetually covered by water, because the sequence of strata is identical to the one that is met with in a depression 20 nautical miles north of the island of Bornholm where

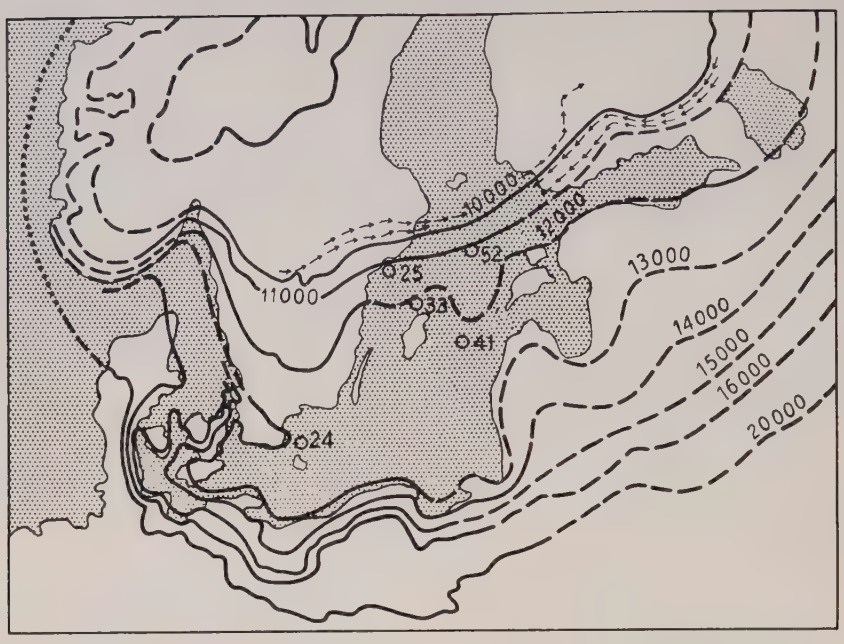

Fig. 1. Positions of coring stations. Milleniar ice-margins B.P. and influxes of salt water to the Baltic from east and west (De Geer 1954)

the depth is about 100 m. In more shallow water near the coast of Scania the bottom is covered by sand over-laying a hard moraine. The extension of the area covered by a complete sequence of varved clay and postglacial sediment strata has not yet been found out in detail. As a preliminary to a systematic examination a detailed survey with echo-sounder to a depth of 40 m was undertaken in May, 1954, using Decca for navigation.

In the Great Belt a layer of peat about 75 cm thick was found in September 1953, near Nyborg at a depth of 28 m during a cruise with the Danish research vessel the "Biologen" using a 3 m piston corer adapted for the rapid collection of the uppermost sediment layers. The core is being worked up at the Danish Geological Survey, and Dr Ödum has kindly informed me that the deepest part of the peat layer dates from lateglacial time. Though several cores were collected in the immediate neighbourhood, only one more of them revealed traces of peat so the peat-bog is evidently quite small. This should be remembered in the search for peat-bogs inundated by the sea, and necessitates that the search be carried out with considerable thoroughness. A peat-bog is in great danger of being removed or having its size reduced by wave action in the process of inundation.

The salinity of the interstitial water of the bottom deposits in the Baltic might be a source of information regarding the salinity of the bottom during the various stages of the Baltic. According to studies in the laboratory, using a beaker as a settling tank, the salinity of the interstitial water in newly deposited sediments is identical to the salinity of the bottom water (Kullenberg 1952). Studies of sediment samples collected in the Mediterranean and the Indian ocean don't rule out the possibility that changes occur as the sediment grows older, and especially that the salinity might be different in adjacent sediment layers with different compositions even though both layers might originally have had the same salinity. This presupposes a diffusion of some major component of the sea salt from one sediment layer to another able to bind the ions in a higher concentration. However, if such changes occur they are too small to be very important in the case of Baltic sediments,

because the salinity changes in the Baltic during the last stages of the glaciation and during postglacial time should be very considerable according to the prevailing views on the history of the Baltic.

The smoothing out of vertical salinity gradients by diffusion might have an influence more prejudicial to our aim. By measurements in the laboratory I have found the coefficient of diffusion to be about $2 \cdot 10^{-6}$ cm^2/sec, but so far I have not studied the influence of the water content on the coefficient of diffusion though such an influence must certainly exist. Further, the texture of the sediment, and its degree of consolidation, should be expected to influence the coefficient of diffusion. Unfortunately, the disturbance caused to a sediment sample when it is collected and during its subsequent treatment may increase the coefficient of diffusion very much, so the value here reported is probably too large. We shall discuss the diffusion in connection with some of the cores collected in the Baltic.

Nearly hundred long cores have been collected in the Baltic and we shall here discuss the ones given in Table 1. The positions of the coring stations together with milleniar ice-margins B.P. (before present) and influxes of salt water to the Baltic from east and west according to De Geer (1954) are indicated in Fig. 1.

Table 1

Station	Latitude	Longitude	Depth	Length of the core
24	N 55°31′	E 15°08′	86 m	15.2 m
25	58 26	17 39	72	8.5
33	58 04	18 57	117	15.0
41	57 28	20 07	183	10.0
52	59 07	20 31	118	9.0

Station 24. The station is situated 20 nautical miles north of the island of Bornholm. At the lower end of the core there is a 3 m thick layer of a moraine consisting of sand, silt, and lumps of clay. Between a sediment depth of 1,240 and 1,020 cm there is a grey glacial clay with rather distinct varves, succeeded by a fine red glacial clay with indistinct varves extending to a depth of 125 cm. Between 125 and 100 cm there is a clayey mud, light bluish grey, which is separated from the adjacent layers by very sharp boundaries. The top of the core down to 100 cm consists of a dark greenish mud with a high content of organic matter.

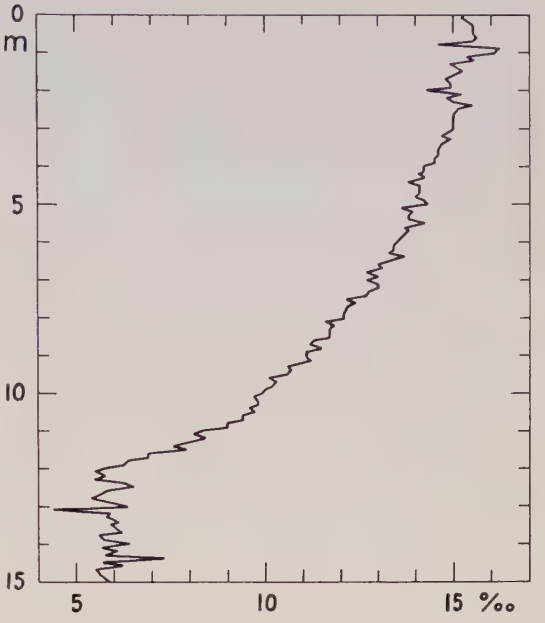

Fig. 2. The salinity of the interstitial water at station 24.

The salinity of the interstitial water as determined at intervals of 10 cm is represented in Fig. 2.

Regarding the postglacial deposits at the top of the core we shall call attention to the fact that there is no outstanding salinity minimum such as the *Ancylus* stage would have left behind itself, as the Baltic is generally considered to have been a lake at that period. Neither has any major salinity minimum indicating the *Ancylus* stage been found in the other cores investigated in the Baltic, some of which have a much thicker postglacial sediment layer than the core now deliberated. It might be that diffusion has removed the salinity minimum. The duration of the *Ancylus* stage is estimated at about 1,500 years, and the sediment layer formed during this period might be quite thin, as in fact it must be at station 24, where the total thickness of the postglacial deposits accumulated during 10,000 years is no more than 125 cm. Accordingly very great salinity gra-

dients would appear in the core if the salinity of the bottom water was coming down to zero during the *Ancylus* stage, and the diffusion would be correspondingly intensified. However, in some areas the postglacial deposits attain a thickness of 20 m, or more, and then diffusion should be less effective. So far, the salinity has not been determined in any core containing such a thick postglacial sediment layer, and a final judgment should be postponed until this has been done. Another explanation of the lack of a postglacial salinity minimum might of course be that the salinity of *the bottom water* was not reduced appreciably during the *Ancylus* stage.

In the glacial clay between 125 and 1,240 cm the salinity of the interstitial water decreases with the sediment depth from 15 ‰ to 6 ‰. In the moraine found between 1,240 and 1,520 cm the salinity is constant except for irregular variations. Here the water content is as small as 14 per cent by weight, so the salinity cannot be determined very accurately.

It is remarkable that the salinity gradient in the clay increases with the sediment depth. This evidence appears to prove definitely that the salinity of the interstitial water in the varved clay was originally high, i.e. 10—15 ‰ even in the lower portion of the layer consisting of varved clay. In fact, a horizontal lamella of clay will lose more salt downwards per unit time than it will receive from above, because the salinity gradient is smaller at the top of the lamella than at the bottom. It is true that the coefficient of diffusion might change with the sediment depth, and if the coefficient of diffusion were reciprocally proportional to the salinity gradient each horizontal lamella of clay would lose equally as much salt downwards per unit time as it receives from above. However, as the clay is getting slightly more coarse with increasing sediment depth the coefficient of diffusion should be expected to *increase* with the depth, if it changes at all. Then a horizontal lamella of clay will certainly lose salt continually in the portion of the core between 200 and 1,200 cm. Accordingly the salinity of the interstitial water in this portion of the core will continually be reduced. The rapidity of this process is dependent on the value of the coefficient of diffusion *in situ*, which is not known but is probably less than $2 \cdot 10^{-6}$ cm²/sec.

The diffusion of the salt is governed by the equation

$$w \frac{\partial S}{\partial t} = k \frac{\partial^2 S}{\partial t^2} \qquad (1)$$

S denoting the salinity of the interstitial water, w the water content in g/cm³ (i.e. practically in fraction of the volume), k the coefficient of diffusion, z the sediment depth, and t the time. We will put $k/w = m$ and, by way of simplification, we will assume m to be a constant. This does not mean that we assume k/w to be generally independent of the character of the sediment (it is certainly not); we just assume this ratio to be a constant in the varved clay here in question, the general properties of which do not change appreciably though the water content does change.

In the depth range 500—1,200 cm the salinity is approximated quite closely by the equation

$$S = 4.5 + 0.363 \sqrt{1{,}220 - z} \qquad (2)$$

This will make

$$\frac{\partial^2 S}{\partial z^2} = -0.091 : (1{,}220 - z)^{3/2} \qquad (3)$$

Putting $m = 3 \cdot 10^{-6}$ we get

$$\frac{\partial S}{\partial t} = -2.7 \cdot 10^{-7} : (1{,}220 - z)^{3/2} \qquad (4)$$

The salinity change in 1,000 years according to eq. (4) is given in Table 2.

Table 2

Depth	$\Delta S_{1{,}000\ \text{years}}$
5 m	— 0.45 ‰
6	— 0.55
7	— 0.7
8	— 1.0
9	— 1.5
10	— 2.6
11	— 6.5

This imports that the salinity of the interstitial water in the varved clay is rapidly decreasing at all depths below 4 m, or that the salinity was originally greater, especially in the deeper parts of the varved clay. Supposing the selected value of the coefficient of diffusion to be approximately correct, the high

rate at which the salinity is changing with time will appreciably influence the second derivative of the salinity in a much shorter time than 1,000 years. Accordingly the figures given in Table 2 are valid for the present only, especially in the deeper parts of the varved clay. Notwithstanding, the salinity will have changed at a very high rate during the past few thousand years, if the coefficient of diffusion is as high as has been assumed here. The main part of the varved clay in this core has an age of more than 12,000 years (De Geer 1954). Even without entering into a detailed calculation it can therefore be maintained, with reference to Table 2, that the original salinity of the interstitital water in the varved clay did not fall much below 15 ‰, not even in the deepest portion of the varved clay. This conclusion would still not be greatly affected even if the coefficient of diffusion *in situ* is only one tenth of the value here adopted. If, on the other hand, there is no diffusion at all, the original salinity is given by Fig. 2.

Regarding the sand underlying the varved clay it appears probable that here the interstitial water is comparatively free to move, which would smooth the salinity gradients effectively. Unless there is a continual supply of fresh water to the sand layer able to carry away the salt brought to the sand layer by diffusion, the salinity of the interstitial water in the sand layer must be increasing and was, accordingly, originally smaller than at present. The corer did not go right through the moraine so we don't know the thickness of the sand layer. Considering the small water content of the sand layer, it has a small capacity as a recipient of salt, and it has to have a thickness of 10—20 m to be able to absorb the amount of salt carried away from the varved clay, if the original salinity of the interstitial water in the varved clay was 15 ‰. If the interstitial water in the sand layer contained sea salt originally, its capacity as a recipient of salt would be even smaller. It is therefore not probable that so much sea salt has flowed from the clay to the sand as would be the case if the coefficient of diffusion *in situ* were really as high as $2 \cdot 10^{-6}$ cm²/sec. In fact, at present the salinity gradient between 11 and 12 m sediment depth is 0.023 ‰ per cm. At $k = 2.10^{-6}$ cm²/sec this would make the amount of sea salt entering the sand layer by diffusion 1,450 mg/cm² in a thousand years. The water content of the sand layer being about 30 % by volume a supply of salt at this rate would raise the salinity of the interstitial water in a sand layer 80 m thick by 6 ‰ in ten thousand years. It is hardly probable that the sand layer is as thick as that.

Regarding the salinity of the bottom water in the South Baltic at the time the varved clay in the core here considered was deposited, it follows that the salinity did not fall much below the salinity found in the bottom water in the South Baltic at present, with the possible exception of the deepest part of the varved clay corresponding to a period no longer than a few hundred years. We conclude that the Baltic ice-lake contained sea water even during the early stage here in question, or at about 12,000 B.P., when only the South Baltic was laid free by the retreating ice. This does not agree with the prevailing view that the South Baltic was a fresh water lake until 10,500 B.P., when sea water began to flow into the Baltic over Finland as the ice-margin left Salpausselkä I.

The low salinity of the interstitial water in the moraine and, possibly, the deepest portion of the varved clay may be occasioned by the nearness of the ice and the ensuing masses of melt water likely to reduce the salinity, unless the cause is a horizontal leaking of fresh water through the sand layer.

Station 25. The station is situated 20 nautical miles east of the Swedish coast, northwest of Gotland. The corer hit a big boulder or solid rock which was covered by 8.5 m sediment. The nose of the corer was smashed by the rock. Immediately above the rock there was about 50 cm of clay and silt with pebbles. Then followed a 265 cm thick layer containing 219 rather distinct varves covered by a 32 cm thick layer containing less distinct and very thin varves. The varves are grey, and the summer sediment consists of silt. Between 490 and 70 cm there is a grey clay which did not display any varves until it had dried and even then the varves were quite indistinct. The top of the core down to 70 cm consists of a bluish grey clay containing a few lumps coloured black by iron sulphide.

The salinity of the interstitial water is represented in Fig. 3. The interface at about 5 m between the deeper part of the core containing well-developed varves, and the upper part containing indistinct varves, is displayed by a sudden decrease of the water content from 55 % by weight to (in the mean) 44 %. Large irregular variations of the water

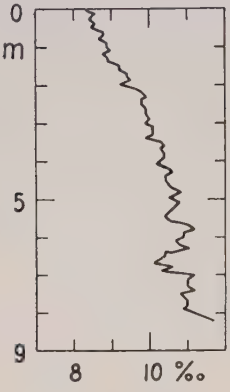

Fig. 3. The salinity of the interstitial water at station 25.

content in the deeper part of the core is due to the fact that the water content of the winter sediment is considerably higher than that of the summer sediment.

The salinity of the interstitial water increases with sediment depth from 8.4 ‰ at the top of the core to 11.7 ‰ at 820 cm, which is about 25 cm above the rock. This appears to prove that the salinity of the bottom water at this station was higher at the time the varved clay was deposited than it is now. The salinity gradient decreases with the sediment depth, and diffusion will therefore diminish the salinity throughout the core, except for the top. This imports that the salinity of the interstitial water in the varved clay was even higher originally than it is now, provided diffusion takes place.

According to Fig. 1 the deeper portion of this core was deposited a little earlier than 11,000 B.P., whereas the inflow of salt water over Finland commenced at about 10,500 B.P. Considering that the ice-margins in the Baltic are estimated on the basis of observations ashore, this discrepancy does not appear serious. On the other hand it is quite possible that the inflow of salt water in the east has nothing to do with the high salinity found in this core. In fact, cores collected nearer the entrance of the Gulf of Finland do not display a similar increase of the salinity with the sediment depth, whereas they should have done so even to a higher degree if the influx of salt water over Finland were the cause of the phenomenon. This core appears therefore to strengthen the evidence supplied by core 24, that the Baltic ice-lake contained sea water at an early stage.

Station 33. The station is situated a few nautical miles to the north of Gotland. The deepest 240 cm of the core consists of silt and sand with occasional pebbles; the colour is light reddish. Above 1,260 cm there is a varved clay containing red summer sediment and grey winter sediment; the thickness of the varves decreases from 5—8 cm at 12.5 m to 6—8 mm at 9 m. Above 915 cm the varves are not distinct, and above 880 cm no varves can be perceived in the homogeneous light reddish clay present up to 645 cm. Between 645 and 510 cm there is a grey clay with occasional thin sand layers and traces of indistinct varves. At 510 cm begins a bluish grey, clayey mud with numerous lumps coloured black by iron sulphide, especially at 510—465 and 375—305 cm. At about 135 cm the grey mud is succeeded by a greenish grey mud smelling of hydrogen sulphide with occasional thin brown layers consisting of plant debris.

The salinity of the interstitial water is represented in Fig. 4. Apart from minor irregular variations the salinity is constant in the top layer 0—135 cm consisting of green mud. It is on the whole increasing slowly with the sediment depth in the postglacial deposits 135—510 cm, from 10.2 to 11.4 ‰. In the layer consisting of homogeneous clay the salinity is again decreasing from 11.4 ‰ to about 10.6 ‰ at the top of the varved clay, and remains then constant to the undermost metre of the sand layer at the bottom of the core where the salinity decreases by about 1 ‰.

The retreating ice margin is supposed to have passed this station at 12,100 B.P., or 1,600 years before the invasion of sea water by Salpausselkä I. The number of varves present below 900 cm is less than 300 so it appears probable that most of the clay between 900 and 510 cm was deposited before Sal-

pausselkä I. It is possible that the clay was deposited in fresh water and the salt was brought into it by diffusion after Salpausselkä I, but this does not appear likely if we consider St 24 and 25, where diffusion has not been able to smooth out the salinity gradients. It is therefore highly probable that the clay at St 33 was deposited in sea water with a salinity slightly higher than the one found there at present. The salinity in the varved clay is slightly lower than in the varved clay at the bottom of core 25 which was deposited about 400 years later according to the ice-margins laid down by De Geer, and in more shallow water.

Station 41. The station is situated between Gotland and Latvia. Only a 10 m corer was used which was not sufficient to reach down into the moraine. The core consists of varved

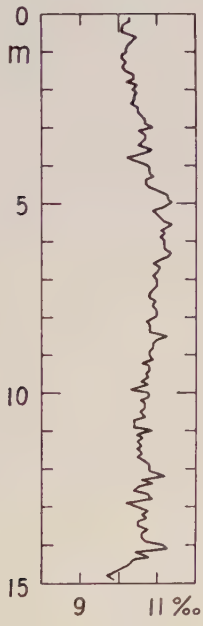

Fig. 4. The salinity of the interstitial water at station 33.

clay from the lower end at 1,000 cm to about 290 cm where it is succeeded by a homogeneous brown-grey clay. This is covered by a bluish-grey clayey mud found between about 170 and 6 cm containing a few layers which are coloured black by iron sulphide. At the top of the core there is a thin layer of green mud. A longer core reaching down to the moraine will be collected at this station.

The salinity of the interstitial water is represented in Fig. 5. The salinity is decreasing with the sediment depth throughout the

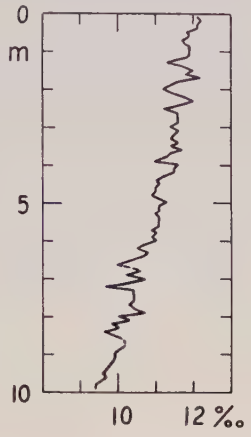

Fig. 5. The salinity of the interstitial water at station 41.

core, from 12,1 ‰ at the top to 9.4 ‰ at the lower end and the salinity gradient tends to increase with the depth in a similar way as at St 24. According to the ice-margins in Fig. 1 the varved clay should be contemporary with the one deposited at St 33. However, in the deeper portion of core 41 the salinity of the interstitial water is lower than in core 33, though the opposite would be the case if the deposits were really contemporary, as the water depth is greater at St 41 than at St 33. The positions of the ice-margins should be verified by varve measurements in cores collected in the Baltic. We shall postpone the discussion until this has been done and a set of cores reaching down into the moraine have been collected in this area.

Station 52. This station is situated in the middle of the Baltic, between the island of Dagö and the Swedish coast. In the Baltic the echo-sounder commonly indicates a stratified bottom with six or more interfaces able to give rise to an echo. One of them divides the glacial clay from the clayey mud usually overlying it. In the area now in question the echo-sounder reveals that one interface

giving a powerful echo rises to the surface very often, forming intervening depressions which are filled with comparatively soft deposits with a higher water content than found below the interface in question, as shown by cores collected in such depressions. At St 52 the interface in question has risen to the surface.

But for an 11 cm thick surface layer consisting of a homogeneous grey mud with a high content of organic matter, the core contains nothing but varved clay with a grey colour. The varves have a thickness of 1—2 cm near the top of the core, i.e. the distal glacial sediment is missing that should be expected on the top of the distinct varves. It would appear that erosion has removed the distal sediment. The varves are quite distinct and can be measured throughout the core. However, the varve sequence will not be discussed until longer cores have been obtained reaching down into the moraine.

The water content decreases with the sediment depth from 55 % by weight at the top of the core to 25 % at 900 cm. The salinity of the interstitial water keeps constant at about 10 ‰ throughout the core. The ice-margin is supposed to have passed this station at the same time as it passed St 25. It is noteworthy that the salinity of the interstitial water is smaller than in the deeper parts of core 25 in spite of the fact that the water depth is more than 40 m greater. As the core does not reach down to the moraine, no definite comparison with St 25 can be made, however, as it is quite possible that a longer core at St 52 would reveal an increase of the salinity with the sediment depth below 900 cm. Notwithstanding, the constancy of the salinity at St 52, as compared with the steady increase of the salinity at St 25 from the very top of the core, appears to contradict the possibility that the sea water apparently present in the Baltic at the time the varves found in the two cores were deposited, entered the Baltic from the east.

REFERENCES

De Geer, Ebba Hult, 1954: Skandinaviens Geokronologi, *Geol. Fören. Förhandl.*, **76**, 299.

Kullenberg, B., 1952: On the salinity of the water contained in marine sediments, *Medd. Oceanogr. Inst. i Göteborg*, No. 21.

— 1947; The piston corer. *Sv. Hydr.-Biol. Komm. skrifter.* 3 ser: Hydr. Bd. 1. H. 2.

Specific Scattering by Uniform Minerogenic Suspensions

By WAYNE V. BURT[1]

Department of Oceanography, University of Washington[2]

(Manuscript received March 25, 1954)

Abstract

The Mie theory has been applied to determine the theoretical scattering from 1 mg per liter concentrations of uniformly-sized spherical particles over the size range from very small particles up to particles with a radius of 6 microns. The theoretical results compare favorably with experimental results recently published by Jerlov and Kullenberg.

Jerlov and Kullenberg (1953) have published the results of laboratory measurements of the Tyndall effect of uniformly-sized suspensions of quartz and feldspar particles. Their results are presented in terms of the scattering coefficient, $s\,(\mathrm{km}^{-1})$, for suspensions with particle diameters of 1, 3, 7, 9, and 12 microns with known concentrations of suspended material. Their coefficient, s, takes into account the effects of suspended materials only. The following empirical relationship was used to convert the Tyndall reading, A, to scattering, s (Jerlov, 1953):

$$s\,(\mathrm{km}^{-1}) = 0.52\,A - 3 \qquad (1)$$

The Mie theory (Gumprecht and Sliepcevich, 1951, 1953a, 1953b) can be used to determine the theoretical value of the scattering coefficient for suspensions of the type employed by Jerlov and Kullenberg. It seems worth while to compare the theoretical results as predicted by the Mie theory to those obtained experimentally in order to use the theory to predict what would occur over a more complete range of particle sizes.

The Mie theory requires the use of the effective area coefficient, K, which is defined as the ratio between the effective scattering cross section and the geometric cross section of a spherical particle. It is computed as a function of the dimensionless parameter, $\alpha = 2\,\pi r/\lambda$, and the relative refractive index, m, between the particle and the suspending medium, in this case water. The particle radius is r and λ is the wave length of the light energy that is being scattered. Gumprecht and Sliepcevich (1951) tabulate K as a function of α for several values of m equal to and greater than 1.20. In addition, Van de Hulst (1946) provides an equation for determining K for values of m near 1.00. The above tables and and equation provide sufficient information to interpolate for K as a function of α for values of m between 1.00 and 1.20.

Considering the effects of scattering only, the theoretical extinction, H, due to uniformly-sized spherical particles is then:

$$H = K\pi r^2 n \qquad (2)$$

where n is the number of particles per unit volume. Equation (2) applies for particles with the same relative refractive index for light of a single wave length.

[1] Now at Oregon State College, Corvallis, Oregon.

[2] This work has been supported by Office of Naval Research Contract N8onr-520/III, Project NR 083 012.

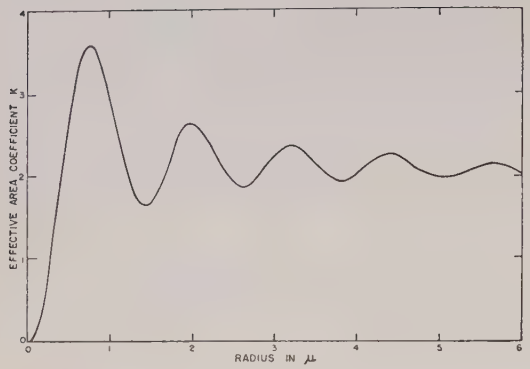

Fig. 1. Mie scattering curve for material with a relative refractive index of 1.15 for blue light (0.470 μ). Adapted from Gumprecht and Sliepcevich (1953a) and Van de Hulst (1946).

The specific scattering is now defined as the extinction per meter, H_0, for a suspension containing 1 mg of suspended material per liter. If the material in suspension has the usually assigned average density of minerals of 2.65, the suspension will contain 0.377×10^{-6} m^3 of suspended material per m^3 of suspension. Equation (2) can then be rewritten

$$H_0 = \frac{3}{4}\frac{K}{r}\left(\frac{4}{3}\pi r^3 n\right) = \frac{3}{4}\frac{K}{r}(0.377 \times 10^{-6}) \quad (3)$$

Taking the length unit for the radius in the conventional unit of the micron, equation (3) becomes:

$$H_0 = 0.283\ K/r \quad (4)$$

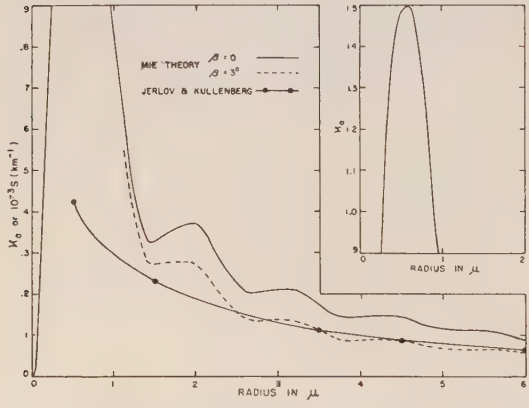

Fig. 2. Theoretical and experimental (Jerlov and Kullenberg, 1953) specific scattering for concentrations of suspended materials of 1 mg per liter.

Jerlov and Kullenberg used quartz and feldspar with relative refractive indices of approximately 1.15. Figure 1 shows the theoretical variation of K, the effective area coefficient, with the radius, r, for spherical particles with relative refractive indices of 1.15 for blue light (.470 μ).

Figure 2 shows the theoretical specific scattering computed from equation (4) and the material presented in figure 1. Whenever these theoretical scattering computations are compared to actual measured values of scattering, a correction should be made to the theoretical computations to take into account the fact that any practical measuring device measures light which is scattered in a nearly forward direction as transmitted light (Gumprecht and Sliepcevich, 1953a). The dashed curve on figure 2 shows the theoretical scattering corrected to exclude light scattered into a cone of half angle β centered about the forward direction. The correction decreases with decreasing particle size until it becomes relatively unimportant for small values of β for particles with radii below approximately 1 micron.

The experimental results for specific scattering from Jerlov and Kullenberg (1953) are also shown on figure 2. Considering the fact that their material was made up of non-spherical particles, the agreement between theory and measurement is striking for all but the smallest-sized particles, particularly if the measurements are compared to the theoretical curve corrected to exclude a part of the nearly forward scattered light.

The large discrepancy between the theoretical specific scattering and the measured specific scattering for the smallest-sized particles with a nominal radius of 1/2 micron is probably due to a combination of the following factors: (a) failure of some of the assumptions, such as the assigned values of the refractive index or the density or the effects of non-spherical particles, in applying the Mie theory; (b) small experimental errors in determining the particle size and concentration down in the size range where Stokes' law becomes increasingly difficult to apply; or (c) the fact that the slope constant in equation (1) cannot be assumed to be a constant over the whole range of particle sizes.

REFERENCES

GUMPRECHT, R. O., and C. M. SLIEPCEVICH, 1951: *Tables of light-scattering functions for spherical particles*, Ann Arbor, Michigan, University of Michigan Engineering Institute, Special Publication: Tables.

— 1953 a: Scattering of light by large spherical particles, *J. Phys. Chem.*, **57**: 1, pp. 90—95.

— 1953 b: Measurement of particle sizes in polydispersed systems by means of light transmission measurements combined with differential settling, *J. Phys. Chem.*, **57**: 1, pp. 95—97.

JERLOV, N. G., 1953: Particle distribution in the ocean, *Reports of the Swedish Deep-Sea Expedition 1947—1948*, **3**, Fasc. 2, pp. 73—125.

JERLOV, N. G., and B. KULLENBERG, 1953: The Tyndall effect of uniform minerogenic suspensions, *Tellus*, **5**: 3, pp. 306—307.

VAN DE HULST, H. C., 1946: Optics of spherical particles, *Recherches Astronomiques de l'Observatoire d'Utrecht*, **11**, part 1, pp. 1—87.

On the Origin of Cosmic Radiation

By HANNES ALFVÉN*, Kgl. Tekniska Högskolan, Stockholm, Sweden

(Manuscript received June 12, 1954)

Abstract

The "local" theory of the origin of Cosmic Radiation is developed. According to the theory the radiation (possibly with exception of the highest energies) is generated in interplanetary space around the sun and trapped in an interstellar magnetic field. The acceleration takes place in electromagnetic fields in the sun's environment which are produced by the solar activity and especially associated with magnetic storms.

A theory of the origin of Cosmic Radiation should at the same time be a theory of the extra-terrestrial variations in the radiation. The present theory incorporates the magnetic storm variation, the diurnal variation and the long time (solar cycle) variation.

The acceleration process of the theory is efficient for protons and especially for for heavy nuclei but is inefficient for electrons. This explains the absence of electrons in the primary Cosmic Radiation. The latitude "knee" is accounted for as a direct effect of the acceleration process.

1. Introduction

Since the discovery of the Cosmic Radiation the general picture has changed drastically several times. The primary radiation was at first believed to be a γ radiation, later a β radiation, until it was proved to consist merely of protons. Recently even heavy nuclei have been found in the primary radiation.

Even the views concerning the isotropy and constancy of cosmic radiation have been revised from time to time. The first measurements indicated strong fluctuations but these were soon found to be due to experimental errors. During a long time cosmic radiation was regarded to be almost completely isotropic and constant in time. Recently this picture has been changed again and the study of the time variations of cosmic radiation is attracting more interest. FORBUSH's ionization chamber measurements, which have continued during more than 15 years, show large variations in the yearly means of the total intensity[1]. THAMBYAHPILLAI and ELLIOT, and SARABHAI and KANE[2] have demonstrated that the phase and the amplitude of the diurnal variation changes considerably with the solar activity. Further, during magnetic storms large fluctuations are observed which cannot be due to terrestrial causes[3]. The neutron counter technique developed by SIMPSON allows a study of the low energy part of the spectrum, which varies very much with time[4]. High altitude measurements by LORD and SCHEIN, by SWETNICK, NEUBURG, and KORFF, and by YNGVE and especially by NEHER indicate variations in the primary radiation[5].

The changing views concerning the properties of the primary radiation have been

* This paper was written during a stay at the Department of Physics and Institute for Fluid Dynamics, University of Maryland, U.S.A.

reflected in the theories of the origin of cosmic radiation. As long as it was generally agreed that the time constancy was the most remarkable feature, it was natural to consider the radiation as a universal, or at least a galactic, phenomenon. As we now realize that the radiation is variable and that the variations are closely connected with the sun, it becomes natural to look for the origin of cosmic radiation in our close environment.

The measurements by SIMPSON and his collaborators[4] demonstrate beyond a doubt that at least a considerable part of the low energy radiation must be of local origin. On the other hand, TELLER-RICHTMYER's suggestion[6] that most of the cosmic radiation, perhaps all, is of local origin, seems not to have been generally accepted, although no decisive arguments against this view have been brought forward. The aim of the present paper is to show that the local origin theory deserves to be taken seriously.

The discussion of the universal and galactic theories have demonstrated that these theories encounter several difficulties. During the last few years FERMI's theory[7] has been in the centre of the discussion. Objections against this theory have been forwarded by UNSÖLD[8]. Introducing values into Fermi's formula for the energy spectrum which from astrophysical point of view are most probable, Unsöld finds that the theoretical value of the exponent should be about 200 instead of the empirical value 1.5. Further, the theory does not explain the abundance of heavy nuclei and cannot account for the low-energy cut-off. These objections seem not to have been overcome altogether by the recent development of the theory by FAN[9], MORRISON, OLBERT and ROSSI[10], and by FERMI[11].

It seems not to be generally observed that even if these difficulties could be successfully overcome – which does not seem likely at present – only half of the problem of the primary radiation would have been solved, because we must also have a theory of the variations. Such a theory will probably be as difficult as a theory of the origin.

The local theory has a different position in this respect, because it attempts to account both for the variations and the origin. Hence, an acceptable local theory would solve the two main problems at the same time. The study of the variations gives us much experimental material by which a local theory can be checked.

2. Acceleration mechanisms

It is most likely that cosmic radiation is generated by acceleration of charged particles in electromagnetic fields in space or in stellar atmospheres. The first mechanism of this kind was proposed by SWANN[12] who pointed out that a betatron acceleration may take place in the growing magnetic field of a sunspot (the "cygnotron"). Other electromagnetic accelerating mechanisms have later been proposed by EHMERT[13], by MENZEL and SALISBURY[14] and by BAGGE, BIERMANN and SCHLÜTER[15].

In this paper we shall study a mechanism of a somewhat similar kind by which charged particles are accelerated by electromagnetic fields in the neighborhood of stars. For the production of fields of the required type it is essential that we have at least two magnetized bodies, moving in relation to each other. In the first attempt to develop a theory along these lines the two bodies were represented by the two components of a double star, which were assumed to possess magnetic fields[16]. It was shown that by their relative motion electric fields could be produced which are powerful enough to accelerate particles up to the energies found in cosmic radiation. Two alternative processes were discussed. In the first one charged particles moving in trochoidal orbits are accelerated by an induced electric field, a process which is equivalent to the betatron effect. In the second alternative the motion of charged particles parallel to the magnetic field was considered and it was shown that under certain conditions accelerating electric fields could be produced.

Mechanisms of these kinds can explain the high energies in cosmic radiation, but it was found more difficult to account for the intensity.

Electromagnetic generators could obviously not generate sufficient cosmic radiation to fill up the whole space, so cosmic radiation could not be a "universal" phenomenon. The assumption of a galactic magnetic field had to be introduced, which should be strong enough to trap all the radiation generated near the stars in our galaxy, but even so, it

was difficult to account for the observed intensity without very far-stretched assumption. In fact, according to any "galactic theory", the energy of cosmic radiation within our galaxy must be of the same order as the kinetic energy of the galaxy[6], and it is difficult to believe that generators near the stars could give as much power as that. On the other hand, one of the successful results of the theory was a prediction of the existence of heavy nuclei in cosmic radiation[17]. This result was confirmed by observation about a decade later.

Thus the theory explained some of the properties of cosmic radiation, but the main difficulty was the intensity. This problem came in different light when TELLER and RICHTMYER[6] pointed out that cosmic radiation may be a "local" phenomenon, confined by trapping magnetic fields to the neighbourhood of the stars. If in this way cosmic radiation fills up only small volumes (of the order of 10^{17} cm) around the stars, the total energy goes down by a factor 10^6 or more and the intensity problem is no longer serious. However, as the radiation we observe must be generated in the neighbourhood of our sun, the initial theory must be modified because the sun is no double star. If we still accept the basic idea, i.e. that cosmic radiation is generated by electromagnetic processes due to the relative motion of magnetized bodies, we must consider the sun and a gas cloud moving in relation to it, instead of the two components of a double star. With this as a background a theory of the generation of cosmic radiation was developed in which the energy source is located in the storm-producing beams emitted from the sun[18]. Of the two alternative processes mentioned in the summary of the double star theory only the first one was considered. As recent experimental and theoretical results support the local theory, it seems worth while to discuss the whole problem again.

3. Magnetic storms

As stated in § 1 a theory of the origin of cosmic radiation should at the same time be a theory of the variations in the primary radiation. Of the different types of variations, the storm variation is of special importance because it gives us information in a rather direct way about the electromagnetic fields in our surroundings.

Occurrences on the sun, such as solar flares, are frequently followed one day later by magnetic storms and aurorae on the earth. Also when a sunspot crosses the solar meridian, a similar disturbance sometimes occurs on the earth after about one day. This has led to the assumption that a beam of ionized gas is ejected from the sun with such a velocity

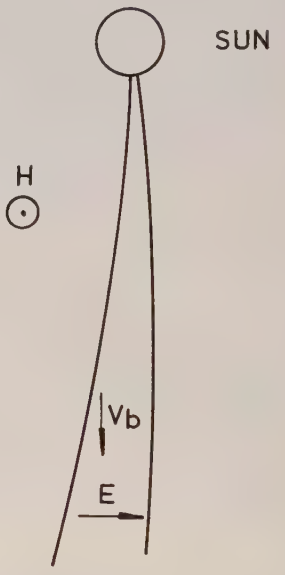

Fig. 1. Storm-producing beam, emitted from the sun (Equatorial plane).

($v_b = 2 \cdot 10^8$ cm sec.$^{-1}$) that the time of travel from the sun to the earth is approximately one day (Fig. 1). This storm-producing beam has never been observed directly, probably because its density is very low. Further, in order to produce a magnetic storm on the earth, the beam must be directed towards the earth and a beam sent out from the sun towards us should be difficult to observe. Gas ejected from the solar limb perpendicular to the sun—earth line has frequently been observed. Usually, the ejection velocity is smaller than the velocity which a storm-producing beam should have, but in many cases velocities of the same order of magnitude have been measured.

The concept of a storm-producing beam consisting of ionized rarified gas was introduced by Schuster. CHAPMAN and FERRARO[19]

have studied the properties of such a beam under the assumption that the magnetic field within the beam is zero. When the beam reaches the neighbourhood of the earth the terrestrial magnetic field is disturbed by the beam, and a magnetic storm should occur. This theory, which has been further developed by MARTYN[20], has not been able to account for the phenomena observed during a magnetic storm, and it seems legitimate to conclude that a magnetic storm cannot be produced by a beam of this type. Nor does it seem possible to account for the magnetic storm variation of cosmic rays in this way.

As it is very difficult to find another way by which a disturbance in the sun could be propagated to the earth in about one day, it seems necessary to preserve the concept of a storm-producing beam consisting of ionized rarified gas. The beam originates at the solar surface, where, no doubt, considerable magnetic fields exist. Hence, it is natural to assume that the ionized gas of the beam initially is permeated by a magnetic field. If this is the case, the conductivity of the beam is no doubt so large that the magnetic field is "frozen" into the beam, so that the beam carries a magnetic field with it as far out as to the earth. A beam with a magnetic field H in it has properties which are fundamentally different from Chapman-Ferraro's beam. Due to the motion with the velocity v_b the beam becomes electrically polarized, the electric field being

$$\vec{E} = -\frac{1}{c}\vec{v}_b \times \vec{H} \qquad (3.1)$$

This electric field seems to be the most important property of the storm-producing beam, and there is good hope that the essential features of magnetic storms and aurorae can be explained as effects of this field[21]. The difficulties of Chapman-Ferraro's theory seem to be due to the fact that they have neglected the electric field of the beam. The cosmic ray decrease, associated with magnetic storms, seems also to require the existence of such an electric field.

4. Storm variations of cosmic radiation

In connection with magnetic storms the cosmic radiation frequently decreases by a few per cent as shown by FORBUSH and others[22]. A study of the storm variations of cosmic rays at different latitudes shows that the variations cannot be caused by a change in the earth's magnetic field. This is evident from the fact that storm variations are observed at all latitudes, even above the latitude knee (FORBUSH)[22]. Recently, SINGER[23] has observed storm decreases even near the magnetic pole. Simpson has shown that the variations of the low energy radiation observed with neutron counters are of extra-terrestrial origin[24].

As the storm variations cannot be produced by any terrestrial phenomenon, it is necessary to assume that cosmic rays are affected in interplanetary space already before they reach the earth. Only an electric field (or a time variation in a magnetic field, which of course is equivalent to an electric field) could produce a change in the cosmic ray intensity. As the cause of magnetic storms seems to be the electric field of the beam, it is reasonable to assume that the storm effect in cosmic rays is a direct effect of this field. A theory along these lines[25] has recently been developed by BRUNBERG and DATTNER[26] and seems to explain the main features of the cosmic ray storm effect.

From the change in cosmic radiation, it is possible to estimate the field and the voltage difference of a storm-producing beam. If the average electric fields is E_b, and the breadth of the beam, in the direction of E_b, is b, the voltage difference is

$$V_b = E_b b \qquad (4.1)$$

Consider cosmic ray particles with energy V_0. When they pass the beam, which we depict as an electric double layer, their energies change by V_b. Further, the space density changes proportional to V_b/V_0. The result is that the measured intensity I changes by

$$\Delta I = k I V_b / V_0 \qquad (4.2)$$

where k is a constant, which depends on the measuring device, and probably has a value of about 3.★

If the average energy of cosmic radiation is $3 \cdot 10^{10}$ ev a change of 1 % means $V_b = 10^8$

★ A recent calculation by S. LUNDQUIST[27] indicates a somewhat higher value.

volt and a change of 10 % means $V = 10^9$ volt. The breadth b of the beam may be estimated from the duration of a magnetic storm. If a storm lasts about two days, as it often does, this is an indication that the beam is so broad that the earth is situated within it during two days. As the synodic period of the sun is 27 days and the earth's orbital radius is $1.5 \cdot 10^{13}$ cm this gives

$$b = \frac{2}{27} \cdot 2\pi \, 1.5 \cdot 10^{13} = 0.7 \cdot 10^{13} \text{ cm}$$

This means that we have $E = 10^{-5}$ to 10^{-4} volt/cm, values which are acceptable in the theory of magnetic storms. With $v_b = 2 \cdot 10^8$ cm sec^{-1} we find $H = 10^{-5}$ to 10^{-4} gauss. It is not necessary that the radius of curvature is larger than the breadth of the beam, because the particle may cross the beam moving in a trochoid.*

In the absence of electric currents outside the sun, the magnetic field in interplanetary space outside the sun derives from the sun. At some distance from the sun this field will be approximately a dipole field. The beam disturbs this field very much. It carries "frozen-in" field from the neighbourhood of the sun outwards. This means that currents flow at the borders of the beam. A possible structure of the field in interplanetary space when disturbed by the beam is seen in Fig. 2. If the beam is switched off the field will after some time resume a dipole character.

5. The interplanetary magnetic field

Magnetic fields in interplanetary space may derive both from the magnetic fields of the celestial bodies and from currents in interplanetary space. It is usually assumed that the field in interplanetary space derives from the solar dipole field (except in small regions near the planets), which tacitly implies that the currents in interplanetary space are negligible.

This assumption seems not to be justified. Instead it is likely that the magnetic field deriving from the sun is violently disturbed by currents in interplanetary space. These currents produce large local irregariulties and make the field vary with time. They also seem to produce a large-scale effect so that outwards from the sun the average field decreases much slower than a dipole field. It is therefore misleading to refer to the magnetic field in interplanetary space as "the solar dipole field" and in the following we shall call it "the interplanetary field". The reasons for assuming that the field deviates very much from a dipole field are the following, of which 1) and 2) refer to the general shape of the field and 3) and 4) to the local irregularities.

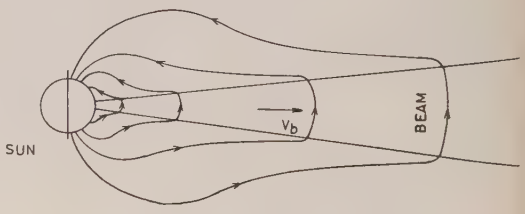

Fig. 2. Simplified model of the interplanetary magnetic field, consisting of the solar field which is very much disturbed by the storm-producing beams. (Meridional plane.)

1. Eclipse photographs of the corona show in the polar regions a structure which may be reconcilable with a magnetic dipole field, in which matter streams along the lines of force. However, in the equatorial region long "streamers" are observed which go out from the sun. Together with the fact that matter often is seen to be ejected from the equatorial regions this shows that there often are outward streams of ionized gas near the equatorial plane. As the magnetic field is "frozen" into the gas, which is a good conductor, an original dipole field will be disturbed very much. The outward motion will in general tend to make the average field decrease slower than a dipole field.

2. Cosmic ray evidence speaks for a much higher field near the earth's orbit than is reconcilable with a dipole field. In § 4 we have estimated the field in the beam to 10^{-5}—10^{-4} gauss. A dipole field with this strength at the earth's distance would be

* Compare. Swann, *Phys. Rev.* **93**, 905, 1954, and H. Alfvén, *Phys. Rev.* **94**, 1,082, 1954. See also Fig. 7.

100—1000 gauss at the sun's surface, which is excluded. Even outside the beam the field probably exceeds 10^{-5} gauss according to BRUNBERG and DATTNER[26].

3. The solar corona seems to be highly turbulent. This must also hold for the magnetic fields, because of magneto-hydrodynamic effects. It is reasonable that the turbulence is not confined to the neighborhood of the sun but spreads out into interplanetary space. The fine-structure of the corona found by radio-astronomy observations by RYLE and collaborators[28], and the "dark prominences" studied by ÖHMAN[29], give further indication of strong local disturbances, which probably are connected with electromagnetic effects.
4. Magnetic storms and aurorae are caused by disturbances originating from the sun and transmitted through the interplanetary space. The irregular and rapidly varying character of these phenomena may be a reflection of the electromagnetic state in interplanetary space.

In the following we shall at first discuss the large-scale variations of the interplanetary field which to a considerable part is produced by the storm-producing beams. The local disturbances of the field which are due to the turbulence will later be found to produce a diffusion of Cosmic Rays which is of essential importance for the generating mechanism we are going to study.

6. Changes in the interplanetary magnetic field

A storm-producing beam carries magnetic flux with it. The flux $\frac{d\varphi}{dt}$ transported per unit time across the earth's orbit by a beam is

$$\left(\frac{d\varphi}{dt}\right)_b = -H_b b v_b = -cV_b \qquad (6.1)$$

where the negative sign means that flux is transported outwards. With $V_b = 10^8$ volt $= \frac{1}{3} \cdot 10^6$ esu we obtain $d\varphi/dt = 10^{16}$ gauss cm^2 sec^{-1} and $V_b = 10^9$ volt gives $d\varphi/dt = 10^{17}$ gauss cm^2 sec^{-1}.

Table 1. Properties of storm-producing beam near the Earth

$\frac{\Delta I}{I}$	V_b (volt)	E volt/cm	H gauss	$\frac{d\varphi}{dt}$ gauss cm^2 / sec
1 %	10^8	$1.4 \cdot 10^{-5}$	$0.7 \cdot 10^{-5}$	10^{16}
10 %	10^9	$1.4 \cdot 10^{-4}$	$0.7 \cdot 10^{-4}$	10^{17}

$b = 0.7 \cdot 10^{13}$ cm $\quad v_b = 0.0067$ c

From the intensity drop ΔI of cosmic radiation the voltage V_b over the beam can be calculated. This gives the field E and H in the beam and the flux transport $d\varphi/dt$

If we consider the general magnetic field of the sun as produced by a homogeneously magnetized body with a polar field of say $H_p = 10$ gauss★, its total flux is $\varphi = \pi R_\odot^2 H_p = 1.5 \cdot 10^{23}$ gauss cm^2. Hence, a beam with $V = 10^8$ volt would be able to empty the whole flux in $1.5 \cdot 10^{23}/10^{16} = 1.5 \cdot 10^7$ sec, which is only half a year, and a beam with $V = 10^9$ volt would produce the same effect in less than one month. The latter case is certainly exceptional, but beams with $V = 10^8$ volt (corresponding to changes in cosmic ray intensity of about 1 %) are quite normal. Several beams may be sent out in different directions at the same time.

From this follows:

1. The storm-producing beams cause a drastic redistribution of the magnetic field in the sun's environment.
2. Magnetic flux must be transported inwards, back towards the sun, in some way.

This conclusion seems inevitable because the storm decrease of cosmic rays can only be accounted for by the existence of an electric field in space and such an electric field means necessarily a change in the magnetic flux.

If the beam is ejected during a very long time so that a stationary state is reached, the back flow of flux will take place outside the beam. A simple model of this is the following (Fig. 3). There is only one beam and this is supposed to be radial; the effect of the solar rotation is neglected. Outside the beam there is a radial flow with velocity v_a in towards the sun; as earlier we consider the conditions

★ This is not in conflict with the Zeeman-effect measurements. Compare H. ALFVÉN, Arkiv f. Fysik 4, Nr 24, 1952.

near the equatorial plane. The magnetic field at the distance R is $H_a(R)$. The electric field is

$$E_a = \frac{v_a}{c} H_a \tag{6.2}$$

The voltage over the backflow is

$$V_a = (2\pi R - b) E_a \tag{6.3}$$

and the flux transport

$$\left(\frac{d\varphi}{dt}\right)_a = H_a (2\pi R - b) v_a = c V_a \tag{6.4}$$

If the same flux is transported inwards as outwards we have

$$\left(\frac{d\varphi}{dt}\right)_a + \left(\frac{d\varphi}{dt}\right)_b = 0 \tag{6.5}$$

and

$$V_a = V_b \tag{6.6}$$

The magnetic field derives in part from the sun, in part from currents at the borders of the beam, and – in case the fields H_a and H_b do not decrease as R^{-3} – in part from currents perpendicular to R.

If at a certain time the interplanetary field derives only from the sun, so that it is a dipole field, and the beam is switched on, it takes some time before this stationary state is reached. During this time we have

$$V_a < V_b \tag{6.7}$$

As a measure of the time which is needed to reach a stationary state we could take the transit time of magneto-hydrodynamic waves. This should be of the order $\tau = R/V = RH^{-1}(4\pi\varrho)^{1/2}$ where R is the distance, V the magneto-hydrodynamic velocity, and ϱ the mass density. As we are especially interested to study the flux transport across the earth's orbit, we put $R \sim 10^{13}$ cm and $H \sim 10^{-5}$ gauss which is a reasonable value for the field near the earth's orbit (BRUNBERG and DATTNER)[25]. The density in the outer corona is 10^{-19} g cm^{-3} and in interstellar space 10^{-24} g cm^{-3}. Hence, it is reasonable to use an intermediate value for ϱ, say $\varrho = 10^{-21}$ g cm^{-3}. This gives $\tau = 10^8$ sec $=$ $=3$ years, a value which obviously could be in error by a factor of 10. Near the sun the stationary state is reached much quicker.

When the beam is switched off it takes a time of the same order before the magnetic field has reached equilibrium, which with no beam on, would be a dipole field. (It is doubtful whether this state is ever reached.) During this resetting time we have

$$V_a > V_b$$

It should be observed that the model of stationary flow can be valid only within certain limits. Inwards it can extend only to a radius $R_{\min} > R_\odot$, because near the sun we must have a tangential flow. There must also be an outer limit $R_{\max}$ outside which stationary conditions have not been reached. Further, the model is applicable only at a certain distance from the equatorial plane. We assume that it holds approximately up to a latitude angle φ. This means that our model is limited by a double cone with the angle $\frac{\pi}{2} - \varphi$ around the solar axis.

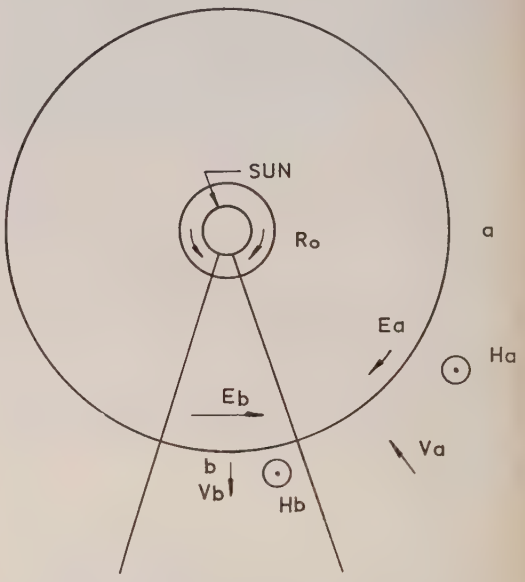

Fig. 3. Simplified model of storm-producing beam, (Equatorial plane). Within the beam with breadth b there is a rapid outflow with velocity v_b which produces an electric field E_b. Outside the beam there is a slow inflow with the velocity v_a, producing the field E_a.

The stationary model is not exactly the same as used by Brunberg and Dattner for computing the storm effect. Their model represents the non-stationary conditions immediately after switching on the beam, be-

cause they assume $E_a = 0$. As the influence of E_a on most of the particle orbits they consider is small, their results remain qualitatively the same.

7. Acceleration

In order to explain the generation of cosmic radiation many different acceleration mechanisms, have been proposed. It is reasonable that cosmic radiation is a result of some very general magneto-hydrodynamic phenomena in space which transfers energy from kinetic or magnetic energy into cosmic ray energy. We shall here study a general type of acceleration of particles in a changing magnetic field.

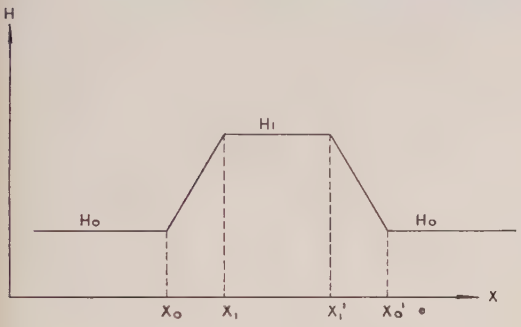

Fig. 4. Accelerator model. A compressible gas with high conductivity flows in the x-direction. Due to change in the flow velocity the magnetic field changes from H_0 to H_1 and back again to H_0.

Besides this effect which may be called a *betatron effect*, it is also necessary to consider the *diffusion* of particles between regions of different magnetic field strength. These two processes, both of a very general character, are the only ones we need to discuss. We shall study them with a model still simpler than that of § 6, and later apply the results to the conditions in interplanetary space.

Let us assume that we have a flow of ionized gas in the x-direction with a variable velocity v. The conductivity of the gas is infinite and there is a frozen-in magnetic field H parallel to the z-axis. The gas has an infinite extension in the y-direction. In the z-direction it is confined between two perfectly reflecting plane surfaces. The velocity v of the gas decreases slowly from an initial high value v_0, to a low value v_1 and increases again to the first value v_0. As the density δ of the gas varies as

$$\delta = \delta_0 v_0 / v \tag{7.1}$$

and as the magnetic field is proportional to δ we have

$$H = H_0 v_0 / v \tag{7.2}$$

The variation in H is shown in fig. 4. The subscript $_0$ denotes the values to the left of x_0.

We assume that the gas contains high energy charged particles which do not interact with the molecules of the gas. Due to the magnetic field the particles move in trochoidal orbits. Suppose that their momentum p has the component $p_\perp$ in the x—y plane.

From the equations of motion we obtain[31]

$$2\frac{dp_\perp}{p_\perp} = \frac{dH}{H} \tag{7.3}$$

which gives

$$\frac{p_\perp^2}{H} = \text{const.} \tag{7.4}$$

Suppose that the initial velocity v_0 of the particle is small compared to c. If the velocity vector has a random direction we have in average

$$\left.\begin{aligned} v_0^\perp &= \sqrt{\frac{2}{3}}\, v_0 \\ v_0^{\parallel} &= \sqrt{\frac{1}{3}}\, v_0 \end{aligned}\right\} \tag{7.5}$$

When the field increases from H_0 to H_1 we have

$$\left.\begin{aligned} p_1^\perp &= \sqrt{\frac{2}{3}}\, m_0 v_0 \left(\frac{H_1}{H_0}\right)^{1/2} \\ p_1^{\parallel} &= \sqrt{\frac{1}{3}}\, m_0 v_0 \end{aligned}\right\} \tag{7.6}$$

If we consider large values of H_1/H_0 we have $p_1^{\parallel} \ll p_1^\perp$, and $p_1 \approx p_1^\perp$. As the kinetic energy W is $W = m_0 c^2 \left\{\sqrt{1 + \frac{p^2}{m_0^2 c^4}} - 1\right\}$ we have

$$W = m_0 c^2 \left\{\sqrt{1 + \frac{2}{3}\left(\frac{v_0}{c}\right)^2 \frac{H_1}{H_0}} - 1\right\} \tag{7.7}$$

Seen from a coordinate system which takes part in the motion the increase in energy could be regarded as produced by the betatron action of the increasing magnetic field. Seen in a fixed coordinate system it can be considered as an effect of the electric field

$$\vec{E} = -\frac{1}{c}\vec{v} \times \vec{H} \tag{7.8}$$

which because of (7.2) is a constant field in the y-direction. As long as the magnetic field H is constant, the particles drift parallel to the x-axis, in a trochoidal orbit due to the combined action of the electric and magnetic field (Fig. 5). The drift velocity $v = cE/H$ equals the flow velocity. As soon as $\frac{dH}{dx} \neq 0$ a drift component parallel to the y-axis is produced. This drift is parallel to the electric field, which means that the energy of the particle changes. It is easily shown that this change in momentum is the same as obtained by considering the betatron effect.

In the double star theory[16] and in the first papers on the present theory[18] the acceleration was presented in the latter way.

The result of this process is that when the particles move from H_0 to H_1, their momentum increases, but when they continue from H_1 to H_0', their momentum goes down again to the initial value. No net momentum gain is obtained.

8. Disturbed magnetic field

So far we have considered the ideal case when the magnetic field is mathematically perfect. In order to approach the real case this assumption is the first one we must drop, because due to the long time the particles spend in the field, even small inhomogeneities are of importance. In order to account for the effect of inhomogeneities of the magnetic field in a simple way, let us assume that a charged particle at intervals τ_i passes a region of disturbed field. The passage does not change the absolute value of the momentum vector, but it changes its direction. The disturbance of the momentum vector could be described as

(1) a change in the angle with the z-axis, and

(2) a change of the angle between the x-axis and the projection of the vector on the x—y plane. The former effect means a *redistribution* of the momentum between $p^{\perp}$ and $p^{\parallel}$. We account for this in a simplified way by assuming that after the disturbance we have $p_{\perp}^2 = \frac{2}{3}p^2$; $p_{\parallel}^2 = \frac{1}{3}p^2$.

The second effect means that in the x—y-plane the centre of curvature is displaced. We account for this by assuming that each disturbance displaces the centre of curvature a distance ϱ in a random direction. The result is a *diffusion*.

In order to discuss the effect of the redistribution let τ_0 be the time it takes for the gas to move from x_0 to x_1, τ_1 the time from x_1 to x_1', and τ_0' the time from x_1' to x_0'. Let us first suppose that

(a) $\tau_1 \gg \tau_i \gg \tau_0$ and τ_0'. The particle will gain momentum according to (7.4) between

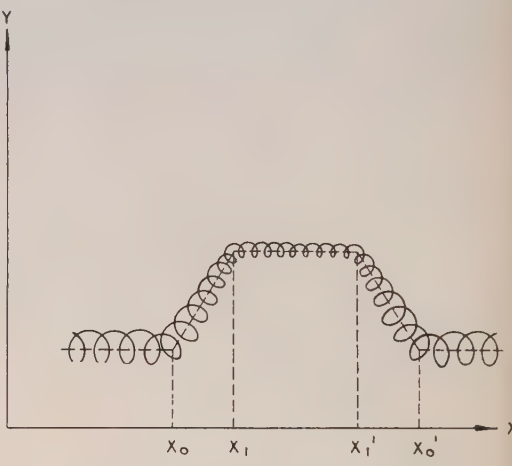

Fig. 5. Path of a high energy charged particle in a flow according to Fig. 5.

x_0 and x_1. Between x_1 and x_1' the gain in $p_{\perp}$ will be equally distributed over the three degrees of freedom, so that part of it is transferred to $p_{\parallel}$. When the particle moves from x_1' it losses momentum again, but this refers only to $p_{\perp}$. Hence the momentum stored as $p_{\parallel}$ is not lost and the result of the whole process is a net gain. – If instead

(b) τ_0 and $\tau_0' \gg \tau_i$, the gain of momentum will be "adiabatic". Of the gain in momentum a part will constantly be transferred to $p_{\parallel}$, so that in average we have

$$\left.\begin{aligned} p_{\perp}^2 &= \frac{2}{3}p^2 \\ p_{\parallel}^2 &= \frac{1}{3}p^2 \end{aligned}\right\} \quad (8.1)$$

This gives from (7.3)

$$3\frac{dp}{p} = \frac{dH}{H} \quad (8.2)$$

or

$$\frac{p^3}{H} = \text{const} \tag{8.3}$$

Instead of (7.6) we have

$$p_1 = m_0 v_0 \left(\frac{H_1}{H_0}\right)^3 \tag{8.4}$$

and

$$W = m_0 c^2 \left\{ \sqrt{1 + \left(\frac{v_0}{c}\right)^2 \left(\frac{H_1}{H_0}\right)^{2/3}} - 1 \right\} \tag{8.5}$$

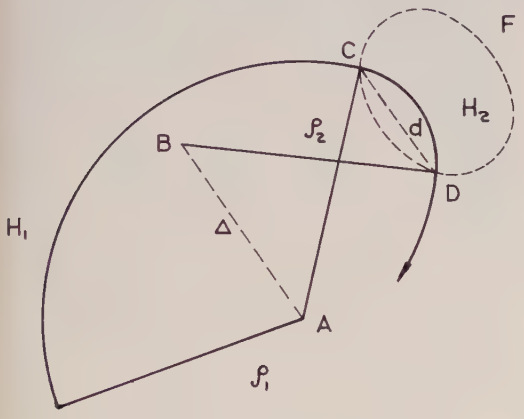

Fig. 6. Diffusion caused by field disturbance.

(c) If either τ_0 or τ_0' is smaller than τ_i momentum is gained as in (a) but the gain is somewhat smaller.

The second effect mentioned above means simply a *diffusion* perpendicular to the magnetic field. Seen in a coordinate system which takes part in the flow, it is obvious that a diffusion can take place without change in momentum. In order to check this result we shall treat the problem also in a fixed coordinate system (Fig. 6). The magnetic field is H_2 everywhere except in a certain region CDF where it is $H_3 (> H_2)$. A particle moves in a circle with radius of curvature ϱ_2 with the centre located in A. At C it crosses the border to H_3. The radius of curvature changes to ϱ_3 and the centre is displaced to B. When the particle has reached D it leaves H_3 so that the radius of curvature is ϱ_2. The centre of the circle is now A'.

Denoting the distance AA' by Δ and CD by d we have

$$\frac{\Delta}{d} = \frac{\varrho_2 - \varrho_3}{\varrho_3} = \frac{H_3 - H_2}{H_2} \tag{8.6}$$

Inside H_3 there is an electric field

$$\vec{E}_3 = -\frac{1}{c}\vec{v} \times \vec{H}_3 \tag{8.7}$$

and outside the field is

$$\vec{E}_2 = -\frac{1}{c}\vec{v} \times \vec{H}_2 \tag{8.8}$$

The field is non-potential. The result of the disturbance is that the trochoidal orbit of the particle is displaced in the x-direction and in the y-direction. The displacement in the x-direction which is perpendicular to the electric field cannot produce any change in energy. The displacement in the y-direction changes the energy by

$$\Delta W = -e\left[\vec{E}_2\left(\vec{\Delta} + \vec{d}\right) - \vec{E}_3\vec{d}\right] \tag{8.9}$$

which because of (8.6), (8.7), and (8.8) gives

$$\Delta W = 0 \tag{8.10}$$

It should be observed that according to (8.6) the displacement of the centre of curvature is independent of the energy of the particle. Hence particles with different energies passing the same distance d in a disturbed region, will have their orbits displaced the same distance. However, as $d \leq 2\varrho$, the distance d can be larger for particles with high energy, which means that high energy particles diffuse more easily.

Without diffusion the density of the particles would be proportional to v^{-1} or to H. Hence the density in H_1 would be much higher than in H_0. The diffusion tends to equalize the densities, so that in general the particles are displaced from H_1 to H_0 and to H_0'.

If the velocity of diffusion in the *x-direction* is larger than the flow velocity v a high energy particle in H_1 can leave this region and move to H_0 without loss of energy. If the diffusion velocity is smaller than v, particles will not be able to move from H_1 to H_0, but they will stay longer in the region x_0x_1 and hence gain more energy. Further, they will pass x_1x_0' more rapidly and hence lose less energy. If the diffusion velocity is of the same order as the flow velocity particles

may stay a prolonged time in the region x_0x_1 and gain much energy.

At the same time low energy particles from H_0 and H_0' will eventually diffuse in H_1. If they later are transported out to H_0' the net result will be a loss of energy. As the diffusion of low energy particles is slower than of high energy particles, this effect will in general not be very important.

If to left of x_0 we feed in particles with energy W_0, some of these particles will follow the flow and be accelerated up to W_1 and then diffuse back to x_0. Other particles will not reach the full energy before they diffuse back. The result is that near x_0 we will find particles with all energies between W_0 and W_1. There will also be particles with still higher energies which have drifted to the right and diffused back several times.

9. Application to interplanetary field

We shall now apply the results from the simple accelerator model of §§ 7—8 to the conditions in interplanetary space. We start with the stationary flow discussed in § 6, and confine the discussion to motions near the equatorial plane. (Fig. 7.) A particle at a where the magnetic field is rather weak will follow the flow inwards to a stronger field. This corresponds to the motion from x_0 to x_1 in the accelerator model. Later it may enter the beam, by crossing the border between the beam and the surrounding region. Then it will follow the beam outwards again, a process corresponding to the motion from x_0' to x_1' in the accelerator model. The distance corresponding to x_1x_1' is small.

In the same way as in the model the increase in energy can be depicted either as due to the betatron action of the increasing magnetic field, or to the trochoidal motion in the combined electric and magnetic field. The latter treatment makes it easy to construct the path, if we know H and E_a. As the flow is stationary we have a potential field and find

$$W = W_0 + e(V - V_0)$$

where W is the energy of the particle and V the potential at an arbitrary point, W_0 and V_0 denoting the same quantities for the starting point. Combined with (6.4) or (7.2) or this gives us the trochoidal path of the particle.

Fig. 7 shows the orbit if the particle is confined to the equatorial plane. The path is a result of the drift due to the inhomogeneous magnetic field which tends to make the particle drift around the sun at constant distance, and the drift due to the electric field, which tends to make the particle drift radially towards the sun.

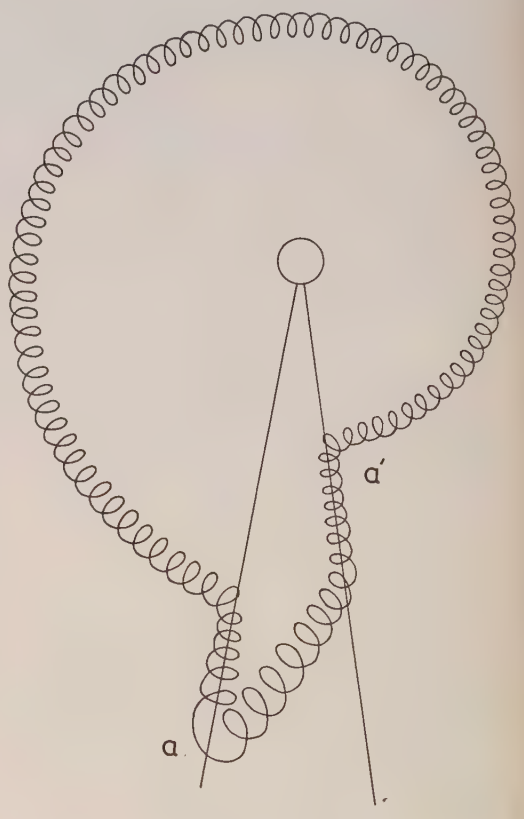

Fig. 7. Path of a high energy particle in the model of Fig. 4. Stationary state $V_a = V_b$.

The energy which a particle can reach in the stationary model of § 6 is limited in two different ways. As we have a potential field the maximum energy gain is given by the maximum potential difference which is V_a. If a particle starts at a with an energy W_a it gains energy and approaches the sun until at a' it has reached the energy $W_a' = W_a + eV_a$. It enters the beam and is carried out again, losing energy. If both processes are either adiabatic or non-adiabatic no energy is gained and the particle returns to its starting point and may continue to move in the same orbit.

If the conditions are non-stationary the particle does not come back to the same point after one turn. If $V_a < V_b$ which is the case if the beam has just been switched on or is increasing in intensity, the particle will lose $e(V_b - V_a)$ for every turn. On the other hand, if $V_a > V_b$ characterizing the conditions when the beam just has been switched off or is decreasing in intensity, the energy of the particle will continue to increase. In this case the whole solar field is resetting, and the particles are carried inwards with the general flow.

Both in the stationary case and non-stationary case an upper limit to the gain of energy is set by the ratio of the magnetic field at the starting point H_0 and the strongest field H_1 the particle reaches. The particle may start far away from the sun in a region where the field may be 10^{-5} gauss or 10^{-6} gauss. When it comes very close to the sun the field may be as high as 1 gauss or even 10 gauss. Hence the field ratio may be as high as $H_1/H_0 = 10^6$. In many cases it may only be brought to the region of the outer corona where $H = 10^{-1}$ or 10^{-2} gauss, giving $H_1/H_0 = 10^4$.

In order to reach very high energies the particles should start the process in a low magnetic field with as high initial energy as possible. Hence, we should look for particles with reasonably high velocities far out from the sun. Without introducing any new assumption we expect to find particles with velocities of the same order as the beam velocity ($v_b = 2 \cdot 10^8$ cm). There are probably regions near the border between the beam and the interplanetary matter at rest, where the relative motion produces an injection of particles. In this way beam particles with the velocity v_b are shot into the surrounding regions, and particles from these regions are injected into the beam with a relative velocity v_b.

In the beam electrons and ions move with the same velocity, so the different particles are injected with the same initial velocity v_i. We put $v_i = v_b = 0.0067\,c$ and use this for the calculation of the maximum energy with different values of H_1/H_0. Depending upon whether we assume the process to obey (8.5) ("adiabatic") or (7.7) ("non-adiabatic") we obtain:

Table 2

$\frac{H_1}{H_0}$	Acceleration according to (7.7)	Acceleration according to (8.5)
10^4	$W = 0.14\ m_0c^2$	$W = 0.010\ m_0c^2$
	Electrons 0.00007 GeV	0.000005 GeV
	Protons 0.13 »	0.009 »
	O nuclei 2.1 »	0.15 »
10^6	$W = 4.5\ m_0c^2$	$W = 0.20\ m_0c^2$
	Electrons 0.0023 GeV	0.00010 GeV
	Protons 4.2 »	0.19 »
	O nuclei 67 »	3.1 »

The energy values shown are obtained if the particles start at H_0 and are carried with the flow to H_1. After the acceleration the particles may diffuse out without loss of energy and eventually start gaining energy again. The absolute value, which in some cases is in the lower energy range of the Cosmic Radiation, is not very interesting, because by multiple processes much higher values can be reached as we shall see later. The relative values for electrons, protons, and heavy nuclei are very important, because they demonstrate that the process we consider, *favours heavy nuclei and strongly discriminates against electrons*. This is only in part due to the assumption that the injection takes place with constant velocity. Even if the particles were injected with the same kinetic energy there would be a similar effect although less pronounced. This is a consequence of the fact that the acceleration is more effective in the non-relativistic then in the relativistic energy range.

It is of interest to observe that the charge of the particles does not enter explicitly into the formulae for the energy. The energy per nucleon is constant. Even charged dust grains should be accelerated, provided the magnetic field is strong enough to keep them trapped.

10. The injection problem

In FERMI's theory[7] the injection constitutes a serious difficulty. In the low energy range protons and especially heavy nuclei pick up energy so slowly that their energy loss in interstellar matter is not covered. We shall investigate the same problem for our case.

The whole acceleration is supposed to take place in a time which is of the order of a month or a year, say 10^7 sec. This means that

the magnetic field doubles its value in about 10^6 sec. During this time a particle moving with $v = 2 \cdot 10^8$ cm/sec has a path of $2 \cdot 10^{14}$ cm. The mass density in interplanetary space may be estimated to 10^{-21} g cm^{-3}. This means that when the particle doubles its energy due to electromagnetic acceleration, it passes $2 \cdot 10^{-7}$ g cm^{-2} of matter. An oxygen nucleus with $v = 0.0067\, c$ can pass 10^{-4} g cm^{-2} before it is absorbed. Hence, the particle certainly gains much more energy than it loses.

Due to the swift acceleration there is no injection difficulty in our case.

The presence of heavy nuclei in Cosmic Radiation is a strong argument in favor of a swift acceleration process. As a process can be expected to be swift only near the stars, it favours the local hypothesis.

11. Multiple processes

The processes we have discussed will accelerate particles up to high energies. In the case of a stationary model the energy gain is limited by V_a, which is of the order 10^8—10^9 volt according to Table 1. In the non-stationary state with $V_a > V_b$ there is no limitation of this kind. In both cases the values given in Table 2 set an upper limit. As summary it may be stated that particles injected by the beam be accelerated up to energies of the order 10^8—10^9 volt in one process of the indicated kind. If the solar magnetic field were undisturbed the accelerated particles would be completely trapped and particles with these energies could be found only close to the sun. Small local disturbances permit a diffusion, but due to the small radius of curvature, this will be rather slow. Only violent disturbances of the solar field will allow them to diffuse out, say to the earth or still further out. For example, a storm-producing beam will disturb the field in its neighbourhood so that there are lines of force running from regions with strong field near the sun far out to regions with low field. (See Fig. 2.) Particles which normally are trapped in a strong field near the sun will be able to move along such lines out to regions with low field without losing energy. (Besides this effect there will also be particles trapped in the beam and transported out, but as within the beam the magnetic field is decreasing with time, the particles will lose energy.) Of course, some particles will also move inwards in a disturbed region, but as in the flow model the density increases with the magnetic field this effect will not be so important.

In this way particles, which have followed the flow inwards and gained energy in the increasing magnetic field, will be able to move out some distance without losing the energy they have gained.

Much higher energies can be reached by such multiple processes. If by a disturbance of this kind particles accelerated to 10^8 or 10^9 e volt are injected in a low magnetic field H_0' and follow the flow to a field H_1', they will be accelerated again. The process may be repeated if they are taken from the field H_1' and without loss of energy are injected in a field H_0'', which later increases to H_1''. The energy gained by this triple process can be calculated from (7.7) or (8.5) if H_1/H_0 is substituted by

$$\frac{H_1}{H_0}, \frac{H_1'}{H_0'}, \frac{H_1''}{H_0''}$$

The energy which can be reached in this way is only limited by the condition that the magnetic field must be able to keep the particle in a trapped orbit. Compare § 17.

If the acceleration takes place during a time when $V_a < V_b$ so that the dominating motion is directed outwards, the acceleration outside the beam is less efficient than the deceleration in the beam, and the chance of a multiple acceleration up to high energies is small. If $V_a > V_b$, the motion inwards dominates. Particles which have been accelerated and been brought outwards by a disturbance will be taken inwards again by the flow. Multiple accelerations are quite normal processes. In the stationary case $V_a = V_b$ the acceleration will in general dominate as we shall see in 12. Also in this case, multiple processes are probable.

As long as ϱ is small the particle cannot leave the acceleration process unless it is captured within the beam. If it is brought out to a weaker field by a disturbance in the field, it will be brought inwards again by the flow. This condition is changed when the energy of a particle, by one process or iterated processes, has increased so much that ϱ becomes comparable to R. Then it is no longer compelled to follow the inward flow to the same

degree as earlier, because its diffusion velocity increases. Hence, it can move outwards not only due to very large disturbances. Even more "normal" disturbances of the solar field will make it possible for it to diffuse outwards. In this way a considerable emission of high energy particles takes place. The condition $\varrho \sim R$ is satisfied, for example, if $\varrho \approx R = 10^{13}$ cm and $H = 10^{-5}$, when $V = 3 \cdot 10^{10}$ e volt. Already when ϱ is sometimes smaller than R, the diffusion is considerable, so that the cosmic ray generator emits particles well below the mentioned energy.

It is of interest to estimate the order of magnitude of the low energy limit for particles emitted by the cosmic ray accelerator. Let us suppose that a particle moving with the velocity u at the solar distance R encounters a disturbed region after having travelled a distance γR, where γ is a constant. Hence, the time τ_c between two disturbances is

$$\tau_c = \gamma R/u \tag{11.1}$$

Each disturbance displaces the orbit a distance ϱ in an arbitrary direction. In order to escape from the generator the path must be displaced a distance of the order R which requires $(R/\varrho)^2$ disturbances. The momentum p is

$$p = \frac{eZ}{c} H\varrho \tag{11.2}$$

Hence, the time τ_d needed to diffuse out is

$$\tau_d = \left(\frac{R}{\varrho}\right)^2 \tau_c = \frac{\gamma e^2 Z^2 R^3 H^2}{c^2 u p^2} \tag{11.3}$$

If during this time the inwards flow which has the velocity

$$v_a = c\,\frac{V_a}{\alpha R H} \tag{11.4}$$

(where α is the angle of the inflew) has carried the particle inwards a comparable distance the particle cannot escape. Hence if we put

$$v_a \tau_d = R \tag{11.5}$$

we obtain an approximate limit to the momentum of the particles which can escape. From (11.3) we obtain

$$\frac{cV_a}{\alpha R H}\,\frac{\gamma e^2 Z^2 R^3 H^2}{c^2 u p^2} = R \tag{11.6}$$

or

$$p = \frac{Ze}{c}\left[\gamma \frac{HRV_a c}{\alpha u}\right]^{1/2} \tag{11.7}$$

Putting $\alpha \approx 2\pi$; $u = c$; $V_b = 3 \cdot 10^8$ volt $= 10^6$ e.s.u.; $H = 10^{-5}$ gauss, $R = 10^{13}$ cm referring to the conditions near the earth's orbit, we obtain

$$\frac{cp}{Ze} = 0.4 \cdot 10^7 \sqrt{\gamma} \tag{11.8}$$

or

$$p = 1.2 \cdot 10^9 \sqrt{\gamma}\ \text{e volt}\ Z/c \tag{11.9}$$

We do not know γ. In order to make $p = 0.5 \cdot 10^9$ e volt, which is the empirical value for the low energy cut-off, we should have $\gamma = 0.2$. This means that the path of a particle is likely to be disturbed considerably after a travel over a distance 0.2 R. This seems to be acceptable. The radius of curvature is $\varrho = 2 \cdot 10^{11}$ cm $= 0.02\ R$.

12. Production of cosmic ray energy

Consider the flow studied in § 6. We treat the conditions in the equatorial plane and assume that these are valid up to a latitude angle φ. A beam with an angular breadth $\beta = \frac{b}{R}$ is emitted with a velocity

$$v_b = c\,\frac{V_b}{\beta R H_b} \tag{12.1}$$

We assume that V_b and β are constant and that

$$H_b = H_b^{\odot}(R_{\odot}/R)^{n_b} \tag{12.2}$$

$H_b^{\odot}$ is the field at the earth's orbit $R_{\odot}$ and n_b is a constant. This gives

$$v_b = \frac{cV_b}{\beta H_b^{\odot} R_{\odot}^{n_b}}\, R^{n_b - 1} \tag{12.3}$$

Outside the beam there is an inflow with the breadth $\alpha R = 2\pi R - b$. In this region H obeys the formula

$$H_a = H_a^{\odot}\,(R_{\odot}/R)^{n_a} \tag{12.4}$$

and

$$v_a = \frac{cV_a}{\alpha H_a^{\odot} R_{\odot}^{n_a}}\, R^{n_a - 1} \tag{12.5}$$

If a particle with energy W moves in a changing magnetic field its energy increases so that

$$\frac{dW}{Wdt} = A\,\frac{dH}{Hdt} \tag{12.6}$$

where A is a factor which depends on the energy.

According to (7.7) and (8.5) we have $1/3 < A < 1$. In the following approximate calculations we shall put $A = 1/2$. If the total cosmic ray energy per unit volume is w we have

$$\frac{dw}{wdt} = \frac{1}{2}\frac{dH}{Hdt} = \frac{v}{2H}\frac{dH}{dR} \tag{12.7}$$

For the beam this gives

$$\left(\frac{dw}{dt}\right)_b = -\frac{w}{2}\frac{n_b}{R}\frac{cV_b R^{n_b-1}}{\beta H_\delta^{n_b} R_\delta^{n_b}} \tag{12.8}$$

and a similar expression outside the beam. From this we can calculate the total energy production P within the distance R_δ from the sun. We obtain

$$P = \int_{R_0}^{R_\delta}\left(\frac{dw}{dt}\right)_a \cdot 2\varphi R^2 \alpha dR - \int_{R_0}^{R_\delta}\left(\frac{dw}{dt}\right)_b 2\varphi R^2 \beta dR \tag{12.9}$$

or

$$P = c\varphi\left[\frac{V_a n_a}{H_a^{n_a} R_\delta^{n_a}}\int_{R_0}^{R_\delta} wR^{n_a} dR - \frac{V_b n_b}{H_b^{n_b} R_\delta^{n_b}}\int_{R_0}^{R_\delta} wR^{n_b} dR\right] \tag{12.10}$$

R_0 is the inner limit of the acceleration process. As $R_0 \ll R_\delta$ this is not important. In order to obtain the whole increase in energy inside R_δ we shall add the transport $\frac{dU'}{dt}$ of particles through the surface R_δ.

$$\frac{dU'}{dt} = 4\pi\varphi R_\delta^2\left[\alpha(wv)_a - \beta(wv)_b\right] \tag{12.11}$$

It is assumed that no energy is transported through the limiting cones. In stationary state the energy increase must be compensated by an energy outflow

$$\frac{dU''}{dt} = \frac{dU'}{dt} + P \tag{12.12}$$

This is effected by outward diffusion of cosmic ray particles. The net outflow of cosmic ray energy through R_δ is $\frac{dU''}{dt} - \frac{dU'}{dt} = P$

As the storing capacity of the volume inside R_δ is negligible in this connection, a unit surface perpendicular to R_δ near the earth's orbit is hit by the same number of particles from outside as from inside. The particles coming from the inside, have been accelerated by the process we have considered and hence have higher energy than those coming from the outside. In this way the produced energy P is emitted. If the energy density outside R_δ is w, the energy flux from outside through the unit surface is wc and through the whole surface we consider

$$\frac{dU_0}{dt} = 4\pi R_\delta^2 \varphi wc \tag{12.13}$$

In a similar way the outflow is

$$\frac{dU_1}{dt} = 4\pi R_\delta^2 \varphi w_1 c \tag{12.14}$$

where w_1 is the average energy density inside R_δ. As

$$\frac{dU_1}{dt} = \frac{dU_0}{dt} + P \tag{12.15}$$

we find from (13), (14), and (15)

$$w_1 - w = \frac{1}{4\pi R_\delta^2 \varphi c}\cdot P$$

13. Diurnal variation

If a measuring instrument shows the intensity I when receiving radiation with average energy w, it gives the reading $I + \Delta I$ for w_1. If we put

$$\Delta I = k' I \Delta w / w \tag{13.1}$$

with $\Delta w = w_1 - w$, the constant k' is as in § 4 between 1 and 10, and probably about 3.

An instrument which rotates with the earth will show a diurnal variation with amplitude D_R and a maximum at 12^h, given by

$$2D_R = \frac{\Delta I}{I} \tag{13.2}$$

Hence we have

$$D_R = \frac{k'}{8\pi R_\delta^2 \varphi c}\cdot\frac{P}{w} \tag{13.3}$$

In order to calculate the diurnal variation it remains only to estimate how w waries. In the energy range of most of the cosmic rays, the radius of curvature ϱ is rather large so that the diffusion is relatively rapid. This means that w cannot vary very much. Even if it increases somewhat when we approach the sun, it is probably legitimate to put it

approximately constant. This gives from (12.10)

$$P=c\varphi wR_{\delta}\left[\frac{n_a}{n_a+1}\frac{V_a}{H_a^{\delta}}-\frac{n_b}{n_b+1}\frac{V_b}{H_b^{\delta}}\right] \quad (13.4)$$

and

$$D_R=\frac{k'}{8\pi R_{\delta}}\left[\frac{n_a}{n_a+1}\frac{V_a}{H_a^{\delta}}-\frac{n_b}{n_b+1}\frac{V_b}{H_b^{\delta}}\right] \quad (13.5)$$

In order to discuss this formula let us assume that there is no solar activity during a long time, so that $V_a=V_b=0$. If then a beam is switched on, we have $V_b>0$ but V_a is still zero. Hence there is a deceleration of cosmic rays: P and D_R are negative and there is an inflow of radiation across the earth's orbit. Let us suppose that V_b remains constant. After some time — of the order of a year — V_a has increased to the same values as V_b and we have stationary conditions. With $V_a=V_b$ we have

$$D_R=\frac{k'V_b}{8\pi R_{\delta}}\left[\frac{n_a}{n_a+1}\frac{1}{H_a^{\delta}}-\frac{n_b}{n_b+1}\frac{1}{H_b}\right] \quad (13.6)$$

According to § 5 the value of n_b is about $n_b=1$. According to estimates by Brunberg and Dattner we may put $n_a=2.5$. This gives

$$D_R=\frac{k'V_b}{8\pi R_{\delta}}\left[\frac{0.7}{H_a^{\delta}}-\frac{0.5}{H_b^{\delta}}\right] \quad (13.7)$$

The magnetic fields are probably of the order $H_a=10^{-5}$ gauss and $H_b=3\cdot10^{-5}$ gauss. Further, we may put $V_b=3\cdot10^{8}$ volt, and $k'=3$. This gives

$$D_R=4\cdot10^{-4} \quad (13.8)$$

i.e. a 12^h component of the diurnal variation of 0.04 %.

If now the beam is switched off so that $V_b=0$ the last term disappears, so that D_R increases. The magnetic field resettles with an inward motion of magnetic flux. This means that both H_a and V_a decreases. Depending on which of them decreases most, the value of D_R may either go up or down.

It is of interest to note that in the stationary state $V_a=V_b$ there is still an energy production if $n_a/(n_a+1)\,H_a^{\delta}>n_b/(n_b+1)\,H_b^{\delta}$. This is not in conflict with the fact that a particle which drift around the sun a whole turn in a closed orbit does not increase its energy, because the drift velocity is smaller inside the beam. In order to have the same Cosmic Ray density outside and inside the beam there must be particles which do not enter the beam. Experimental evidence speaks rather for a lower density inside the beam.

14. Comparison with observations

The results we have obtained could be compared with observations of the diurnal variation and the variation of the total intensity.

THAMBYAHPILLAI and ELLIOT[2] have pointed out that the phase of the diurnal variation varies in a systematic way with the solar cycle. This variation has further been discussed by SARABHAI and KANE[3]. Using the results of their terrella experiment BRUNBERG and DATTNER[26] have shown that if reduced for the deflection in the terrestrial field the maximum of the diurnal variation occurs at 18^h or during some years a few hours earlier. Their interpretation is that the diurnal variation consists of a "*tangential*" component with a maximum at 18^h and a "*radial*" component with maximum at 12^h. The tangential component is due to an excess of particles coming in parallel to the earth's orbit, which possibly is an effect of the solar rotation in which most of the Cosmic Rays in our environment may take part. We are here more interested in the radial component D_R because it shows us how much cosmic ray energy is streaming out across the earth's orbit. This has been calculated theoretically in § 13 so a comparison between observations and theory is possible.

The variation of D_R with time can best be followed from the long-time registrations with ionization chambers by Forbush. Fig. 8 shows his results for Huancayo, Cheltenham, Christchurch, and Godhavn plotted in harmonic dials.

Before we use these values we must correct them for the deflection of cosmic rays in the terrestrial magnetic field. If we know the energy of the variable component, the time angle correction Ψ_E can be found from Brunberg and Dattner's curves. The energy is not known with certainty but could be expected to be between 20 and 40 GeV. Table 3 shows the corrections for the zenith direction. It is evident that we do not make a large error if we use 30° for Godhavn and 40° for Cheltenham and Christchurch. The value for Huancayo is uncertain.

Table 3

Station	Geom. Lat.	Correction Ψ_E for zenith			
		20 GeV	30 GeV	40 GeV	Adopted
Godhavn	79°.8	30°	31°	30°	30°
Cheltenham	50°.1	44°	40°	35°	40°
Christchurch	— 48°.0	42°	40°	35°	40°
Huancayo	— 0°.6	110°	64°	45°	90°

An ionization chamber measures rays from all directions although the atmospheric absorption makes it most sensitive to rays from zenith. BRUNBERG and DATTNER[26] have recently estimated the integrated effect and calculated the average value of Ψ_E. They find that at Godhavn the diurnal variation should be a complex phenomenon because rays from very different primary directions reach the ionization chamber. For Cheltenham and Christchurch they obtain values of Ψ_E which are about 5° higher than those adopted in Table 3.

This indicates that the corrections are most reliable for Cheltenham and Christchurch. For Huancayo the value is uncertain. As we shall see a good agreement between all those three stations is obtained if we adopt the correction 90° for Huancayo. This corresponds to an energy of 25 GeV for the zenith direction.

In each of the harmonic dials a line making the angle Ψ_E with the 18^h axis is drawn. The distance of the dots from this line gives the 12^h component D_R of the diurnal variation. The values of D_R obtained in this way are plotted in Fig. 10. The agreement between Cheltenham, Christchurch and Huancayo is good. The absolute values for Huancayo are uncertain. The variations in D_R at Godhavn are small and not very well correlated with the variations at the other stations, probably for the reasons given above. The average for Cheltenham, Christchurch and Huancayo is shown in Fig. 9. The position of the zero line is uncertain due to possible errors in Ψ_E. An error of 10° means a shift in the zero line of 0.025 %. Further, atmospheric effects may influence the diurnal variation.

The value of D_R reaches a maximum in 1944 when the sunspot cycle has a minimum, and a minimum in 1947, coinciding with the sunspot maximum. It increases to high values

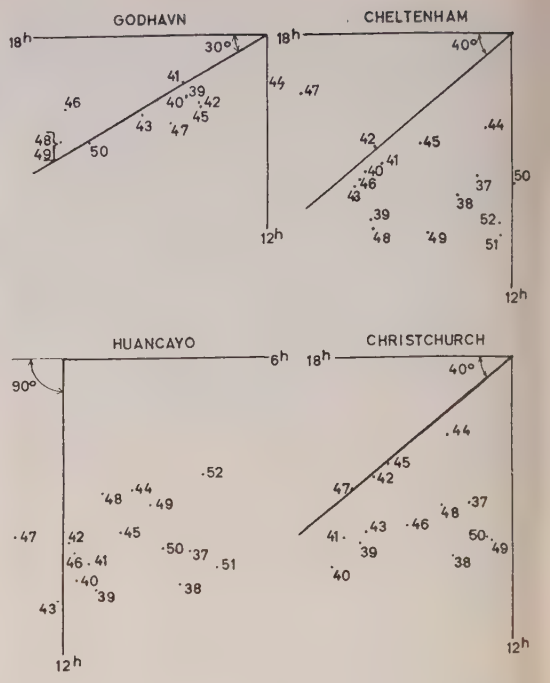

Fig. 8. Harmonic dials of diurnal variation in Godhavn, Cheltenham, Huancayo, and Christchurch. Yearly means 1938—1952. (FORBUSH.)

in 1952 when we approach next minimum. There is a sunspot maximum at 1938, but D_R does not go down to a low value until 1939, and it stays at this low value during some years.

The same variation can be traced in BRUNBERG and DATTNER's diagram of the phase angle.[26]

Thus the general tendency seems to be that an increased solar activity gives a decrease in D_R. This is in a qualitative agreement with the theoretical results of § 13.

From (13.7) a value of $D_R = 0.04$ % was estimated for the stationary state. This is well reconcilable with the average of the D_R curve in Fig. 9, but this agreement is not very convincing, because there is considerable uncertainty regarding the zero value. It is seen from (13.5) that the variations in D_R should be of a comparable order of magnitude. The observational values show a difference of 0.16 % between the highest value in 1952 and the lowest value in 1947. Taking into account the many uncertain factors the quantitative agreement is encouraging.

15. Variation of the total intensity

According to FORBUSH[28] the total intensity I of Cosmic Radiation varies with the solar cycle by as much as 4 %. The variation at Huancayo, Cheltenham, and Godhavn is shown in Fig. 9. (There is no reason to exclude Godhavn as in the case of the diurnal variation.) The variation seems to have a negative correlation with the sunspot curve. The amplitude has no systematic dependence on the latitude, so it is likely that it is not only the low-energy part of the spectrum which varies.

The observed variation is of decisive importance to the question about the trapping field. As obviously the intensity in the whole galaxy cannot change by 4 % in three years, the intensity variations must be confined to a relatively small volume around the solar system. Consequently we must assume that there is some sort of screening, most likely produced by a "trapping field". The intensity we measure characterizes the conditions inside the screen.

A more difficult question is how perfectly the trapping field screens. There are two alternatives:

1. There is so much leakage in the trapping field that averaged over a very long time, there can only be a small difference in intensity. This means that in average the intensity in e.g. the whole galaxy should be about the same as here. The consequence is that besides the local generation which we have considered here, there must also be a galactic generation, and further, we must assume a galactic trapping field, which prevents the radiation in the galaxy from leaking out into intergalactic space.

2. The leakage in the trapping field may be so small that a large difference in intensity can be established. This means that we are not concerned with the intensity outside the trapping field. This intensity may be very low. We need not assume any appreciable galactic generation, and it is not necessary to postulate a galactic trapping field.

Although at present there is no decisive argument in either direction, the latter alternative seems more attractive because we do not need so many *ad hoc* assumptions.

Variations in the total intensity are expected from the point of view of the theory of § 12. The efficiency of the generating mechanism varies with the solar activity as discussed in § 13. How this should affect the total intensity depends on what assumptions we make about the diffusion of Cosmic Rays through the trapping field and its storing capacity. The observational result is that the total intensity shows a negative correlation with the sunspot activity. This means that the intensity near the earth may be a direct measure of the efficiency of the energy production, and should vary according to (13.4).

Forbush's curves of I are somewhat similar to the curves of D_R. Especially the rapid rise from 1944 to 1947 is the same. The similarity during the first years of the registrations is less convincing.

16. Total energy production

The total energy produced within the earth's orbit can be found from (13.3):

$$P = \frac{8\pi}{k'} R_\odot^2 \varphi c w D_R \qquad (15.1)$$

using essentially only empirical data. We put $\varphi = 1$ and $k' = 3$. As an average for D_R we may put $D_R = 4 \cdot 10^{-4}$. This gives

$$P = 2 \cdot 10^{34}\, w$$

With $w = 10^{-12}$ erg cm^{-3} we find $P = 2 \cdot 10^{22}$ erg sec^{-1}.

It is of interest to compare this with the kinetic energy of the beam. If near the earth its cross-section is $S = 10^{25}$ cm^2 and the density is ϱ g cm^{-3}, the outward transport of energy is

$$\frac{dU_b}{dt} = S \frac{\varrho v_b^3}{2} = 4 \cdot 10^{49} \varrho$$

Hence even if the density were as low as $\varrho = 10^{-24}$ g cm^{-3} corresponding to 1 particle/cm^3 the beam energy would be 2,000 times as large as the cosmic ray production. If the half-life of cosmic rays in interstellar space is say $T = 10^6$ years $= 0.3 \cdot 10^{14}$ sec, this energy production is enough to fill a volume of the order

$$\Phi = \frac{T}{w} P = 10^{48} \text{ cm}^3$$

which has a diameter of 10^{16} cm. The beam has probably only dissipated a small fraction of its energy inside the earth's orbit.

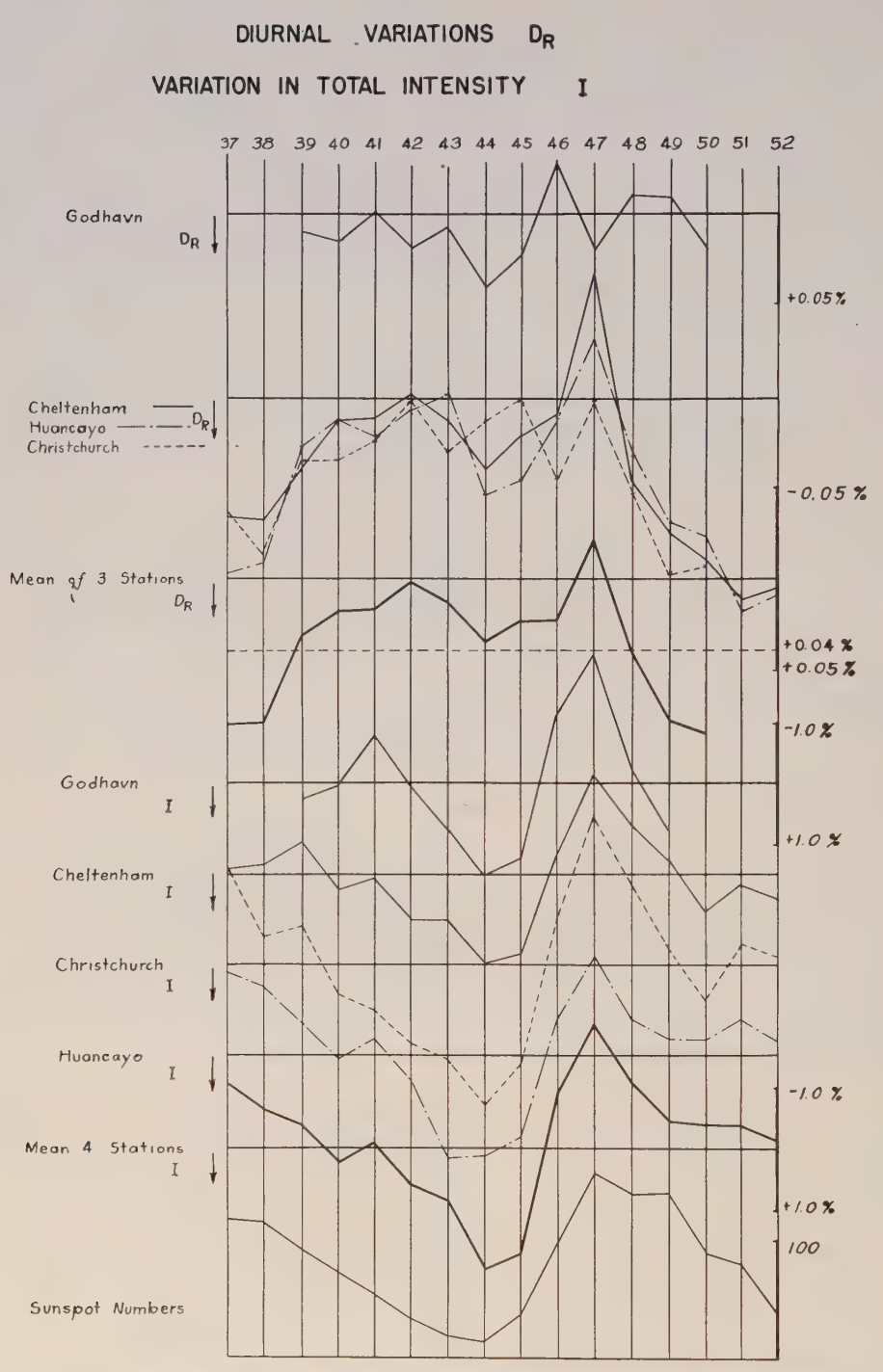

Fig. 9. Radial component D_R of the diurnal variation, in Godhavn, Cheltenham, Huancayo and, Christchurch, obtained from Fig. 8 after correction for the terrestrial magnetic field.

Mean of the three latter stations. Departure from average intensity I at the four stations. Mean of these stations. Sunspot numbers.

Processes of similar kind may go on outside the earth's orbit so the total energy production may be enough to fill up a much larger volume.

The number of particles which must be injected is

$$\frac{dn}{dt} = \frac{1}{eV_0} P$$

where eV_0 is the average energy per particle. As the number of particles per unit volume is $n = w/eV_0$ we have

$$\frac{dn}{dt} = 2 \cdot 10^{34}\, n$$

With $n = 10^{-10}$ cm^{-3}, we obtain

$$= 2 \cdot 10^{24} \text{ particles/sec.}$$

As the injection takes place with $v = 2 \cdot 10^8$ cm, an injection cross-section of only $S = 10^{16}$ cm^2 is enough even if we assume a density as low as 1 particle cm^{-3}. Hence there seems to be no difficulty of injecting a sufficient number of particles.

17. Upper energy limit

The present theory has been developed in order to account for the properties of that part of the Cosmic Ray spectrum which is measured by ionization chambers and counters, i.e. 10^{10}—10^{11} e volt. The neutron counter measurements, which cover the lower part of the spectrum, seem to fit into the picture rather well, although much more work in this field is desired. Concerning the high energy part of the spectrum ($> 10^{11}$ e volt), we know at present very little about its properties, and the different types of variations have not been studied. Hence it is believed that the time is not yet ripe for a detailed discussion of the highest energies. In this paragraph we shall at first show to what energies it is possible to extend the present theory and then make some speculations about possible ways to account for the highest energies.

A local theory cannot be expected to account for energies above a certain limit. This limit may be given either

(1) by the accelerating mechanism; or

(2) by the trapping field which we must assume in order to make the radiation isotropic.

The accelerating mechanism can produce particles up to the maximum momentum which can be kept in trochoidal orbits close to the sun. In the case of a dipole field near the sun the maximum momentum p of a trochoidal path in the equatorial plane is given by the Störmer orbit of a particle which just does not hit the sun. For this we have

$$p = \frac{Ze H_\odot R_\odot}{c} \left(3 - 2\sqrt{2}\right) \qquad (17.1)$$

where Ze is the charge of the particle and $H_\odot$ the field at the sun's equator. Putting $H_\odot = 5$ gauss we find

$$p = 1.8 \cdot 10^{13} \text{ e volt } Z/c \qquad (17.2)$$

In a dipole field there may be more complicated orbits which give somewhat higher values. Further, if the field is not a dipole field it is possible that still higher values could be obtained, but the above figure is likely to give the order of magnitude.

The corresponding value of the rigidity is

$$H\varrho = 6 \cdot 10^{10} \text{ gauss cm.} \qquad (17.3)$$

This means that a trapping field of 10^{-5} gauss could keep the particles within a distance of some 10^{16} cm.

Multiple charged heavy nuclei with $Z = 30$ or somewhat higher brings us up to a maximum energy of the order of 10^{15} e volt, but higher energies could not be accounted for by a local theory. Although at present we know too little about the energies above 10^{15} e volt to be able to discuss the matter very seriously, the following speculations about the energies 10^{15}—10^{17} e volt may be of interest.

1. The most energetic particles may derive from other stars which generate Cosmic Rays in a similar way but possess much stronger magnetic fields. Some of the particles may leak out and reach us.

2. As Cosmic Rays may travel some million years in space before they are absorbed, some of the particles which we observe may have been generated very long ago. It is possible that the sun has had a much stronger magnetic field during some period the last million years. If so, very energetic particles may have been generated. In order to keep them trapped we need a trapping field of for example 10^{-4} gauss extending 10^{17} cm (giving $p = 3 \cdot 10^{15}$ e volt Z/c, or with $Z = 30$, $p = 10^{17}$ e volt/c).

3. The existence of primary particles with very high energies is proved only by measuring the total energy of extended air showers. It seems at present not to be possible to exclude that such showers originate from multiple charged dust grains which are accelerated by the mechanism we have discussed. Possible values would be: charge 10^4 e, mass 10^6 nucleons, total energy 10^{17} e volt, energy/nucleon 10^{11} e volt, $H\varrho = 3 \cdot 10^{10}$ gauss cm.

18. The trapping field

Both the galactic and local theories must postulate the existence of a trapping field in order to prevent the cosmic radiation from filling up the whole universe with the same intensity. In both cases the properties of the trapping field are *ad hoc* assumptions which at present cannot be checked in any other way. The problem has been treated by UNSÖLD[8] and BIERMANN and SCHLÜTER[30].

The local theory requires a trapping field which is stronger and more "insulating" than in the galactic theories.

If the magnetic field in our environment is produced only by *local* currents it may easily be insulating over large regions. In order to discuss a very simple model, let us assume that the field is produced by a current in a circular loop. Suppose that charged particles having a radius of curvature which is small compared to the size of the loop are produced in the field. They are free to move along the lines of force. Due to the inhomogeneity of the field they will have a superimposed drift in circles around the axis. From a small region near the axis they could leak out to infinity but they will be trapped in a large portion of the field.

As at some distance the field from a loop is a dipole field the problem is related to Störmer's problem. It is well known that in a dipole field there are regions from which there are no trajectories out to infinity.

Hence if the trapping field is caused by a system of local currents, it may very well be insulating. However, in the case of the interplanetary field we have seen that a diffusion of charged particles is caused by small-scale irregularities in the field. The same kind of disturbances may cause a diffusion out of the trapping field. It is reasonable that the disturbances which are caused by the solar activity, are much more important near the sun. As the trapping field is far from any source of disturbance, it is possible that the small-scale irregularities have been smoothed out, so that the diffusion is small.

If besides the field from a local current system there are also fields from other sources, the combined field has a complicated structure and leakage is more probable. Hence, the necessity of assuming an insulating trapping field probably sets an upper limit to a galactic field in our neighbourhood.

In the earlier discussion[18] of the local theory it was pointed out that a trapping field may be produced by magneto-hydrodynamic effects of the motion of the solar system in relation to interstellar matter. Another possibility is that it may be generated by the storm-producing beams. When after the ejection from the sun the beams pass the earth's orbit, they have certainly much energy left and it is possible that far outside the earth's orbit this energy is used to build up a trapping field.

As a summary of this brief discussion we may state that the assumption of a trapping field which makes the radiation isotropic is not in conflict with any known facts. On the other hand we know so little about it that at present it is hardly worth while to try to make a detailed theory of it.

19. Summary of the accelerating mechanism

The generating process we have studied takes place in interplanetary space around the sun, to a large extent at solar distances comparable to the earth's distance. The process has been found to have the following properties.

1. *Absence of electrons.*

   The accelerated particles have an energy which is proportional to their rest mass. This means that the process is inefficient for electrons but favourable for protons and still more so for heavy nuclei.

   This explains the absence of electrons in cosmic radiation, and the fact that heavy nuclei constitute an important part of the radiation.

2. *Latitude knee.*

   The diffusion is slow below a certain momentum, which is of the order 10^9 e VZ/c. Accelerated particles below this limit are found only close to the sun. Above this

limit the diffusion becomes more rapid and cosmic ray particles diffuse outwards. This seems to account for the low energy cut-off in the cosmic radiation energy spectrum and also for the large variability in the lowest energy range.

3. *Intensity variation with the sunspot cycle.*

The acceleration process is a result of the solar activity, and must be expected to vary with the solar cycle. At the beginning of the sunspot cycle when the solar activity is strong the outflow dominates and the decelaration may be as strong as the acceleration or even stronger, resulting in a decrease in cosmic ray intensity. At the end of a sunspot cycle the inflow dominates and the acceleration becomes more efficient so that the intensity becomes large. This is in agreement with Forbush's curves, which show intensity variations of 4 %.

4. *The diurnal variation.*

The diurnal variation of the primary radiation seems to consist of two effects. One of these is due to an excess of particles coming in from the 18^h direction. Superimposed on this is the radial flow of cosmic ray energy which gives a component D_R with a maximum at 12^h. This component is a measure of the energy produced by the accelerating process inside the earth's orbit. From Forbush's curves it is evident that it varies in roughly the same way as the total intensity, and is correlated with the solar activity.

I wish to thank Dr S. E. Forbush for permission to study his very valuable unpublished material and for many discussions. I also thank Dr F. Singer for discussions and kind help in various ways.

The investigation has been made during a stay at the University of Maryland, for which I am most obliged to Dr J. Toll and Dr M. H. Martin. My journey was supported by a Fulbright grant.

Miss R. Turner and Mrs C. Smith have kindly helped me with the preparation of the manuscript.

REFERENCES

1. S. E. Forbush, *Physical Rev.* – In the press.
2. T. Thambyahpillai and H. Elliot. *Nature* **171**, 918, 1953.
   V. Sarabhai and R. P. Kane, *Phys. Rev.* **90**, 204, 1953; **91**, 688, 1953.
3. S. E. Forbush, *Terr. Mag.* **43**, 203, 1938. See also H. Elliot, *Time Variations of Cosmic Ray Intensity.* Contained in J. G. Wilson, *Progress in Cosmic Ray Physics*, 1952.
4. J. A. Simpson, W. H. Fonger, and S. B. Treiman, *Phys. Rev.* **90**, 934, 1953.
5. J. J. Lord and M. Schein, *Phys. Rev.* **78**, 484, 1950; M. J. Swetnick, H. A. C. Neuburg and S. A. Korff, *Phys. Rev.* **86**, 589, 1952. H. V. Neher, V. Z. Petterson and E. A. Stern, *Phys. Rev.* **90**, 655, 1953.
6. R. D. Richtmyer and E. Teller, *Phys. Rev.* **75**, 1729, 1949. Compare also *Rep. Progr. Physics*, **17**, 154, 1954, where Teller seems to have changed his opinion.
7. E. Fermi, *Phys. Rev.* **75**, 1169, 1949.
8. A. Unsöld, *Phys. Rev.* **82**, 857, 1951.
9. C. Y. Fan, *Phys. Rev.* **82**, 211, 1951.
10. Ph. Morrison, S. Olbert, S. and B. Rossi, *Phys. Rev.* **94**, 440, 1954.
11. E. Fermi, *Conference on Cosmic Rays*, Duke, Durham, 1953.
12. W. F. G. Swann, *Phys. Rev.* **43**, 217, 1933.
13. A. Ehmert, *Zeitschrift f. Naturforsch.* **3 a**, 264, 1948.
14. D. H. Menzel and W. W. Salisbury, *Nucleonics* **2**, 867, 1944. See also E. M. McMillan, *Phys. Rev.* **79**, 498, 1950.
15. L. Biermann, *Die Entstehung der Höhenstrahlung* contained in W. Heisenberg, *Kosmische Strahlung*, Berlin 1953.
    E. Bagge and L. Biermann, *Naturwissenschaften* **35**, 120, 1948.
    A. Schlüter, *Zeitschrift für Naturforschung* **7 a**, 136, 1952.
16. H. Alfvén, *Zeitschrift f. Physik* **105**, 319, 633, 1937, **107**, 579, 1937, *Arkiv för mat. astr. och fysik* 25 B, Nr 29 1937.
17. H. Alfvén, *Nature* **143**, 1939.
18. H. Alfvén, *Phys. Rev.* **75**, 1732, 1949; **77**, 375, 1950.
19. See S. Chapman and J. Bartels, *Geomegnetism*, Oxford 1940.
20. D. F. Martyn, *Nature* **167**, 1951.
21. H. Alfvén, *Cosmical Electrodynamics*, Chapter VI, Oxford 19.50; See also Tellus 7, 1955
22. S. E. Forbush, *Terr. Mag.* **43**, 203, 1938; *Phys. Rev.* **54**, 975, 1938. S. E. Forbush, T. B. Stinchcomb, and M. Schein, *Phys. Rev.* **79**, 501, 1950.
23. F. Singer, *Phys. Rev.* In press.
24. J. A. Simpson, *Phys. Rev.* In press.
25. H. Alfvén, *Cosmical Electrodynamics*, p. 215.
26. E. A. Brunberg and A. Dattner; *Tellus* **6**, 73, 1954; **6**, 254, 1954.
27. S. Lundquist, *Tellus* **6**, 260, 1954.
28. M. Ryle, Accademia Nazionale Dei Lincei Convegno Di Science Fisiche Matematiche e Naturali 14 – 19 sept. 1952, p. 276.
29. Y. Öhman, *Astrophys. J.* **114**, 367, 1951.
30. L. Bierman and A. Schlüter, *Phys. Rev.* **82**, 863, 1951.
31. E. Åström, (in course of preparation).

Variations of the Cosmic Ray Intensity During Magnetic Storms

By ERNST-ÅKE BRUNBERG and ADAM DATTNER

Royal Institute of Technology, Stockholm

(Manuscript received June 12, 1954)

Abstract

A simple mechanism has been suggested by H. Alfvén to explain the main features of the variation of cosmic ray intensity during magnetic storms.

Cosmic ray particles are accelerated or retarded in the electric fields of ionized beams, which are sent out from the sun. Particle orbits hitting the earth have been calculated for different momenta and for solar magnetic fields decreasing with distance as r^{-3}, r^{-2} and r^{-1}. The influence on the particles of beams of different length and breadth has been analyzed.

A beam length of a few times the orbital radius of the earth and particles with momenta in the range 20—40 *GeV Z/c* give a time variation in cosmic ray intensity similar to the variation measured during a magnetic storm. This requires a solar magnetic field of 10^{-5} gauss at the earth's orbit.

As discovered by FORBUSH (1937) the typical variation of cosmic ray intensity during a magnetic storm is a decrease of the intensity soon after the beginning of the main phase of the storm. This result was obtained from measurements with ionisation chambers and G-M counters (cf. also WILSON, "Progress in Cosmic Ray Physics", *1952*, Chapter VIII). After the decrease a slow recovery to normal value occurs and during the whole time of the storm there is a pronounced diurnal variation as seen in fig. 1, (SEKHIDO and YOSHIDA, 1950, ELLIOT and DOLBEAR, 1951). The decrease is not proportional to the intensity of the magnetic storm. During some storms no decrease takes place whereas some small magnetic storms have caused rather big decreases in the intensity of cosmic radiation. (TRUMPY, 1953.)

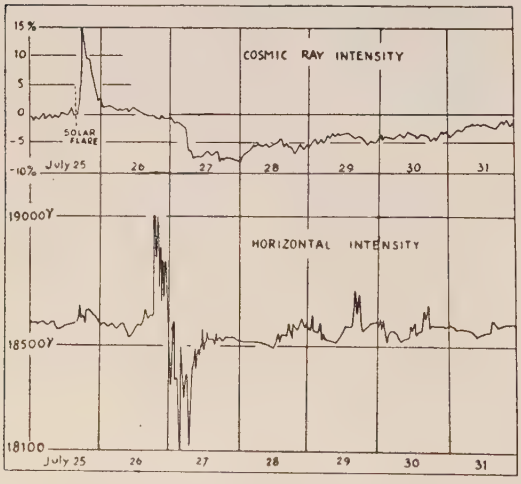

Fig. 1. Typical variation of the cosmic ray intensity during a magnetic storm. (WILSON, 1952, *Progr. in Cosm. Ray Phys.* p. 495.)

An increase in cosmic ray intensity has sometimes been observed approximately one hour after a solar flare and 24 hours before the main phase of the storm *(Progress in Cosmic Ray Physics)*. We shall here not discuss this immediate effect of the solar flare, which is without a doubt a quite different phenomenon.

The properties of an ionized beam

ALFVÉN (1949) has suggested that the magnetic storm effect is caused by the electric field of a beam of ionized gas, which is sent out from the sun in connection with a magnetic storm. In order to discuss this problem we shall first give an account of the main properties of such a beam.

We consider the phenomena in the equatorial plane of the sun and assume that a stream of ionized gas is sent out from the sun with the velocity $\bar{v}$, which is of the order of 10^6 m/s, fig. 2. The solar magnetic field polarizes the beam. Seen from a coordinate system which is at rest in relation to the sun the magnetic field strength is supposed to be $\bar{B}$ inside and $\bar{B}_0$ outside the beam. The positive and negative space charges give rise to an electric field $\bar{E}$ across the beam with field strength

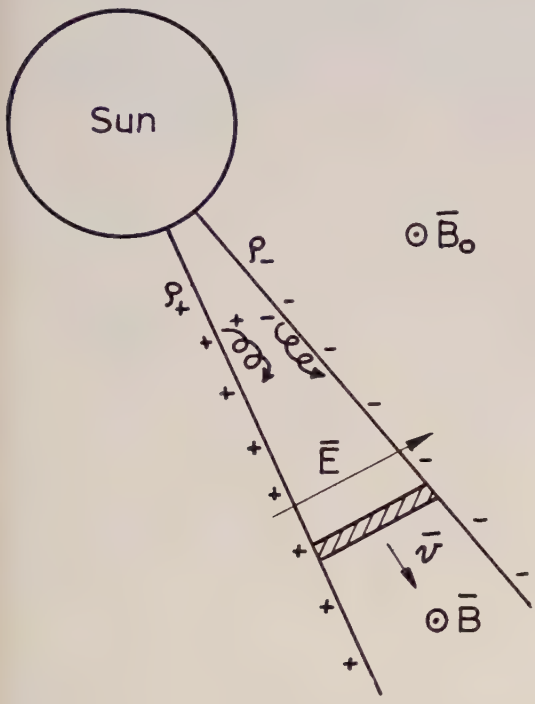

Big. 2. The beam of ionized gas, sent out from the sun.

$$\bar{E} = -\bar{v} \times \bar{B} \qquad (1)$$

and pointing in the same direction as the sun rotates.

In the combined electric and magnetic fields, charged particles move out from the sun in trochoidal orbits. The radius of curvature of a particle orbit depends on the mass and the energy of the particle but the translation velocity is equal for all particles and given by

$$v = \frac{E}{B} \qquad (2)$$

MKS units are used. (cf ALFVÉN, 1950. Ch. II.)

Cosmic rays in the field of the beam

During a magnetic storm the earth passes regions with electric and magnetic fields where the conditions are different from that in other parts of the earth's orbit. Cosmic particles are affected by these fields and the intensity measured on the earth is changed. In the following example we suppose the beam to be very thin so that it can be considered as an electric double layer. Hence the effect on a cosmic particle crossing the beam must be a change of the particle energy. Particles which cross the beam from the negative to the positive side lose energy, and particles moving in the opposite direction gain energy.

The change in energy is $\Delta W = e \int \bar{E} ds$.

However, there are further effects to be considered. The particles reach the earth from all directions (except in the forbidden cones) and they may or may not cross the beam. Furthermore the extension of the beam in the meridional plane of the sun is unknown, as well as the length of the beam in the equatorial plane. We also know little about the solar magnetic field. Nevertheless it is possible to discuss the phenomenon of the magnetic storm variations by means of a study of a simple model, as explained in the following.

The discussion is confined to the phenomena in the equatorial plane of the sun.

Generally the radius of curvature is

$$\varrho = \frac{\sqrt{V^2 + 2\, m_0 c^2 V}}{B}$$

but $B = \frac{M}{r^n}$

and hence $\frac{\varrho}{R_{S-E}} = k \left(\frac{r}{R_{S-E}} \right)^n$

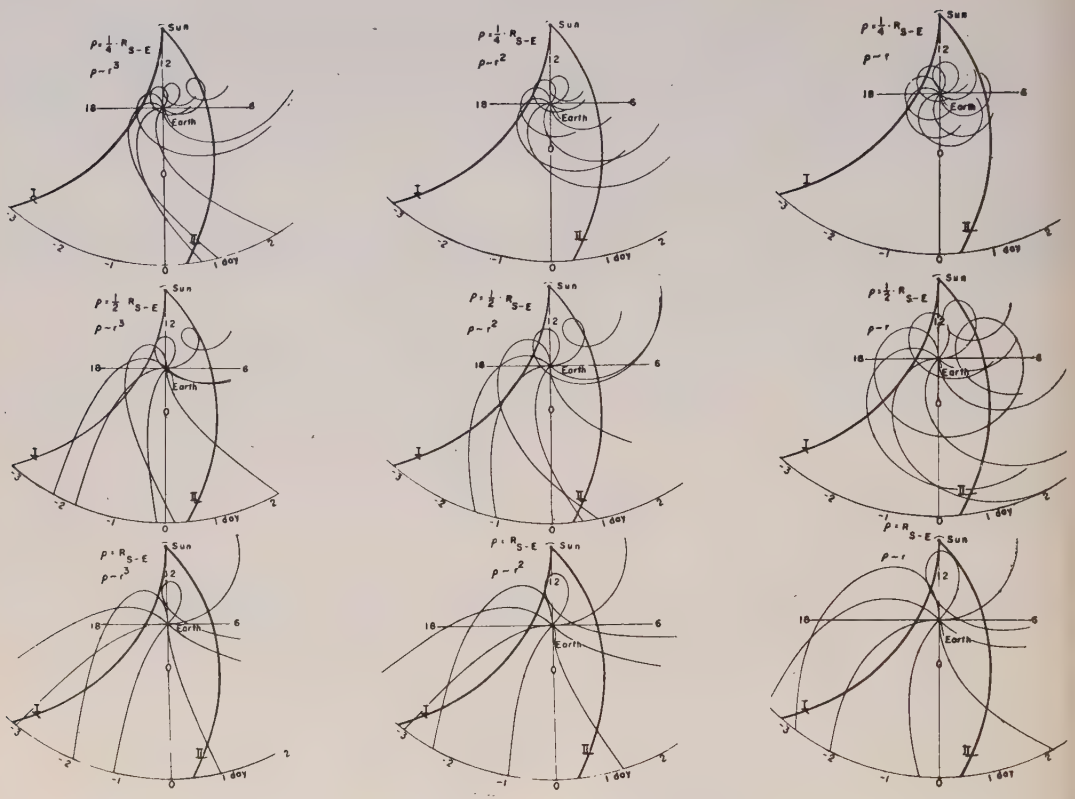

Fig. 3. Charged particle orbits in the solar magnetic field, calculated for different values of k and n.

where r = distance to the sun
B = magnetic field strength at distance r
k and n are constants
R_{S-E} = distance between the sun and the earth
The particle orbits are calculated graphically for
$k = 1$, 0.5, and 0.25
$n = 1$, 2, and 3

and those which hit the earth from the zenith direction at eight different points with the local time 12 h, 15 h, 18 h, 21 h and so on. The magnetic field of the earth is neglected. A correction for this can be applied according to BRUNBERG and DATTNER (1953). In such a way nine diagrams were obtained, each consisting of eight different orbits (see fig. 3).

Then we consider a beam of a geometrical shape as given by CHAPMAN and BARTELS, (*Geomagnetism* vol. II, p. 806). Before the magnetic storm the beam is situated in position I (fig. 4), and moves towards the earth. In order to define the problem it is necessary to introduce the length of the beam. This is arbitrarily put equal to 2 or 3 R_{S-E}.

Starting from these assumptions the variation of cosmic ray intensity during a magnetic storm may be explained in the following way.

Particles crossing the beam either gain or lose energy. Those crossing from the left gain energy, those crossing in the opposite direction lose energy. Finally particles crossing the beam and returning again through the beam do not change their energy.

The deflection of particles in the magnetic field is altered by the change in energy but this is a small effect and has not been taken into account in the present model.

After the beam has passed the earth a decrease in intensity takes place because most cosmic particles reaching the earth have passed the double layer of the beam and hence become retarded. The rays which are least affected are those entering between 12 h and 18 h. (See fig. 4 Beam in position II.) From this it is evident that the beam length plays an impor-

tant part for the phase of the diurnal variation. It is shown further on that good agreement with observations of cosmic ray intensity during the magnetic storms can be obtained if the beam length is assumed to be three times the radius of the earth's orbit. Other

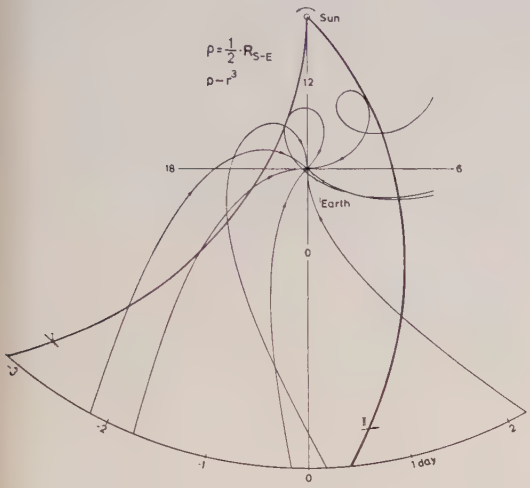

Fig. 4. Charged particle orbits in the equatorial plane of the solar magnetic field.

beam lengths are likely to give similar results, but a more precise discussion requires more data about the phase of the storm time diurnal variation.

The intensity variation

We consider the beam in a certain position and observe particles coming from the zenith to a point on the earth's equator. We follow this point while the earth rotates and the beam moves towards the earth and passes it. The observed intensity varies as for example in fig. 5 depending on the initial position of the beam and the point of observation. The same has been repeated for other initial positions of the beam and similar intensity diagrams have been obtained.

We have so far assumed the beam to be infinitely thin and shall now discuss what happens if the beam has a finite breadth. If the beam is supposed to have a breadth corresponding to an 18 hours arc ($18/24 \cdot 1/365\ R_{S-E}$) of the earth's orbit, a beam with this breadth can be used in fig. 4. We must take into account that a particle which passes only a part of the beam changes its energy in proportion to this fraction of the beam breadth.

The difference between the magnetic field inside and outside the beam produces some change in this picture as pointed out by SWANN (1954) and ALFVÉN (1954). This effect will be studied in detail in a subsequent paper. The results are essentially the same as those obtained here.

The effect of the beam breadth was calculated by integrating the already obtained intensity diagrams of a thin beam in the following way. We assumed a beam breadth such that the earth is enveloped in it for 18 hours and 6 diagrams were plotted, representing the state of things at 3 hours intervals (8 diagrams correspond to 24 hours). We began with diagram 12 h and added diagram 15 h moved 3 hours back. The same was repeated for diagram 18 h but with a displacement of 6 hours and so on. The result is the smoothed intensity curve of figs 6 and 7.

This graphical method has been repeated for magnetic fields decreasing as r^{-2} and r^{-1}, for different radius of curvature, for two values of beam breadth and also for a beam length of twice the orbital radius.

Intensity diagrams with a beam length of 3 times the orbital radius, a beam breadth corresponding to 18 h and 36 h and magnetic fields decreasing as r^{-3} and r^{-2} are most interesting and shown in figs 6 and 7.

Results obtained by the model

Four diagrams have been found which give a variation similar to observed variations in cosmic ray intensity during magnetic storms, figs. 6b, 6e and figs. 7b and 7e. In all cases the beam length is 3 times the orbital radius of the earth and $\varrho = 0.5\ r^n$. In figs. 6b and 7b

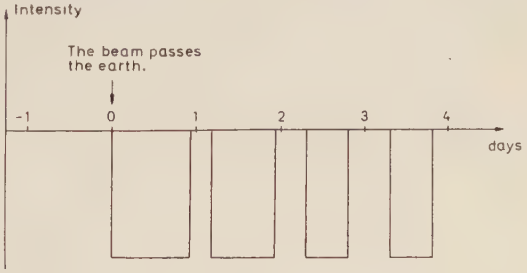

Fig. 5. The variation of the cosmic ray intensity when the beam is assumed to be infinitely thin.

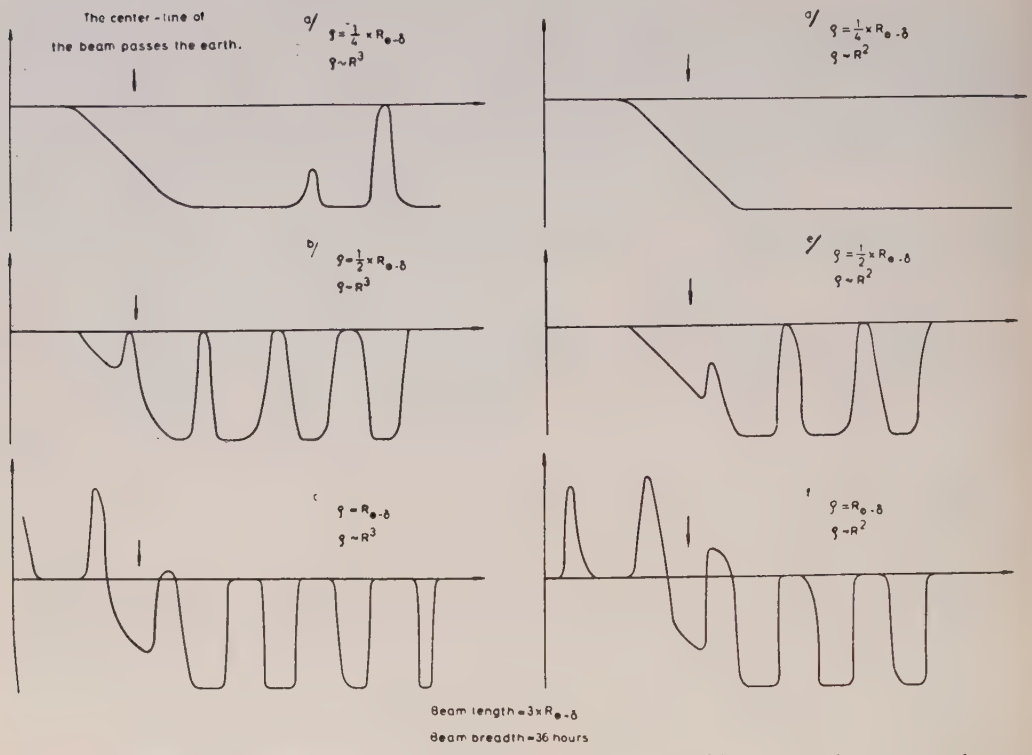
The center - line of
the beam passes the earth.
a/ $\varrho = \frac{1}{4} \times R_{\odot} - \delta$
$\varrho \sim R^3$
a/ $\varrho = \frac{1}{4} \times R_{\odot} - \delta$
$\varrho \sim R^2$
b/ $\varrho = \frac{1}{2} \times R_{\odot} - \delta$
$\varrho \sim R^3$
e/ $\varrho = \frac{1}{2} \times R_{\odot} - \delta$
$\varrho \sim R^2$
c $\varrho = R_{\odot} - \delta$
$\varrho \sim R^3$
f $\varrho = R_{\odot} - \delta$
$\varrho \sim R^2$
Beam length = $3 \times R_{\odot} - \delta$
Beam breadth = 36 hours

Fig. 6. The variation of the cosmic ray intensity for a beam with a breadth corresponding to an 36 hours arc.

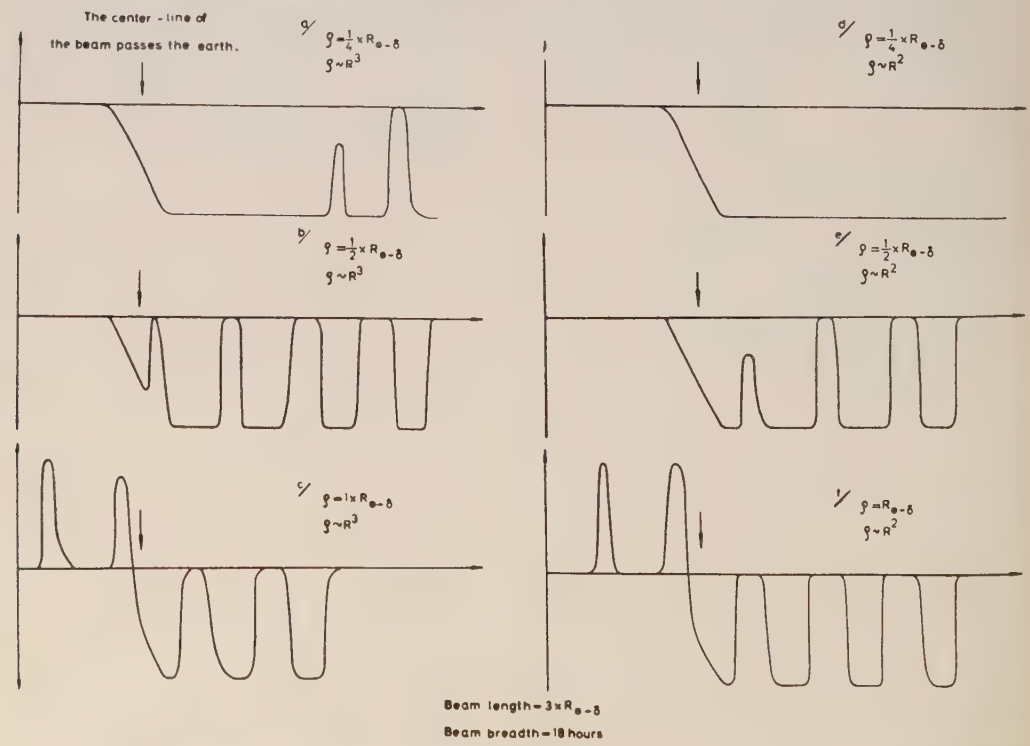
The center - line of
the beam passes the earth.
a/ $\varrho = \frac{1}{4} \times R_{\odot} - \delta$
$\varrho \sim R^3$
d/ $\varrho = \frac{1}{4} \times R_{\odot} - \delta$
$\varrho \sim R^2$
b/ $\varrho = \frac{1}{2} \times R_{\odot} - \delta$
$\varrho \sim R^3$
e/ $\varrho = \frac{1}{2} \times R_{\odot} - \delta$
$\varrho \sim R^2$
c/ $\varrho = 1 \times R_{\odot} - \delta$
$\varrho \sim R^3$
f/ $\varrho = R_{\odot} - \delta$
$\varrho \sim R^2$
Beam length = $3 \times R_{\odot} - \delta$
Beam breadth = 18 hours

Fig. 7. The variation of the cosmic ray intensity for a beam with a breadth corresponding to an 18 hours arc.

$n=-3$ and in fig. 6 e and 7 e $n=-2$. The breadth of the beam seems to be of little importance for the general appearance of these diagrams.

From the ordinary diurnal variation we know that the particles which cause the observed diurnal variation have momenta in the range 20 – 40 *GeV* Z/c (BRUNBERG and DATTNER, 1954). It is probable that the diurnal variation during magnetic storms is caused by particles in the same momentum range.

Moreover the analysis of figs. 6 and 7 has shown that the radius of curvature for the trajectories of the relevant particles is $\varrho = \frac{1}{2} R_{S-E}$, where R_{S-E} is the radius of the earth's orbit. Thus we know the energy of the particles and the curvature of the trajectories, and we can deduce the strength of the solar magnetic field at the earth's orbit. The result is

$$B=\frac{p}{\varrho e}=\frac{eV}{c\varrho e}=10^4\cdot\frac{3\cdot 10^{10}}{3\cdot 10^8\cdot 0{,}75\cdot 10^{11}}=$$

$$=1{,}3\cdot 10^{-5}\ \text{gauss}$$

Suppose the solar magnetic field decreases as r^{-n}. Consideration of the model of the present paper gives no possibility to determine exactly the value of n. However, it has been shown that a value of n between 2 and 3 is in agreement with the general appearance of the intensity variation measured during magnetic storms. If the solar magnetic field is 10 gauss at the sun and 10^{-5} gauss at the orbital radius of the earth the exponent n shall be 2.6.

We point out that a 27-day recurrence tendency can be explained by this mechanism if a beam lasts for a rather long time and passes the earth several times.

We are indebted to Professor H. Alfvén and Dr N. Herlofson for many discussions and good advice. We also want to thank Dr H. Elliot for valuable criticism.

The investigation has been made possible by a grant from Knut and Alice Wallenberg's Foundation which is gratefully acknowledged.

REFERENCES

ALFVÉN, H., 1949. On the solar origin of cosmic radiation. *Phys. Rev.* **75**, 11.

ALFVÉN, H., 1950. *Cosmical Electrodynamics*, Oxford.

ALFVÉN, H., 1954, On the origin of cosmic radiation *Tellus*. **6**, 2.

ALFVÉN, H., 1954. *Phys. Rev.* **94**, 1082.

BRUNBERG, E.-Å., and DATTNER, A., 1953. Experimental Determination of electron orbits in the field of a magnetic dipole. *Tellus*. **6**, 2.

BRUNBERG, E.-Å., and DATTNER, A., 1954. On the interpretation of the diurnal variation of cosmic rays. *Tellus*. **6**, 1.

CHAPMAN, S., and BARTELS, J., 1940. *Geomagnetism*, Oxford.

ELLIOT, H., and DOLBEAR, D. W. N., 1951. Directional measurements of the diurnal variation of cosmic ray intensity. *Journ. of Atm. and Terr. Phys.* **1**.

FORBUSH, S. E., 1939. *Phys. Rev.* **51**, p. 1108.

SEKHIDO, Y., and YOSHIDA, S., 1950. On the diurnal variation of cosmic rays. *Rep. of Ionosph. Research in Japan*. Vol. IV, No. 1.

SWANN, W. F. G., 1954. *Phys, Rev.* **93**, 905.

TRUMPY, B., 1953. Time variations of cosmic ray intensity associated with geomagnetic and solar activity. *Physica*. XIX, p. 645.

WILSON, J. G., 1952. *Progress in cosmic ray physics*. North-Holland Publ. Comp. Amsterdam

A Note on the Variation of Cosmic Ray Intensity Produced by an Electric Field

By S. LUNDQUIST

Royal Institute of Technology, Stockholm

(Received June 12, 1954)

The variation of the cosmic ray intensity during a magnetic storm has been ascribed to the electrically polarized beam of particles from the sun.[1] The loss of particles due to the total reflection in the electric field has been calculated.[2] For comparison with observations, however, the change of the intensity I per surface element dS, solid angle $d\Omega$, and energy interval dW should be considered.

For the motion of particles in electromagnetic fields there exists a Hamiltonian. In a slowly varying field the density of particles in ordinary momentum space (x, p), $D = dN/dV_x dV_p$, is constant along a trajectory.[3] Putting $dV_x = dSpdt/m$ (m = mass), $dV_p = p^2 d\Omega dp$ and $dN = I(W) dW dS d\Omega dt$ one finds

$$I = Dp^3 dp/mdW$$

or since $c^2p^2 = W(W + 2W_0)$, $mc^2 = W + W_0$

$$I = W(W + 2W_0)D$$

For particles reaching the earth with the energy W and the intensity $I'(W)$ and having far away the energy $W + \Delta W$ and the intensity $I(W + \Delta W)$

$$I'(W)/I(W + \Delta W) = W(W + 2W_0)/(W + \Delta W)(W + \Delta W + 2W_0)$$

or for ΔW small

$$\Delta I/I = [I'(W) - I(W)]/I(W) = [WdI/IdW - 2(W + W_0)/(W + 2W_0)]\Delta W/W$$

Assuming an undisturbed spectrum $I(W) = AW^{-k}$

$$\Delta/I = I - (k + k_1)\Delta W/W$$

with $1 \leq k_1 \leq 2$ and $k \approx 2.5$. ΔW is the decrease of energy of the particle due to its motion in the electric (not necessarily electrostatic) field. The two terms of ΔI are shown in fig. 1.

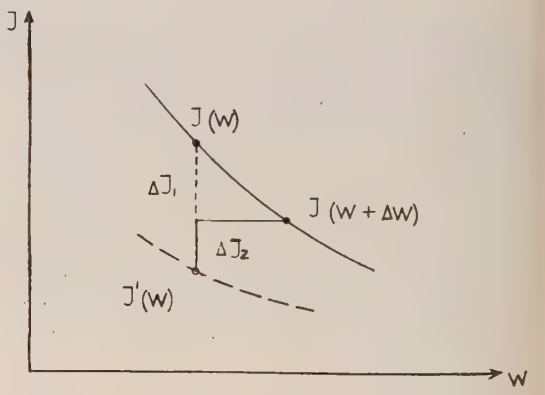

Decrease of cosmic ray intensity I due to a change in the earth's electric potential corresponding to a change of particle energy = $\triangle W$. I = undisturbed spectrum, I' = observed spectrum. $I_1 = WdI/IdW \cdot \triangle W/W$, $I_2 = 2(W + W_0)/(W + 2W_0) \cdot \triangle W/W$.

The result is valid for any direction in which particles can reach the earth. If the electromagnetic field of the beam introduces forbidden cones, these should be considered. The change of intensity here is considerably lower than that given in (2).

[1] H. Alfvén, *Cosmical Electrodynamics*, Oxford, 1950.
[2] B. Trumpy, *Physica* XIX, 645, 1953.
[3] L. Jánossy, *Cosmic Rays*, Oxford 1948, p. 266.

Composition of Atmospheric Precipitation in Sweden

By

A. EMANUELSSON, Institute of Soil Fertility and of Soil Management, Royal Agricultural College, Uppsala

E. ERIKSSON, Institute of Meteorology, University of Stockholm

H. EGNÉR, Institute of General and Inorganic Chemistry, Royal Agricultural College, Uppsala

(Manuscript received Sept. 29, 1954)

Abstract

Preliminary charts are presented based on two years of data, to demonstrate the geographic distribution over Sweden of the annual amounts of Na, Cl, K, Ca, NH_3-N and NO_3-N brought to the surface of the earth by precipitation. The ratios of these total amounts to the total amounts of Na deposited during the same time interval are shown to possess systematic geographic distribution patterns. Comparisons are made between these ratios and the corresponding quantities in sea water. The investigation is now being resumed to provide additional data from a larger number of stations and for longer time periods.

The present paper contains an analysis of some of the results obtained in an investigation of the chemical composition of atmospheric precipitation and in particular of the geographic distribution over Sweden of the various chemical deposits brought down by rain or snow. This investigation, which was carried out during the period October 1, 1947—September 30, 1950, was initiated by professor G. Torstensson and Dr H. Egnér at the Royal Agricultural College of Sweden and by Dr A. Ångström, Director of the Swedish Institute of Meteorology and Hydrography. Financial support was obtained from the Agricultural Research Council of Sweden. The sampling technique and the analytical methods were worked out by the authors and have been described earlier (EGNÉR et al., 1947). The planning of the network of sampling points and the installation of sampling devices was done by Egnér and Eriksson and all analyses were carried out under the supervision of Egnér. Some data from this investigation, on the content of ammonia and nitrate in precipitation, have been published by ÅNGSTRÖM and HÖGBERG (1952 a, b). A detailed but unpublished discussion of the results has been given by one of the authors (Emanuelsson) as part of the requirements for an agronomic licentiate degree at the Royal Agricultural College of Sweden. The geographic distribution charts presented in this paper were analysed jointly by Emanuelsson and prof. C.-G. Rossby.

General information

The accumulated amounts of atmospheric precipitation were collected monthly at 28 places. The geographic position of these (except one which represents a pollution center) are shown on the map in Fig. 1. It is seen that southern Sweden is much better represented than the northern part since the original purpose of the investigation was to study the

agricultural importance of chemical compounds in atmospheric precipitation.

The precipitation samples were shipped to Ultuna and analysed for sodium, calcium, potassium, ammonia, chloride and nitrate. Due to the sampling technique used sulphur had to be excluded. The data on nitrate, and in some measure also those on chloride, are somewhat doubtful but will nevertheless be presented here. Magnesium, which seems to be a significant element in precipitation was not determined due to difficulties associated with the analysis technique used at the time.

The data include all kinds of atmospheric precipitation, except dew and rime; the collecting funnels, which were mounted approximately 1.6 m above the ground, were exposed at all times. The data thus represent chemical compounds brought to the ground by gravitational forces. Excepting those measurements which represent deposits from sources of local character, these data should provide us with information of considerable importance for the interpretation of the general circulation of atmospheric compounds. By far the larger portion of these compounds were brought down by rain or snow.

The mean annual precipitation (rain and snow) for the two-year period October 1, 1948 to September 30, 1950 at the sampling points is also given in Figure 1. It is seen that the Swedish westcoast and the adjacent inland have the highest precipitation values whereas the remaining stations, with the exception of Riksgränsen in the north, have fairly uniform rates. The station at Riksgränsen is located in

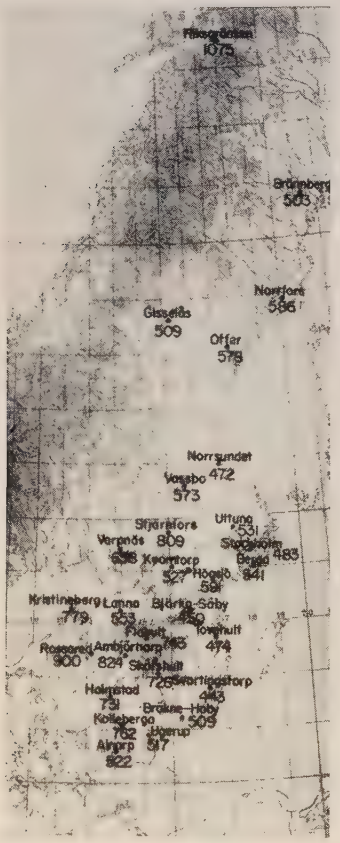

Fig. 1. Station locations and precipitation in mm per year during 2-year period 1 October 1948—30 September 1950.

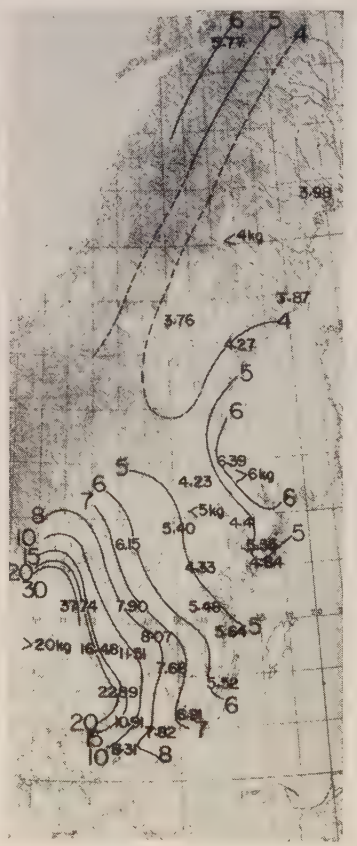

Fig. 2. Yearly amounts of Na (kg/har).

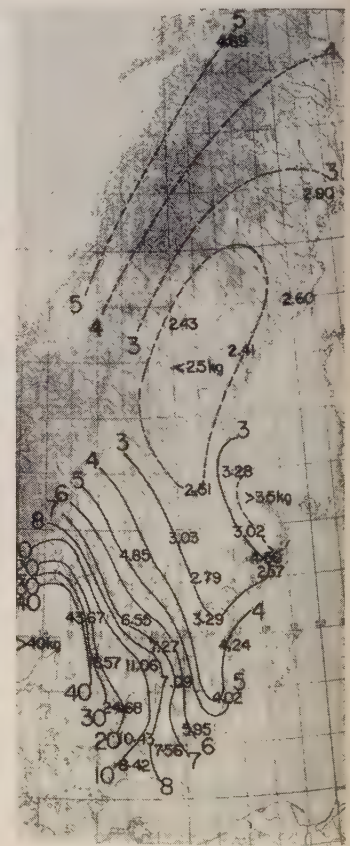

Fig. 3. Yearly amounts of Cl (kg/har).

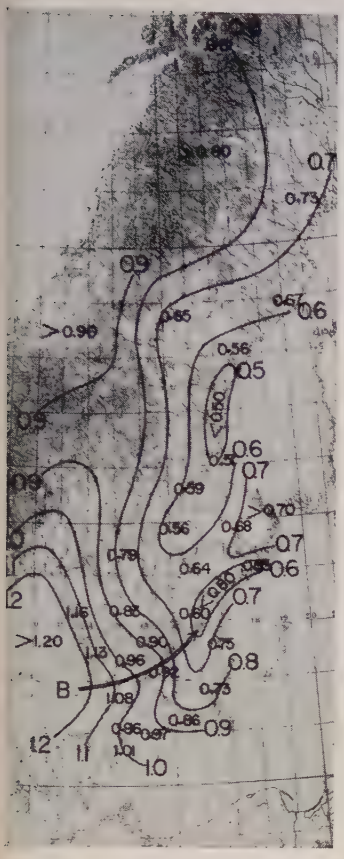

Fig. 4. Weight ratio Cl/Na.

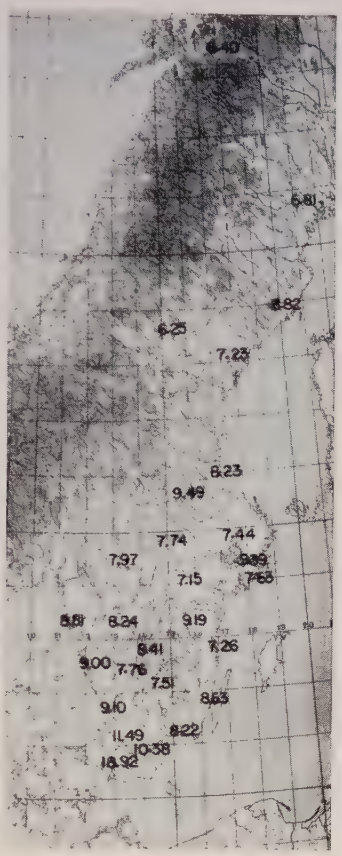

Fig. 5 Yearly amounts of Ca (kg/har).

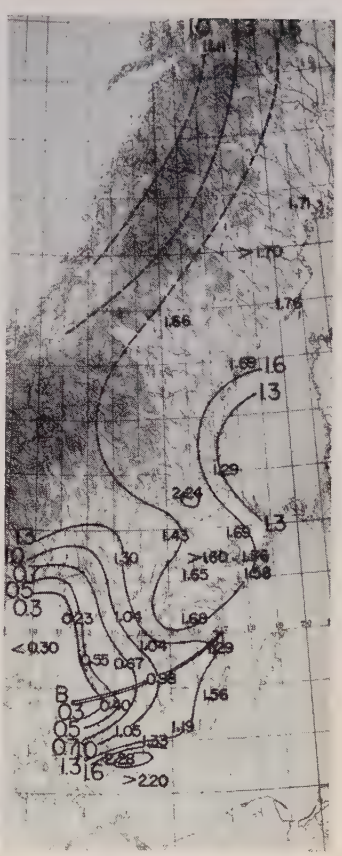

Fig. 6. Weight ratio Ca/Na.

a mountain pass at an elevation of 508 m and is the only one representing mountain conditions.

During the first year of the investigation nitrogen compounds only were determined. Therefore the data given here are based on the two-year period October 1, 1948 to September 30, 1950, in order to provide a fair comparison between ammonia nitrogen and the other elements. The monthly variations in the amounts brought down at the different stations are of considerable interest but will not be discussed here. The average yearly values only will be given because of their obvious geochemical importance. All data have been plotted on maps, and, to give the general patterns of the distribution of the elements, isolines have been drawn. The yearly amounts are given in kg/ha (1 ha = 10^4 m^2). When multiplied with ten these figures give the amounts in μg/cm^2.

On another series of maps the weight ratios of the different elements to sodium have been plotted and are represented by isolines. These values are computed from the total amount of any particular chemical component deposited over the entire two-year period and from the total amount of sodium deposited during the same period at the same station. Data on the ratios of the different elements over sodium in sea water are shown in Table 1.

Table 1. The ratios of some elements over sodium in sea water

Cl/Na	Ca/Na	K/Na	H_3N-N/Na	NO_3-N/Na
1.8	0.038	0.036	$\sim 5 \cdot 10^{-7}$ (at surface)	$\sim 7 \cdot 10^{-7}$

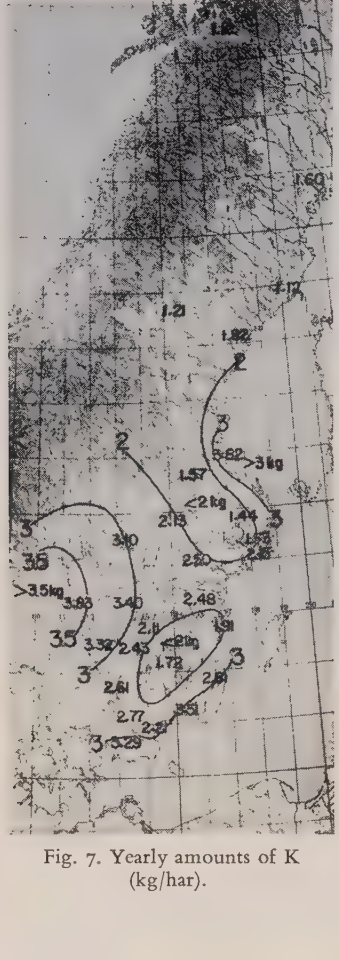

Fig. 7. Yearly amounts of K (kg/har).

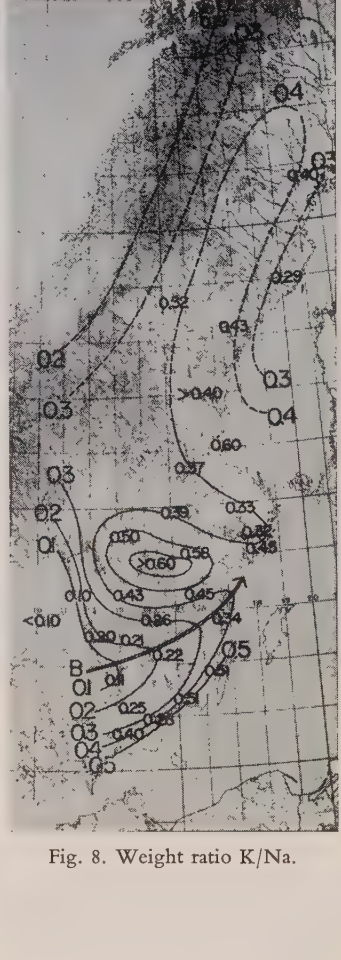

Fig. 8. Weight ratio K/Na.

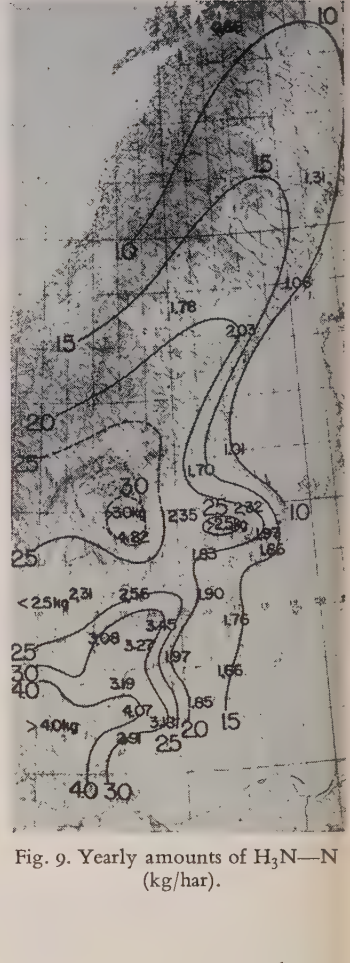

Fig. 9. Yearly amounts of H_3N—N (kg/har).

Sodium and chloride

The yearly amounts of sodium are shown in Fig. 2. The highest values are, of course, found on the freely exposed part of the west coast; inland the amounts decrease roughly logarithmically with distance from the coast. There is a slight indication of a weak secondary maximum along the Baltic coast north of Stockholm. In this region northeasterly winds from time to time give rise to cyclonic-orographic precipitation from low-level clouds; one may perhaps venture a guess that it is this type of precipitation that gives rise to the weak secondary maximum in the deposit of sodium and of some of the other elements observed along this part of the Baltic coast.

A fairly broad minimum or saddle area runs from NNW to SSE across lake Mälaren, just west of Stockholm. To the north the stations are too far apart to permit any conclusions regarding the detailed distribution of the sodium deposit.

The distribution of the yearly deposits of chloride is shown in Fig. 3. The pattern if similar to that of sodium, as might be expected, the sea presumably being the only important source for both of these elements.

Finally the weight ratio Cl/Na is shown in Fig. 4. It is seen that there is a significant geographic variation also in this ratio which, furthermore, even near the coast has a much lower value, around 1.2, than that characteristic of sea water (1.8). This low ratio of Cl/Na at the coast and the further decrease inland certainly is of great geochemical interest. The land surface can hardly be a significant source for either Na or Cl. With the sea as the only significant terrestrial source and disregarding

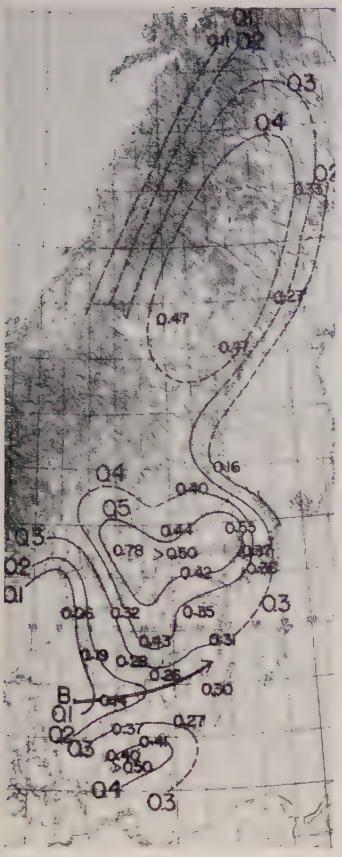

Fig. 10. Weight ratio NH_3—N/Na

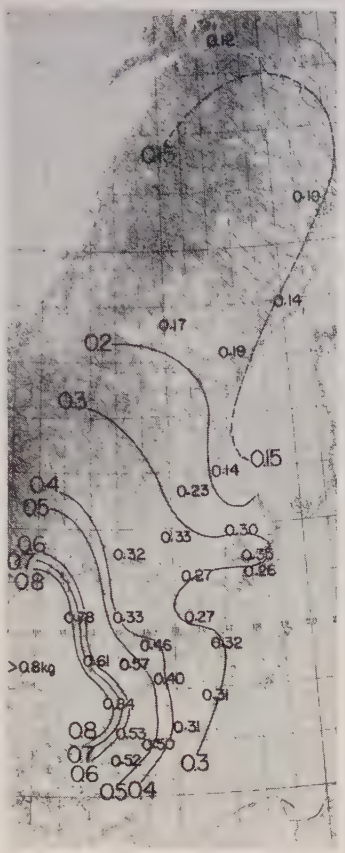

Fig. 11. Yaerly amounts of NO_3—N (kg/har).

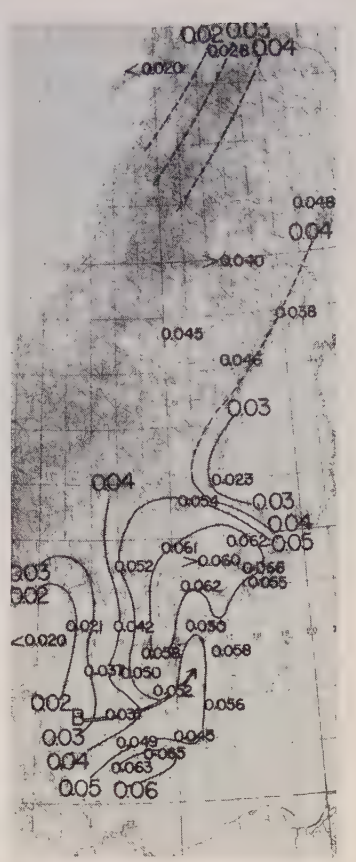

Fig. 12. Weight ratio NO_3—N/Na.

extraterrestrial sources for either of these elements, the distribution of the Cl/Na ratio becomes somewhat of an enigma.

If it is supposed that Na and Cl are brought from the sea to the atmosphere in the same ratio as in the sea (mainly by spray) and that both elements are brought to the ground entirely by precipitation, then either an addition of sodium or a removal of chloride must have taken place in the air during its travel or during the formation of precipitation. Also, these processes must have started before the air entered land. Further, if Na is added and there are no extraterrestrial sources for this element, or if chloride is removed and there are no extraterrestrial sinks for this element then there must be regions on our planet where precipitation contains relatively more Cl than Na as compared to sea water. It seems fruitless at our present state of knowledge to enter into speculations on various possibilities to explain the variation in the Cl/Na ratios. It should be mentioned, however, that CAUER (1949) has suggested a process whereby Cl can be released from solution as Cl_2, chlorine. But in this case the Cl_2 released has to be accounted for in some other way as it is most likely that it ultimately must be brought down by precipitation.

In this connection it is pertinent to refer to an experimental investigat on by KÖHLER and BÅTH (1952), in which they reported on the composition of droplets formed by blowing air over a sample body of sea water. Their conclusion is that »all our experiments indicate that there are droplets of splitted sea water with ratios between the components significantly different from the ratios in sea water in bulk. Droplets with relative excess of Mg and Na

are presumably positively charged, whereas excess of Cl^- (and SO_4^{--}) entails negative charge. Droplets with relative excess of either Mg or Cl are smaller than droplets with normal ratios. It is not possible to conclude from the experiments if there is a relative excess of Mg or Cl in the smallest droplets."

Calcium

The yearly amounts of calcium are shown in Fig. 5 where it is seen that they are fairly uniform, decreasing somewhat to the north. A high value in the south is due to local pollution from a cement factory. No gradient from the west coast can be detected, indicating that this element is fairly widespread in the atmosphere. As the Ca/Na ratio in the sea is 0.038 the sea can hardly be any appreciable source for Ca in precipitation. The soil must be a considerable source as Ca is the most abundant soluble element in soils. However, extra-terrestrial sources can not be excluded completely.

In Fig. 6 the ratios Ca/Na are plotted. As Ca is fairly uniform the pattern is entirely dominated by the variation in Na.

Potassium

In Fig. 7 the yearly amounts of K are plotted. There is a small but definite gradient from the west coast and a slight increase at the east coast north of Stockholm. As potassium in sea water is low (K/Na = 0.036) the sea cannot be the only prominent source although the gradient would so suggest. In Fig. 8 the ratios K/Na are plotted. They increase to a maximum inland and, further, there is a through line in the south indicated by the arrow B. On the west coast the ratio K/Na is about 0.10, which is about three times higher than that in sea water. As the ratios increase inland this means that potassium decreases at a slower rate than sodium. Some of the high values inland may be due to local pollution from cement factories.

As to the origin of K some no doubt comes from the sea but K may also be a rather widespread component in the atmosphere. Some may be released in combustion, forming very small condensation nuclei which, as they are growing slowly, are not readily washed uot by precipitation. Extra-terrestrial addition of K is also conceivable.

Ammonia nitrogen

ÅNGSTRÖM and HÖGBERG (1952) have earlier published results for ammonia and nitrate nitrogen for the whole period October 1947—September 1950. As the period here investigated is limited to two years it may be of interest to include ammonia and nitrate also for this shorter period.

The yearly amounts of H_3N—N are shown in Fig. 9. One of the most outstanding features is the ridge of high amounts in the southwest where the influence of Denmark on the prevailing soutwesterly winds over Sweden is very pronounced. The origin of this maximum is, no doubt, Denmark and as ammonia is mainly released from the ground as gas it is readily picked up and washed out by precipitation. In the east coast area the amounts are generally small, presumably due to washing out by precipitation. There is a small maximum in the Lake Mälaren district which may be significant as this is an important agricultural area. The other maximum to the west is more doubtful and may be due to the effect of local pollution on the readings taken at Varpnäs. The amounts in the north are smaller than in the south since there are but few source regions of ammonia in this part of the Scandinavian peninsula.

In Fig. 10 the ratios H_3N/Na are plotted. The only remarkable is again the trough line indicated by the arrow B.

Though agricultural areas are no doubt important source regions over land, the sea may also contribute to the ammonia content of the air.

Nitrate nitrogen

The NO_3-N also includes NO_2-N which at most can amount to five or ten per cent of the total. In Fig. 11 the yearly amounts are plotted. One remarkable thing is the general pattern of isolines which runs parallel to the coast. Now, it must be admitted that the sampling technique used was not favourable to nitrates, therefore too much weight should not be given to this figures until the results have been confirmed through more reliable data. It is uncertain if these will change the general pattern in Fig. 11 though the amounts may be changed. The NO_3 – N/Na ratios are shown in Fig. 12. Also here a through is in-

dicated by the arrow B on the same place as before. This trough, which appears fairly well-marked in the three charts for $\frac{NH_3-N}{Na}$, $\frac{N}{Na}$, and $\frac{NO_3-N}{Na}$, extends from the Swedish west coast eastward and northeastward through a forest district (Småland) of southern Sweden where the population density, agricultural and industrial activities are lower than in the rich agricultural plain to the south and also somewhat lower than in the areas to the north. It is not inconceivable that this fact is reflected in the slower increase in the relative amounts of K, NH_3-N and NO_3-N along the axis of tongue B.

Though there exist many earlier investigations on the composition of atmospheric precipitation, the present study is the only one which gives a coherent picture of the distribution over a larger area. As such it should be of some geochemical interest. The present investigation suffers from several defects both in planning and inexecution but from the experience gained it has been possible to plan a similar investigation on a much larger scale (Eriksson 1954) which will start operating very soon. From the results of this it should be possible to confirm the distribution patterns over Sweden or to correct them, if necessary, and to get the distribution patterns for various elements over a much larger area. Then it may be possible to gain more definite information on the origin of atmospheric compounds than we now possess.

REFERENCES

Cauer, H., 1949: Ergebnisse Chemisch-meteorologischer Forschung, Archiv für Meteorologie, *Geophysik und Bioklimatolopie*, Serie B, Band I, 221—256.

Egnér H., Eriksson, E. & Emanuelsson, A., 1947: Compositon of Atmospheric Precipitation, I: Sampling Technique. *Ann. Royal Agric. Coll., Sweden* **16**, 593—602.

Eriksson, E., 1952: Composition of Atmospheric Precipitation, I and II, *Tellus* **4**, 215—232, 280—303.

— 1954: Report on an informal conference in atmospheric chemistry held at the Meteorological Institute, University of Stockholm, May 24—26, 1954. *Tellus* **6**, pp. 302—307.

Köhler, H. and Båth, M, 1952: Quantitative chemical analysis of condensation nuclei from sea water. *Nova Acta Regiae Societatis Scientiarium Upsaliensis*, Ser IV, No. 7.

Ångström, A. & Högberg, L., 1952: On the Content of Nitrogen in Atmospheric Precipitation in Sweden II. *Tellus* **4**, 271—279.

Commentaries Concerning Research on the General Circulation

By V. P. STARR, Massachusetts Institute of Technology, Cambridge, Mass.

(Manuscript received February 27, 1954)

Abstract

Several phases of research significant for the general circulation are reviewed briefly. The effect of rotation on convective regimes is discussed. An example is given showing that mean meridional circulations are not essential for the release of potential energy.

During the past several years the present writer has been conducting observational studies on an extensive scale with the aim of securing measures of various quantities chosen on the basis of their direct dynamic significance for the primary mechanism of the general circulation.[1] An outcome of central importance which emerges from this work is that the required meridional transports of angular momentum in the atmosphere are due primarily to horizontal eddy exchange processes, together with the closely allied concept that the kinetic energy of the mean zonal motions is maintained against friction to a large extent by a transference of kinetic energy from the large-scale horizontal eddy kinetic energy to these mean motions.

This action of the eddies is so marked and unambiguous that probably no amount of additional data, if properly brought to bear upon the question, would controvert it.[2] Furthermore, this link in the operation of the general circulation as depicted by the data is so dissimilar to the picture given by most classical schemes which ascribe the drive for the mean zonal motions to the Coriolis force on net meridional flow of air at individual levels, that no really successful manipulation of language or logic can identify them as being, after all, one and the same. We are thus confronted by a state of affairs which, although not completely unsuspected before, is relatively novel in character and hence intriguing—and in many ways puzzling. We must, however, be on the qui vive in our thinking in order to eliminate such difficulties as are merely apparent and not real, and free ourselves of incorrect prepossessions.

In order to show that this behavior of the atmosphere is not unique we may call attention to recent developments of paramount importance for the resolution of the general circulation problem, in the field of experimental hydrodynamics due principally to the original work of D. Fultz and R. Long at the University of Chicago. The particular experiments in question involve the generation of flow patterns in a rotating shallow cylindrical vessel of water resulting from differential heating, which under specified circumstances

[1] It would now appear that the long range planning originally involved in formulating this protracted program has already borne sufficient fruits not only to justify it, but also to suggest rather forcefully the desirability of placing such activities on a firmer footing than has hitherto been possible. Such steps have been advocated before by the writer elsewhere (see STARR 1951), on the basis of preliminary results.

[2] See Appendix.

assume forms similar with respect to a variety of detail to those comprising the atmospheric general circulation (see FULTZ 1952). Some of this work has recently been repeated by A. Faller at the Massachusetts Institute of Technology.

For the purposes of this discussion (and, it should be added, in this writer's opinion) the outstanding new concept made available through these experiments is that the otherwise simple and familiar regime of convective motions is profoundly altered as soon as the rate of rotation exceeds a definite value determined by external parameters such as the intensity of the differential heating. The more intense the heating, the higher becomes this critical rate of rotation. For slow rotation, below the limiting rate, the convection proceeds in an axially symmetric manner with zonal motions developing in much the same fashion as presupposed in the classic explanations of the general circulation. In this case the mean meridional circulations are quite apparent. For rotations higher than the critical one similarity to the atmosphere is obtained as to the following properties (among others): (a) The mean meridional circulations are no longer obvious except perhaps in the form of weak remnants as boundary layer phenomena. (b) Horizontal exchange processes appear to be dominant in the meridional transport of momentum and no doubt other properties as well (see STARR and LONG 1953). The eddies involved are again "waves in the westerlies" as in the atmosphere. (c) The motions appear to be quasi-geostrophic except in the boundary layers. (d) Some evidence of structures within the fluid having the characteristics of occluding cyclones with attendant frontal phenomena has been noted.

To the statement of these experimental findings one should add here a remark concerning some theoretical analyses suggested by them. The symmetrical one is of course the more tractable of the two regimes to study thus, and here the subject has received attention notably from T. V. DAVIES (1952). Still more recently, through the inclusion of the effects of heat advection, H. L. KUO (1953, 1954) has been able to state a necessary condition for the existence of an axially symmetric Hadley type convection in this so-called dishpan experiment. It turns out that a non-dimensional number P involving (among other parameters) the rate of rotation and the axis-to-rim density contrast, is the governing quantity which discriminates between the two regimes and assumes a critical value P_c at the turn-over point. The actual experiments seem to fit in with the theoretical value of P_c in a very satisfactory manner. Preliminary estimates of an analogous parameter for the atmosphere indicate the presence of unmistakable high rotation conditions.

To summarize the situation, it appears that the effect of rotation, if it be rapid enough, is to inhibit large scale convection as ordinarily conceived, and to substitute for it a process which produces the necessary radial transfer of heat and of certain other properties through the agency of quasi-horizontal eddy motions of which cyclones, anticyclones and their attendant upper troughs and ridges are the prime example.

In discussing these matters with other meteorologists the writer has noted frequent skepticism. These reactions seem to imply that any scheme which does not contain some form of the classic convective motions as a starting point is in a general sense too unnatural to be valid, although it is usually not easy to proceed further in order to discover wherein precisely the alleged difficulty lies. It turns out, however, that these attitudes spring mainly from a belief, whether articulate or not, that mean meridional circulations of the toroidal type are indispensable for the utilization of the potential energy inherent in the equator-to-pole temperature gradient in the atmosphere. It is to be sure first necessary to define terms more accurately, but speaking generally this claim is but a delusion, which in actuality the atmosphere circumvents without any real difficulty.

In order to exhibit the nature of the fallacy involved, it suffices to treat a very simple case in the dishpan. Let it be supposed that in the initial state there are two fluids of differing density separated by a vertical discontinuity concentric with the rim as shown in cross section in (a) of the figure and by the inner circle in (b) which is a view seen from the top. It is of course clear that if one of the fluids, say the inner one, is denser the system possesses a certain available potential energy, and the question now is whether some or perhaps all of it can be released without resorting to mean

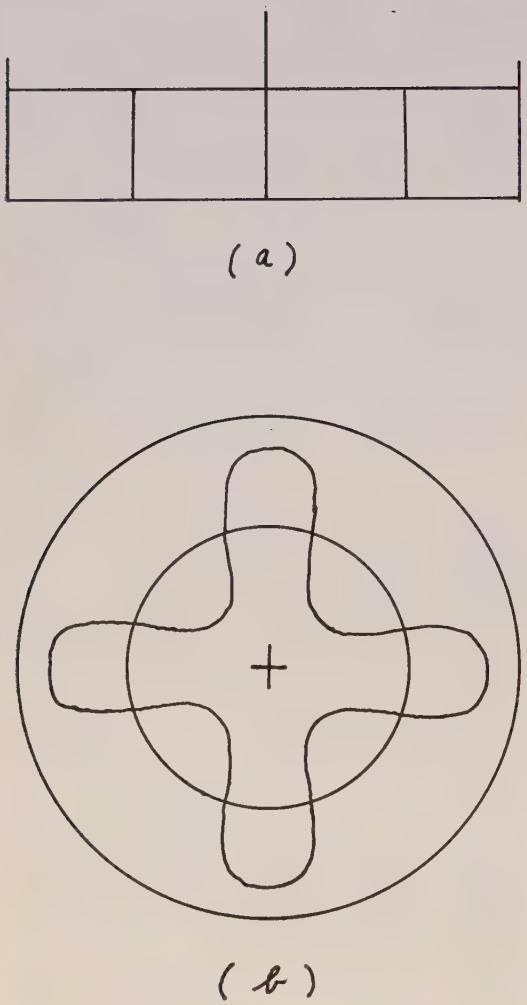

Fig. 1. Diagrams showing a possible rearrangement of two fluids in a cylindrical vessel, prior to the release of potential energy.

meridional circulations, or whether this is precluded through some topological constraint of the continuity principle or other kinematic consideration. It is here assumed that

$$\frac{d\varrho}{dt} = 0; \quad \nabla \cdot \vec{C} = 0; \quad [v] = 0$$

during the readjustment. In these relations ϱ is density, $\vec{C}$ is the vector velocity, v is the inward radial component of velocity, t is time and the square brackets denote zonal space averaging completely around the pan at a given radius and given depth so that the third relation constitutes the stipulation of no mean meridional circulations.

The answer is rather obvious. The total displacements may be divided into two stages so that in the first the vertical velocity w everywhere vanishes and $[v]$ is therefore identically zero because of the continuity requirement. The vertical discontinuity may therefore be deformed by purely two-dimensional motion into the lobed form shown. In the second stage vertical motions are supposed to take place in such a way as to release potential energy but still so as to make $[v]$ zero, say by having $v \equiv 0$, and allowing each lobe to diverge zonally near the bottom and converge zonally near the top (i.e., by having a downward eddy transport of mass).

With a little thought it becomes evident that the simplified model used here may be generalized to include much more complicated initial states involving continuous density distributions of various types, and that the separate stages of motion may be suitably combined. Also one could without difficulty modify the motions so as to liberate potential energy even in spite of a reverse mean meridional circulation, if the downward eddy transport of mass is vigorous enough.

The outlines of the analogous processes in the actual atmosphere are easily recognized on synoptic charts and are very basic meteorological phenomena, appealing as such even to a casual observer.[1] They are embodied in the large-scale outbreaks of cold and warm air so typical of weather conditions over a wide range of latitude. Viewed from the present standpoint these facts suggest anew the importance of such endeavors as those of ROSSBY (1949) and PHILLIPS (1949) to study the mechanism for the release of potential energy by the sinking of cold air domes.

[1] We here make the tacit (but probably correct) assumption that the release of geopotential energy is necessary for the maintainance of the general circulation. Since the total geopotential energy of the atmosphere must on hydrostatic principles bear a fixed ratio to its total internal heat energy, and futhermore since the sum is maintained at a more or less fixed value when radiational and other effects are included, it becomes a philosophical problem of considerable complexity to ascertain whether the generation of kinetic energy takes place more directly from one of the forms of energy mentioned rather than the other.

Appendix

As pointed out by STARR (1953) the transfer of kinetic energy from the eddies to the mean zonal motions is a deep-seated process intense enough to generate in a short period of time an amount of such energy as is normally present—even according to measurements which are probably underestimates of its true potency. The inquiring reader may nevertheless propose that in spite of the fact that it is difficult to secure accurate measurements of the mean meridional circulations in the atmosphere due to their smallness, as an experiment a direct calculation should be made of their efficacy in generating mean zonal kinetic energy through the action of the Coriolis force, using the best data at hand. Formally this can be done with the aid of the compilations of actual wind statistics for the calender year of 1950 given by STARR and WHITE (1954) and used in the reference given above. However, as has been stated frequently by these authors, much is left to be desired in such use of the data, and the calculations made here can indeed be viewed as an experiment only.

The hemispheric wind statistics were compiled from daily data for 13°, 31°, 42°, 55° and 70° N latitude for levels from 1000 to 100 mb. The first consideration is that due most probably to a bias in the selection of the station network so as to favor unduly conditions either to the front of troughs on the one hand, or of ridges on the other, small net mean velocities were obtained across the several latitude walls. These, in order, were −22, −03, −17, +37 and +64 cm sec^{-1} (velocities taken positive northward). Only the last two are really serious in regard to magnitude and would imply a mean rising motion in the polar regions at practically all levels in the troposphere and into the stratosphere, if taken literally. In view of this situation, these mean values of the meridional velocities were subtracted out from the data at all latitudes in an effort to minimize spurious effects. All mean meridional circulations were taken to be zero at the equator.

The effect of the Coriolis forces associated with the mean meridional circulations in producing kinetic energy of mean zonal motions is an amount $\varrho f [\overline{u}] [\overline{v}]$ per unit volume (see, e.g., KUO 1951). Here ϱ is density, f the Coriolis parameter, u the eastward and v the northward component of wind velocity; brackets signify zonal averages and bars time averages. The (volume) integrals of this quantity by latitude belts and also for the whole northern hemisphere (up to 100 mb) are given in the table below in units of 10^{20} ergs per second.

No measures of statistical significance were calculated for these figures, although this could have been done, let us say by computing the daily results and then finding the standard error of the mean. It was not deemed worth the while to do this.

Although it is true that not much reliance can be placed upon the particular outcome here obtained, it should be carefully observed that there exists no valid reason which would necessarily exclude the possibility of such a small negative value of the integral for the hemisphere. The contribution of the energy transfer from the eddies is sufficiently large to allow for this (see STARR 1953 and ARAKAWA 1953). Also one may note that it is the (indirect) cell in middle latitudes which is most effective for the present problem, because an equally intense one at low latitudes is rendered much less potent due to the smallness of the Coriolis parameter, while nearer to the pole the length of latitude circles and hence the amount of air involved becomes small. A net destruction of kinetic energy of mean zonal motions by mean meridional circulations would imply as suggested by CHARNEY (1951), that these latter are merely secondary effects, or perhaps associated with surface friction as discussed by FLOHN (1953), for example.

It is doubtful whether the technique of subtracting out the over all mean velocities across latitude walls really eliminates all the unwholesome consequences of any appreciable bias in the sense of sampling of conditions to the east of troughs unduly, as probably was the case at 55° and 70° N. In the forward portions of troughs at high latitudes there usually is found an increase with elevation in the troposphere of the northward component of the wind. Mere subtraction of the over all mean velocity still leaves an abnormally large sampling of this vertical shear in the data, which then manifests itself as a spuriously strong direct mean meridional cell at a northerly location. The positive contributions shown in the table north of 55° N may owe their origin in part to such an artificially introduced circumstance.

In the computations made above, only the effect of the Coriolis term in generating kinetic energy of mean motions was evaluated. This term, however, occurs in combination with others which likewise represent means through which the mean meridional circulations can contribute to the generation of this kinetic energy. For example the term $[\varrho w] [u] \frac{\partial}{\partial z} [u]$ also enters the problem (see KUO 1951). Here w is the vertical component of velocity and z is height. This quantity could be evaluated from the data already used, although the work was not actually done. Since in the troposphere the term normally takes the algebraic sign of the vertical motion, and since this motion is apt to be downward in the latitudes of the strongest vertical shear in the westerlies, it is quite possible that the total effect is negative.

Many findings will no doubt be reported in the course of time relative to direct evidences of mean meridional circulations. What has been said here makes it evident that such claims must not only be scrutinized carefully as to their reliability, but also it is essential that their importance for maintaining the mean zonal motions be properly assessed from a sufficiently realistic viewpoint. For we have reached such a stage in the development of our subject, that the halcyon, free-wheeling days when investigators could propound mean meridional cells in a rough and ready manner to explain each feature of the mean zonal wind distribution, are irretrievably behind us.

Table 1. Volume integral up to the 100 mb level of quantity $\varrho \cdot f [\overline{u}] [\overline{v}]$ in 10^{20} erg sec^{-1}.

Lat. Belt	0—13°	13—31°	31—42°	42—55°	55—70°	70—90°	Hemisphere
Integral	+ 0.01	— 0.35	— 3.55	— 2.65	+ 2.69	+ 1.76	— 2.09

REFERENCES

Arakawa, H., 1953: On the time rate of work done by the eddy stresses in the free air, and the maintenance of the westerlies in middle latitudes. *J. Met.*, **10**, pp. 392 – 393.

Charney, J., 1951: On baroclinic instability and the maintenance of the kinetic energy of the westerlies. *Un. Geod. et Geophys. int. neuvieme ass. gen.*, Brussels.

Davies, T. V., 1953: The forced flow of a rotating viscous liquid which is heated from below. *Phil. Trans, Roy. Soc. London*, **246**, pp. 81 – 112.

Flohn, H., 1953: Wilhelm Meinardus und die Revision unserer Vorstellungen von der atmosphärischen zirkulation. *Zeitschrift für Meteorologie*, **7**, pp. 97 – 108.

Fultz, D., 1952: On the possibility of experimental models of the polarfront wave. *J. Met.*, **9**, pp. 379 – 384.

Kuo, H. L., 1951: A note on the kinetic energy balance of the zonal wind systems. *Tellus*, **3**, pp. 205 – 207.
1953: On convective instability of a rotating fluid.
– Symposium on hydrodynamic model experiments, Johns Hopkins University, Baltimore, Maryland, September 1 – 4, 1953.
– 1954: Symmetrical disturbances in a thin layer of fluid subject to a horizontal temperature gradient and rotation. *J. Met.* (in press).

Kuo, H. L., 1954: On convective instability of a rotating fluid with a horizontal temperature contrast. (unbublished).

Phillips, N. A., 1949: The work done on the surrounding atmosphere by subsiding cold air masses. *J. Met.*, **6**, pp. 193 – 199.

Rossby, C.-G., 1949: On a mechanism for the release of potential energy in the atmosphere. *J. Met.*, **6**, pp. 163 – 180.

Starr, V. P., 1951: The physical basis for the general circulation, pp. 541 – 550 in *Compendium of Meteorology* Boston, Amer. Met. Soc., 1334 pp.
– 1953: Note concerning the nature of the large-scale eddies in the atmosphere. *Tellus*, **5**, pp. 494—498 .

Starr, V. P., and White, R. M., 1951: A hemispherical study of the atmospheric angular momentum balance. *Q.J.R.M.S.*, **77**, pp. 215 – 225.
– 1952: Meridional flux of angular momentum in the tropic. *Tellus*, **4**, pp. 118 – 125.

Starr, V. P., and Long, R. R., 1953: A study of the flow of angular momentum in rotating model experiments. Geophysical Research Papers, 24, Geophysics Research Directorate, Cambridge, Mass.

Starr, V. P., and Collaborators, 1954: Final report, general circulation project, No. AF 19 – 122 – 153. Massachusetts Institute of Technology (in press).

Energy Transformations and Meridional Circulations associated with simple Baroclinic Waves in a two-level, Quasi-geostrophic Model[1]

By NORMAN A. PHILLIPS

Institute for Advanced Study, Princeton

(Manuscript received April 5, 1954)

Abstract

The changes in geostrophic kinetic energy predicted by the "$2-\frac{1}{2}$ dimensional" quasi-geostrophic vorticity equations without friction are shown to be compatible with the mechanical energy equation. The second-order effects on a zonal current due to the presence of very simple unstable baroclinic waves are then analysed, using a two-level model of finite lateral width without friction or heat sources. In addition to the poleward transport of sensible heat and the creation of kinetic energy by these waves, it is shown that they are accompanied in this model by a weak meridional circulation. This circulation consists of an indirect cell in middle latitudes with direct cells to the north and south. The possible importance of this mechanism in providing appropriately distributed sources and sinks of relative zonal momentum (and therefore in prescribing the distribution with latitude of the surface zonal winds) is demonstrated with the aid of Widger's observations of the horizontal momentum transfer by eddies during January 1946. Finally it is shown that about 95 per cent of the perturbation energy in the unstable waves of this type comes from the "potential energy" of the basic current, the small remainder coming from the kinetic energy of that current.

1. Introduction

It is now quite generally recognized that the large-scale disturbances of extra-tropical latitudes play an important role in the maintenance of the "general circulation" of those latitudes. Their role as agents for the poleward transport of sensible heat was pointed out some time ago by DEFANT (1921), and a few years later, JEFFREYS (1926) suggested that they were also important in the latitudinal transport of angular momentum. These first considerations have been verified in recent years by the actual measurement of these transports using aerological charts and data [WIDGER (1949), WHITE (1951)].

Theoretical investigations of the dynamic and kinematic properties of these turbulence elements have also been carried out in recent years, using the technique of the linearized perturbation theory, where the disturbances are considered to be small perturbations superimposed on a zonal basic current. These theoretical studies may be divided into two principal types. The first, to which we may apply the adjective "baroclinic", has considered the basic current to be a function of height only, latitudinal variations in this basic current being neglected (CHARNEY, 1947). The second type, which we may call "baro-

[1] A portion of the research reported on in this paper was performed at the Institute for Advanced Study under contract N-6-ori-139 with the Office of Naval Research and the Geophysics Research Directorate, Air Force Cambridge Research Center.

tropic", has neglected the vertical increase of the zonal current but has considered instead the effect of latitudinal variations in this quantity (KUO, 1949).

In both analyses, unstable (amplifying) and stable (damped) types of waves are mathematically possible. However, the kinematics of these theoretical motions are such that the disturbances one encounters on actual weather charts seem to be best described by a combination of the *amplifying baroclinic* wave and the *damped barotropic* wave. The pure amplifying baroclinic wave transports energy northward and generates kinetic energy (KUO, 1952). The pure damped barotropic wave does not change the total amount of kinetic energy, but the kinetic energy of the wave is instead organized into the kinetic energy of the basic zonal motion. This last process is accompanied by latitudinal momentum transports of the type described by Jeffreys (see also STARR, 1948).

The combination of the barotropic and baroclinic effects in a perturbation analysis has not yet been accomplished. Furthermore, the effects of non-adiabatic heat changes and friction have not been included in these theories. The mathematical difficulties involved are not trivial, and it may be that the analysis of the role the large-scale disturbances play may be best accomplished with the aid of high speed computing machines in the following manner. Using an appropriate system of prediction equations for the large-scale motions, including friction (surface skin friction is probably most important) and some simplified representation of the non-adiabatic effects (perhaps as a simple function of latitude and height), the machine could be instructed to forecast the development of the flow pattern with time, beginning, say, with some simple initial situation. One would then examine the forecast after some time to see what types of disturbances appeared and what kind of zonal wind distribution was created.

The present paper is written partly as a prelude to such an experiment (which the writer and his colleague Dr Jule Charney hope to carry out at the Institute for Advanced Study) and also to describe some interesting properties of the simple baroclinic waves with special reference to the importance of these properties for the general circulation in extra-tropical latitudes.

2. The quasi-geostrophic equations and boundary conditions

In investigating the role of baroclinic disturbances in the general circulation, we shall, for simplicity, assume that these motions are adequately described by the geostrophic equations for a "2 1/2 dimensional model" (CHARNEY and PHILLIPS, 1952). With some slight additional simplification, these may be written

$$D_1 (f+\zeta_1)/Dt - p_0^{-1}\, 2 f\omega_2 = 0 \qquad (1)$$

$$D_3 (f+\zeta_3)/Dt + p_0^{-1}\, 2 f\omega_2 = 0 \qquad (2)$$

$$p_0^{-1}\, 2\, \omega_2 - f^{-2}\lambda^2 D_{1,3}\,(\varphi_1 - \varphi_3)/Dt = 0 \qquad (3)$$

The subscripts 1, 2, and 3 refer to quantities measured at the 250-, 500-, and 750-mb levels, respectively. The operator D/Dt is defined by

$$D/Dt = \partial/\partial t + \boldsymbol{v}\cdot\nabla$$

where ∇ is the horizontal gradient operator on a constant pressure surface and $\boldsymbol{v}$ is the horizontal (geostrophic) velocity vector. ω_2 is equal to the value of dp/dt at the 500-mb level. φ is the geopotential and λ^2, assumed to be constant, is given by the formula

$$\lambda^2 = \{\Phi_1 - \Phi_3\}^{-1} f^2 [\Theta_2/(\Theta_1 - \Theta_3)]$$

where Θ is potential temperature and $\{\Phi_1 - \Phi_3\}$ represents a typical value of the geopotential difference between levels one and three. p_0, which we have taken as 1000 mb, is the (constant) approximate value of the pressure at the ground. We shall describe the motion in a cartesian coordinate system (x to the east, y to the north) so that the relative vorticity ζ is given by $\partial v/\partial x - \partial u/dy$. The coriolis parameter, f, is considered to be a constant everywhere except in the term Df/Dt, where we assume that $\partial f/\partial y = \beta = \text{constant}$ (ROSSBY, 1939).

We shall represent the extra-tropical atmosphere as being limited "latitudinally" at $y = \pm w$ by fixed vertical walls. In the x-direction we shall assume cyclic continuity, i.e. the motion at $x = L$ is identical with that at $x = 0$.

The solution of (1), (2), and (3) requires boundary conditions at $y = \pm w$ in addition to the cyclic conditions at $x = 0$ and L. The

kinematic boundary condition at the walls requires that $v=0$ at $y=\pm w$. Geostrophically this implies

$$\partial\varphi/\partial x=0 \quad \text{at} \quad y=\pm w \tag{4}$$

Thus, at any one value of t, φ at the walls must not vary with x. This is not sufficient, however, to determine a unique solution to (1), (2), and (3) since this constant value of φ may vary with time. Another condition may be obtained by integrating the first equation of motion in the form

$$u_t+uu_x+vu_y-fv+\varphi_x=0$$

with respect to x, with $v=0$. (The subscripts here indicate differentiation.) We find that all terms disappear except u_t and we get, geostrophically,

$$\int_0^L (\partial^2\varphi/\partial y\,\partial t)\,dx=0 \qquad y=\pm w \tag{5}$$

This, together with (4), is enough to determine uniquely the solution of (1), (2), and (3).[1]

3. The mechanical energy equation for geostrophic motions

The simplified system of quasi-geostrophic equations (1), (2), and (3) allows accelerations of the motion to occur in spite of the fact that according to the equations of motion, geostrophic balance corresponds to zero acceleration. This by now familiar paradox is of course explainable in that the geostrophic approximation is not introduced directly into the equations of motion but is introduced instead into the vorticity equation after the horizontal divergence (which cannot be measured geostrophically) has been eliminated (Charney, 1948).

Since any change in the kinetic energy of horizontal motion must be accompanied by horizontal accelerations, a legitimate question may arise as to the extent to which the motions (and accelerations) predicted by the quasi-geostrophic equations satisfy the energy equation. We shall now demonstrate that (1), (2), and (3) do satisfy the mechanical energy equation in a certain sense.

We first derive a form of the mechanical energy equation suitable to our model, following to some extent the technique introduced by Starr (1951 b). Multiplication of the horizontal equations of motion in the x, y, p, t-coordinate system by u and v first yields

$$q_t+\boldsymbol{v}\cdot\nabla q+\omega q_p+\boldsymbol{v}\cdot\nabla\varphi=0$$

where q is the horizontal kinetic energy per unit mass, $1/2\,(u^2+v^2)$. It would clearly be meaningless to introduce the geostrophic approximation here, since then the last term would vanish. We therefore postpone this step and utilize the continuity equation in this coordinate system (Eliassen, 1949)

$$\nabla\cdot\boldsymbol{v}+\partial\omega/\partial p=0 \tag{6}$$

to derive another form of the equation:

$$q_t+\nabla\cdot(q+\varphi)\boldsymbol{v}+(\omega q)_p+\varphi\omega_p=0 \tag{7}$$

(7) may now be specialized to our model by evaluating it at levels one and three and introducing the approximations (Charney and Phillips, 1952)

$$\omega_{p\,1}=-\omega_{p\,3}=p_0^{-1}\,2\,\omega_2, \text{ and}$$
$$(\omega q)_{p\,1}=-(\omega\varphi)_{p\,3} \tag{8}$$

Adding the two equations which result, and integrating over the region $-w\leqslant y\leqslant w$, $0\leqslant x\leqslant L$, we get finally

$$\left.\begin{aligned}&\frac{\partial}{\partial t}\int\int(q_1+q_3)\,dx dy+\\&+\frac{2}{p_0}\int\int(\varphi_1-\varphi_3)\omega_2 dx dy=0\end{aligned}\right\} \tag{9}$$

This is the form of the mechanical energy equation which is applicable to our 2 1/2-dimensional model. It states that the total kinetic energy q_1+q_3 may change as a result of a net correlation between the thickness $(\varphi_1-\varphi_3)$ and ω_2.

The geostrophic assumption *has not been* used in deriving (9). We now propose to demonstrate that (9) is satisfied if both ω_2 and the kinetic energy q are determined and

[1] Except for a constant of integration determined by the average value of $\partial(\varphi_1+\varphi_3)/\partial t$ over the entire region. The value of this integration constant plays absolutely no part in the conclusions we shall come to in the remainder of this paper; for convenience, therefore, it has been set equal to zero.

measured *geostrophically* by (1), (2), (3) and the boundary conditions (4) and (5).

(1) and (2) may be written

$$f^{-1}\nabla^2\varphi_{1t}+\boldsymbol{v}_1\cdot\nabla(f+\zeta_1)-p_0^{-1}2f\omega_2=0$$

$$f^{-1}\nabla^2\varphi_{3t}+\boldsymbol{v}_3\cdot\nabla(f+\zeta_3)+p_0^{-1}2f\omega_2=0$$

where we have introduced the geostrophic approximation for $\partial\zeta/\partial t$. Multiplying these two equations respectively by $-\varphi_1$, and $-\varphi_3$, using the identity $\nabla\cdot\varphi\nabla\varphi_t=\varphi\nabla\varphi_t+\nabla\varphi\cdot\cdot\nabla\varphi_t$, and then adding, we obtain

$$f^{-1}(\nabla\varphi_1\cdot\nabla\varphi_{1t}+\nabla\varphi_3\cdot\nabla\varphi_{3t})-$$
$$-f^{-1}\nabla\cdot(\varphi_1\nabla\varphi_{1t}+\varphi_3\nabla\varphi_{3t})-$$
$$-[\varphi_1\boldsymbol{v}_1\cdot\nabla(f+\zeta_1)+\varphi_3\boldsymbol{v}_3\cdot\nabla(f+\zeta_3)]+$$
$$+p_0^{-1}2f(\varphi_1-\varphi_3)\omega_2=0$$

$\boldsymbol{v}_1$ and $\boldsymbol{v}_3$ in this equation are of course geostrophic. It is then simple to show that when this equation is integrated over the region $-w\leqslant y\leqslant w$, $0\leqslant x\leqslant L$, the boundary conditions (4) and (5) make the contribution from the second and third terms vanish (remember that f as a coefficient is constant). We are then left with

$$\left.\begin{aligned}\frac{\partial}{\partial t}\int\int\frac{1}{2f}[(\nabla\varphi_1)^2+(\nabla\varphi_3)^2]\,dxdy+\\+\frac{2f}{p_0}\int\int(\varphi_1-\varphi_3)\,\omega_2 dxdy=0\end{aligned}\right\}\quad(10)$$

which, after division by f, is the geostrophic equivalent of (9).

The appearance of only the *geostrophic* kinetic energy in (10), and not the total horizontal kinetic energy is not too surprising. It is, in fact, quite analogous to the case of simple hydrostatic motion, where the energy equation does not include the kinetic energy of the vertical motion. We may remark finally that since (10) was derived without the use of (3), our demonstration of the compatibility of the mechanical energy equation (9) and the quasi-geostrophic equations does not involve any assumption of adiabatic motion.

4. The perturbation equations

The theoretical treatment to date of the non-stationary disturbances of extra-tropical latitudes has been carried out under the assumption that the motion is both adiabatic and frictionless. The linearized perturbation theories then demonstrate the possibility of unstable waves which grow exponentially with time. These unstable waves, especially those which are most unstable (Eady, 1949), are presumably to be identified with the disturbances we actually see on upper air charts. Good evidence for this is to be found in the fact that the pressure, temperature, and vertical motion fields in many actual developing disturbances are quite similar to those in the theoretical perturbations (Kuo, 1952).

In the remainder of this paper we will study the kinematic features of the unstable baroclinic waves (although in a very simplified form), and use these results to compute the effects of these motions on the basic zonal current. This will be done by using the perturbation solutions to evaluate the nonlinear "stress" terms which appear in the zonally averaged equations for the rate of change of the mean current. We will then attempt to show that the effects induced in this manner are such as to counteract the neglected effects of (surface) friction and nonadiabatic processes on the mean motion. The reasoning therefore embodies the tacit assumption that the overall kinematics of the *disturbances* are not influenced significantly by the neglected physical processes and the mathematical simplifications introduced by the perturbation theory.

The most detailed analysis to date of the kinematics of the unstable baroclinic wave has been made by Kuo (1952), who has shown that the waves transfer sensible heat northward, create kinetic energy, and may be important in the vertical transport of zonal momentum. However, Kuo's analysis has the limitation that his calculations are based on the assumption that the perturbations are completely independent of the y-coordinate. Since the latitudinal extent of the actual disturbances is of the same order of magnitude as the x-wavelength of the most unstable wave in this theory, it seems reasonable that the additional kinematic effects introduced by lateral limitations on the motion may not be insignificant.

We are led thus to the study of the properties of small perturbations superimposed on a zonal flow limited at $y=\pm w$ by fixed walls.

For simplicity we will again use the "2 – 1/2 dimensional" equations (1), (2), and (3) as a crude approximation to the more realistic equations employed by CHARNEY (1947) and KUO (1952).

The basic current will be defined by the process of averaging with respect to x; such averaged quantities will be denoted by a bar, $\bar{}$, or by a capital letter. Deviations from this zonal average will be indicated by a prime superscript, $'$. Using this convention, equations (1), (2), and (3) may now be combined into the following two equations:

$$\left.\begin{aligned}
&\left[f\frac{\partial}{\partial t}-(\Phi_{1\,y}+\varphi'_{1\,y})\frac{\partial}{\partial x}+\varphi'_{1\,x}\frac{\partial}{\partial y}\right]\\
&[f\beta y+\Phi_{1\,yy}+(\varphi'_{1\,xx}+\varphi'_{1\,yy})-\lambda^2(\Phi_1-\\
&\qquad-\Phi_3+\varphi'_1-\varphi'_3)]=0\\
&\left[f\frac{\partial}{\partial t}-(\Phi_{3\,y}+\varphi'_{3\,y})\frac{\partial}{\partial x}+\varphi'_{3\,x}\frac{\partial}{\partial y}\right]\\
&[f\beta y+\Phi_{3\,yy}+(\varphi'_{1\,xx}+\varphi'_{3\,yy})+\lambda^2(\Phi_1-\Phi_3+\\
&\qquad+\varphi'_1-\varphi'_3)]=0
\end{aligned}\right\}\quad(11)$$

where f, β, and λ^2 are constants. The equations for the rate of change of the mean motion are obtained by averaging these with respect to x:

$$\left.\begin{aligned}
&\Phi_{1\,yyt}-\lambda^2(\Phi_{1\,t}-\Phi_{3\,t})=\\
&=f^{-1}\overline{\left[\varphi'_{1\,y}\frac{\partial}{\partial x}-\varphi'_{1\,x}\frac{\partial}{\partial y}\right]}\\
&\overline{[(\varphi'_{1\,xx}+\varphi'_{1\,yy})-\lambda^2(\varphi'_1-\varphi'_3)]}\cdot\\
&\Phi_{3\,yyt}+\lambda^2(\Phi_{1\,t}-\Phi_{3\,t})=\\
&=f^{-1}\overline{\left[\varphi'_{3\,y}\frac{\partial}{\partial x}-\varphi'_{3\,x}\frac{\partial}{\partial y}\right]}\cdot\\
&\overline{[(\varphi'_{3\,xx}+\varphi'_{3\,yy})+\lambda^2(\varphi'_1-\varphi'_3)]}
\end{aligned}\right\}\quad(12)$$

Thus the time rate of change of the basic current, as described by $\Phi_{1\,t}$ and $\Phi_{3\,t}$, is influenced by "stress" terms which arise from non-linear interactions of the deviations from zonal flow. In the perturbation theory the deviations φ'_1 and φ'_3 are considered to be small, of the first order. (12), in combination with (5) and (4), then states that $\Phi_{1\,t}$ and Φ_{3t} are at most of the second order.

We may now separate out the first order terms in (11), making the additional assumption that Φ_1 and Φ_3 are linear functions of y, i.e. we assume that the basic current velocities $U_1=-f^{-1}\Phi_{1\,y}$ and $U_3=-f^{-1}\Phi_{3\,y}$ are initially independent of y. (Note, however, that we do not place this restriction on the second order quantities $U_{1\,t}$ and $U_{3\,t}$).

$$\left.\begin{aligned}
&\left[\frac{\partial}{\partial t}+U_1\frac{\partial}{\partial x}\right]\\
&[\varphi'_{1\,xx}+\varphi'_{1\,yy}-\lambda^2(\varphi'_1-\varphi'_3)]+\\
&+[\beta+\lambda^2(U_1-U_3)]\varphi'_{1\,x}=0\\
&\left[\frac{\partial}{\partial t}+U_3\frac{\partial}{\partial x}\right]\\
&[\varphi'_{3\,xx}+\varphi'_{3\,yy}+\lambda^2(\varphi'_1-\varphi'_3)]+\\
&+[\beta-\lambda^2(U_1-U_3)]\varphi'_{3\,x}=0
\end{aligned}\right\}\quad(13)$$

5. Kinematics of the unstable perturbations

For convenience we define

$$\left.\begin{aligned}
V&\equiv 1/2\,(U_1-U_3),\\
B&\equiv\lambda^{-2}\beta,\\
\mu&\equiv\pi/2\,w,\\
k&\equiv 2\pi/L,\ \text{and}\\
\alpha&\equiv\lambda^{-2}(k^2+\mu^2).
\end{aligned}\right\}\quad(14)$$

(13) will then be satisfied by wave solutions of the form $\varphi'\sim\cos\mu y\exp ik(x-ct)$. [The $\cos\mu y$ term is present to satisfy the boundary condition (4).] The phase speed c must satisfy the equation

$$\left.\begin{aligned}
&c={}^1\!/_2\,(U_1+U_3)+[\alpha(2+\alpha)]^{-1}\\
&\left[-(1+\alpha)\,B\pm\sqrt{B^2-\alpha^2(4-\alpha^2)\,V^2}\right]
\end{aligned}\right\}\quad(15)$$

We see that for a given value of α there are two possible values of c, and that when $\alpha<2$, it is possible that c may be complex. The exact condition for complex c is

$$V^2\alpha^2(4-\alpha^2)>B^2\qquad(16)$$

A complex value of c means that the perturbation either amplifies or damps exponentially with time. We are interested in the amplifying type, which we are taking as representative of the disturbances in the real extra-tropical atmosphere. These are obtained by taking the plus sign in (15) when (16) is satisfied. For this case it is easily shown that the pertur-

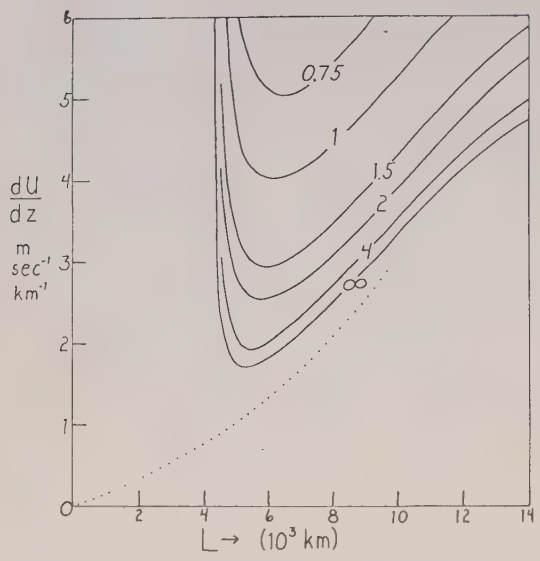

Fig. 1. The time in days required for an unstable wave in the two-level model to double its amplitude, given as a function of the vertical wind shear in the basic current and the wavelength. The dotted line represents the curve $\nu_i = 0$ for the perturbation analyses of Charney and Kuo.

bations φ_1' and φ_3' are given by the following formulae:

$$\left.\begin{aligned} \varphi_3' &= D e^{\nu_i t} \cos \mu y \cos k(x - c_r t) \\ \varphi_1' &= \sigma D e^{\nu_i t} \cos \mu y \cos [k(x - c_r t) + \psi] \end{aligned}\right\} \quad (17)$$

The constant D, which determines the absolute amplitude of the disturbance, is completely arbitrary because of the linearity of (13). However, the relative amplitude σ is determined, as is the phase angle ψ:

$$\left.\begin{aligned} \sigma &= [(2\alpha V + B)/(2\alpha V - B)]^{1/2} \\ \tan \psi &= (2+\alpha)\, \nu_i/(k\alpha V) \end{aligned}\right\} \quad (18)$$

where $\nu_i = k c_i$ is the "frequency of flight", given by

$$\nu_i = k [\alpha^2(4-\alpha^2) V^2 - B^2]^{1/2} [\alpha(2+\alpha)]^{-1} \quad (19)$$

Thus in the amplifying wave ($\nu_i > 0$) the φ_1' wave is larger in amplitude than the wave in φ_3' and lags behind it (for $\nu > 0$). The real phase speed is given by c_r:

$$c_r = 1/2\, (U_1 + U_3) - [\alpha(2+\alpha)]^{-1} (1+\alpha) B$$

To obtain an idea of the magnitude of this instability, the time $\tau = \nu_i^{-1} \ln 2$ required for a given perturbation to double in size is shown in fig. 1 as a function of the wind shear and the wave length L. Numerical values of the other parameters used are as follows:

$$\left.\begin{aligned} \{\Phi_1 - \Phi_3)\} &= 9.81 \times 8.16 \times 10^3 \text{ m}^2 \text{ sec}^{-2} \\ \Theta_2/(\Theta_1 - \Theta_3) &= 316/36 \sim 8.8 \\ \mu &= 3/R_e \\ dU/dz &= 2\, g V \{\Phi_1 - \Phi_3\}^{-1} \end{aligned}\right\} \quad (20)$$

R_e is the radius of the earth, so the distance $2w$ corresponds to sixty degrees of latitude. The constant values of f and β were evaluated at 45° latitude.

For reference it may be of interest to note that the mean value of dU/dz on the winter meridional cross sections published by Hess (1948) and by Palmén and Newton (1948) is about 2.3 m sec^{-1} km^{-1}, the maximum value of dU/dz on Hess's section being about 4.3 m sec^{-1} km^{-1} at 35° N. This corresponds to a time of between one to three days for a doubling of the size of the disturbance.

The wave length of maximum instability seems to be about 6,000 km. This corresponds to a wave number of about five at 45 degrees latitude.

Although the stability criterion (16) has been derived on the assumption that V is independent of latitude, it is interesting to examine the summer and winter cross sections of Hess (1948) to see at what latitudes (16) is satisfied. The most favorable conditions are obtained by choosing L so that $\alpha^2 = 2$. Replacing α^2 by 2 in (16) we find that the criterion for instability is satisfied when

$$\frac{\cos \varphi}{\sin^2 \varphi} < \frac{4\, \Omega\, R_e \Theta_2}{\{\Phi_1 - \Phi_3\}\, (\Theta_1 - \Theta_3)} |V| \sim 0.1\, |U_1 - U_3|$$

where $U_1 - U_3$ is in m sec^{-1} and φ is latitude. Ω is the angular velocity of the earth and R_e the radius of the earth. This relationship is shown in fig. 2, and may perhaps be taken as a partial explanation of the seasonal changes in cyclone activity, both in intensity and latitude.

A more exact solution of the quasi-geostrophic perturbation equations has been made by Charney (1947) and Kuo (1952). Their results differ from those above primarily in that sufficiently short waves may always be unstable. In fig. 1 this would mean that the region of instability would be delineated by

the dotted line. However, Kuo has shown that the values of ν_i in the added region of instability are very small. Since in this discussion we shall be most interested in the waves with large ν_i, it seems reasonable to accept the results we have derived here as a reasonably good first approximation to the kinematics of the baroclinic waves.

6. Second order changes in the basic current

Equation (12) and the boundary condition (5) tell how the basic current will change with time. The perturbation analysis has given us expressions for the perturbations φ_1' and φ_3' which are correct to the first order. We are therefore in a position to evaluate the right side of (12) correct to the second order, and thereby obtain $\Phi_{1\,t}$ and $\Phi_{3\,t}$ correct to the second order.

In using (17) to evaluate the right side of (12), we find that the terms involving $\varphi'_{xx} + \varphi'_{yy}$ drop out, i.e. the perturbation advection of perturbation vorticity is zero. This is a consequence of our assumption that U_1 and U_3 are (initially) independent of y. The other terms, representing the advection of perturbation thickness by the perturbation velocities, do not drop out. We find then that (12) may be written

$$\left.\begin{aligned} \Phi_{1\,\xi\xi t} - \gamma\,(\Phi_{1\,t} - \Phi_{3\,t}) &= -\tfrac{1}{2}\,A \sin 2\,\xi \\ \Phi_{3\,\xi\xi t} + \gamma\,(\Phi_{1\,t} - \Phi_{3\,t}) &= \tfrac{1}{2}\,A \sin 2\,\xi \end{aligned}\right\} \quad (21)$$

where

$$\left.\begin{aligned} A &= [\lambda^2 D^2 (\exp 2\,\nu_i t)\,\alpha\,(2+\alpha)\nu_i]\,[f\mu\,(2\,\alpha V - B)]^{-1} \\ \gamma &= \mu^{-2}\lambda^2 \end{aligned}\right\} \quad (22)$$

and we have introduced the new dimensionless variable

$$\xi \equiv \mu y = (\pi/2)\,(y/w)$$

The solution of (21) satisfying the lateral boundary condition (5) at $\xi = \pm\pi/2$ is

$$\left.\begin{aligned} \Phi_{1\,t} &= -\Phi_{3\,t} = \frac{A}{2\,(2+\gamma)} \\ &\left[\frac{\sinh\sqrt{2\,\gamma}\,\xi}{\sqrt{2\,\gamma}\cosh\sqrt{2\,\gamma}\,\pi/2} + \frac{1}{2}\sin 2\,\xi\right] \end{aligned}\right\} \quad (23)$$

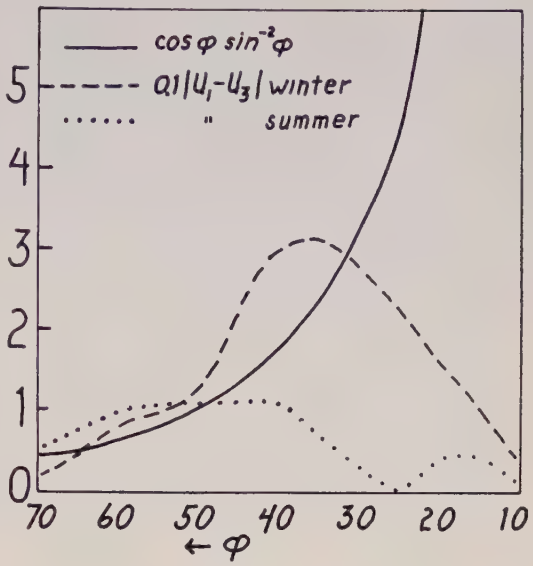

Fig. 2. The satisfaction of the stability criterion for baroclinic waves in the two-level model as a function of latitude and season. The curves of 0.1 $(U_1 - U_3)$ (in m sec^{-1}) are taken from the cross sections of Hess.

Fig. 3 contains a picture of these solutions. In the northern half of the region $\Phi_{1\,t} - \Phi_{3\,t}$ is positive, while in the southern half it is negative. This corresponds to an average warming up of the northern half and a cooling of the southern half of the region. Therefore, as has been shown previously by Kuo (1952), one effect of the unstable waves is to counteract the latitudinal variation in heating and cooling due to non-adiabatic causes.

The size of the disturbance necessary to have the correct magnitude of this effect is readily estimated. From the hydrostatic equa-

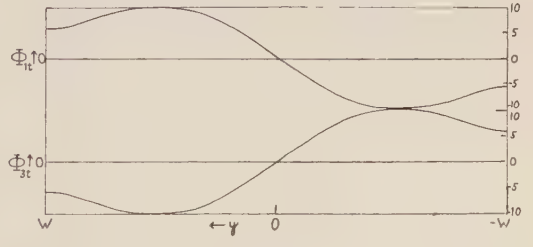

Fig. 3. Graph of the solutions $\Phi_{1\,t}$ and $\Phi_{3\,t}$ of the averaged vorticity equations. The scale on the right side shows the corresponding value of the mean height tendency in m day^{-1} when $T_t^\star$ is taken as 0.5 °C day^{-1}.

tion we first obtain the approximate relation $\partial \bar{T}_2/\partial t \sim R^{-1}(\Phi_{1t} - \Phi_{3t})$ where $\bar{T}_2$ is the 500-mb temperature and R is the gas constant for dry air. Defining $T_t^* \equiv (2/\pi)\int_0^{\pi/2} \bar{T}_{2t}\, d\xi$ as the average value of the warming up of the northern half of the region by the disturbances, we find

$$T_t^* = \frac{A\,(1+\gamma - \operatorname{sech}\sqrt{2\gamma}\,\pi/2)}{\pi R\gamma\,(2+\gamma)}$$

A reasonable estimate of the order of magnitude T_t^* must have in order to balance the yearly average cooling over the northern half of the northern hemisphere is about 0.5 °C per day (see BJERKNES, 1933). With $\mu = 3/R_e$ and $\lambda^2 = 1.17 \times 10^{-12}$ m^{-2} [see (20) and the definition of λ^2 following (3)], we find that $\gamma \sim 5.3$, and that

$$T_t^*\,(\text{deg day}^{-1}) \sim 15.4\,A\,(\text{m}^2\,\text{sec}^{-3}) \quad (24)$$

Defining v_0 as the maximum value of v at level three (750 mb) we may write

$$v_0 = [f^{-1}\varphi'_{3x}]_{\max} = f^{-1}k\,De^{\nu_i t}$$

Introducing this into (22) we then obtain

$$v_0^2 = Ak^2\mu\,(2\alpha V - B)\,[f\lambda^2\alpha\,(2+\alpha)\,\nu_i]^{-1}$$

Taking A as equal to $(30.8)^{-1}$ m^2 sec^{-3} and the following values in addition to those in (20),

$$k = 2\pi\,(6\times 10^6)^{-1}\ \text{m}^{-1}$$
$$V \sim B \sim 14\ \text{m sec}^{-1}$$
$$\nu_i = (\ln 2/1.245)\ \text{days}^{-1}$$

we find that v_0 is about 10 m sec^{-1}. In other words, a disturbance of a size such that v_0 is 10 m sec^{-1} will cause a second-order effect on the mean flow of the correct order of magnitude to balance the average latitudinal variation in heating and cooling. This is a rather small value of v_0, but we have assumed that the perturbation is of the most efficient type (i.e. that with the maximum value of ν_i). Furthermore, the observed eddy motion in the atmosphere is partly due to features such as longitudinal irregularities in orography which probably do not contribute significantly to the latitudinal transport of energy.

7. The meridional circulation

In this section we shall see that the presence of the baroclinic waves implies the existence of a small meridional circulation. Our assumption of quasi-geostrophic motion does not allow us to use the second equation of motion to discuss the creation of a meridional circulation and we must therefore demonstrate its existence in another manner. Averaging (1), we first obtain

$$\bar{\omega}_2 = (2f^2)^{-1}\,p_0\Phi_{1\,\gamma\gamma t} = (2f^2)^{-1}\,p_0\mu^2\Phi_{1\,\xi\xi t}$$

which, when we use (23), yields the following formula for $\bar{\omega}_2$:

$$\left.\begin{aligned} \bar{\omega}_2 &= \frac{p_0\mu^2 A}{4f^2\,(2+\gamma)} \\ &\left[\frac{\sqrt{2\gamma}\,\sinh\sqrt{2\gamma}\,\xi}{\cosh\sqrt{2\gamma}\,\pi/2} - 2\sin 2\xi\right] \end{aligned}\right\} \quad (25)$$

We now integrate the continuity equation (6) with respect to x, define

$$\bar{v}_1 \equiv p_0^{-1}\,2\int_0^{p_0/2} \bar{v}\,dp$$

$$\bar{v}_3 \equiv p_0^{-1}\,2\int_{p_0/2}^{p_0} \bar{v}\,dp$$

and, as we have already done in deriving (1) and (2), assume that ω vanishes at $p=0$ and $p=p_0$. $\bar{v}_1$ and $\bar{v}_3$ are then related to $\bar{\omega}_2$ by the formulae

$$\frac{\partial \bar{v}_1}{\partial \xi} = -\frac{\partial \bar{v}_3}{\partial \xi} = -\frac{2\,\bar{\omega}_2}{\mu p_0}$$

These may now be integrated with respect to ξ from $\xi = -\pi/2$ to $\xi = \xi$, using the boundary condition that $\bar{v}_1$ and $\bar{v}_3$ are both equal to zero at $\xi = -\pi/2$.

$$\left.\begin{aligned} -\bar{v}_1 = \bar{v}_3 &= \frac{\mu A}{2f^2\,(2+\gamma)} \\ &\left[\frac{\cosh\sqrt{2\gamma}\,\xi}{\cosh\sqrt{2\gamma}\,\pi/2} + \cos 2\xi\right] \end{aligned}\right\} \quad (26)$$

(Note that the boundary condition that $\bar{v}_1$ and $\bar{v}_3$ also vanish at $\xi = \pi/2$ is satisfied automatically.)

The meridional circulation given by (25) and (26) is shown in fig. 4, with A taken to

correspond to $T_t^* = 0.5$ °C day^{-1}. It consists of three "cells", a "direct" cell at the northern and southern ends, and a larger "indirect" cell in the central part of the region. It is very weak and therefore questionable whether it could be detected with the present observational network.

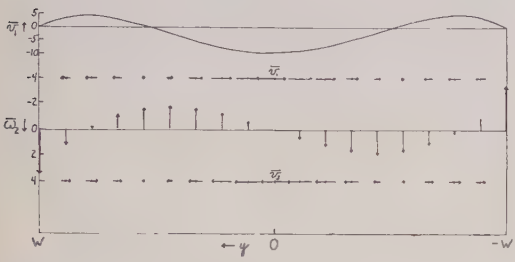

Fig. 4. The meridional circulation due to the baroclinic waves. The arrows indicate the direction and intensity of the flow. Values of $\overline{\omega}_2$ and $\overline{v}_1$ when T_t^* is taken as 0.5 °C day^{-1} are indicated by the scales on the left side; $\overline{\omega}_2$ is in units of mb day^{-1} and $\overline{v}_1$ (top line) is in units of cm sec^{-1}.

The existence of this meridional circulation was not incorporated into our equations (1), (2), and (3). It if had been, the meaned equations (12) would have included a term $f\overline{Bv}$. Having obtained an explicit expression for $\overline{v}$, it is now possible to justify its neglect in (12). If we compute the ratio of the mean values over the interval $-\pi/2 \leq \xi \leq \pi/2$ of the square of the neglected term $f\beta\overline{v}$ with the square of the retained term $\Phi_{1\,yyt}$ we obtain a value of about .03. This crude comparison demonstrates that the presence of the mean circulation (25) and (26) is relatively unimportant in the solution of the zonally averaged vorticity equations (12).

The latitudinal transport of energy in our model, as reflected in the distribution of $\Phi_{1\,t} - \Phi_{3\,t}$ [reference should here be made to (31)], can be shown to be brought about by both a horizontal eddy-transport and by the meridional circulation (25), (26). [A discussion of the manner in which this transport may be broken up into contributions of these two types has been given by STARR (1951 b).] The transport of energy by the meridional circulation is always in the same direction as $\overline{v}_1$, and therefore gives a poleward transport in the northern and southern portions of the region and an equatorward transport in the central portion. The eddy transport on the other hand, is always poleward, and in the central part is much larger than the contribution from the meridional circulation.

Some measurements of the actual eddy transport of sensible heat across latitude circles have been made by WHITE (1951). He has also summarized the amounts of energy which must be transported across latitude circles in order to counteract the effects of radiation. His data suggest that the observed eddy flux is slightly too large in middle latitudes and perhaps too small in higher and lower latitudes to account for the required transports. Although the data are perhaps not representative enough to place too much reliance on this last remark, it is interesting to note that if the discrepancies were to be made up by a meridional circulation, the meridional circulation would be similar to that in fig. 4.

Since most of the heat transport in regions removed from the walls is accomplished by the eddies, it is not surprising that fig. 4 is vastly different from that hypothetical meridional circulation which would provide *all* of the required transport of energy. An example of such a circulation has been computed by BJERKNES et al. (1933), and, as one would expect, it is much more intense than that in fig. 4.

8. Changes in zonal momentum

The second-order changes in Φ_1 and Φ_3 given by (23) show that the baroclinic waves are modifying the distribution of mean zonal momentum. Differentiating (23) with respect to y, we see that the changes in the basic current velocities are given by

$$\left.\begin{aligned} U_{3\,t} &= -U_{1\,t} = \frac{A\pi}{2f(2+\gamma)} \\ &\left[\frac{\cosh\sqrt{2\gamma}\,\xi}{\cosh\sqrt{2\gamma}\,\pi/2} + \cos 2\xi\right] \end{aligned}\right\} \quad (27)$$

The distribution of $U_{3\,t}$ when A is taken as $(15.4)^{-1}$ m^2 sec^{-3} (corresponding to $T_t^* = 1$ °C day^{-1}) is shown in fig. 5.

Before discussing what implication this might have for the general circulation, we note the following two facts about (27):

1. Comparing (27) with (26), we see that

$$U_{1t} - f\bar{v}_1 = 0, \text{ and } U_{3t} - f\bar{v}_3 = 0 \quad (28)$$

Therefore the velocity changes (27) in the basic current are to be explained by the presence of the "implicit" meridional circulation (25), (26).[1]

2. Since $U_{3t} = -U_{1t}$, there is no change in the average velocity $1/2\,(U_1 + U_3)$ at any value of ξ. Therefore our perturbations do not include any mechanism for a net transport of momentum across latitude circles as studied by KUO (1949).

Attempts to explain the existence of the subtropical easterlies, middle-latitude westerlies, and polar easterlies in the surface zonal wind profile have long fascinated meteorologists. In general, all such attempts have begun with the familiar model of HADLEY (1735) for the trade wind zone and have then attempted to extend this type of reasoning to higher latitudes, bringing in various types of frictional effects as needed in order to "explain" the successive appearance of the westerlies and polar easterlies at the surface.

In 1948 STARR drew attention again to the suggestion of JEFFREYS (1926) that the angular momentum budget of different latitude belts might be greatly influenced by asymmetries in the large-scale horizontal flow patterns. These asymmetries could give non-vanishing values of ϱuv (ϱ = density) when integrated around a latitude circle and from the ground up to the top of the atmosphere, and thereby give a net flux of momentum across that latitude. The several synoptic investigations of this process which have since been made have shown that this transport does exist. Furthermore, the net transport of momentum into the various latitude belts by this process accounts rather well for the loss or gain in momentum which each of the latitude belts experiences through the effects of surface friction and the torque due to the pressure differential across large mountain ranges. [A summary of these results and a general discussion of their interpretation has been made by STARR (1951 a).] However, as soon as one examines the momentum budget of a typical latitude belt in more detail, it becomes apparent that other types of momentum transfer must exist in addition to the horizontal transport by the correlations in u and v. Let us consider for the moment a latitude belt in middle latitudes. This ring is losing angular momentum at the surface of the earth but gains an approximately equal amount through the convergence of the horizontal eddy transport. But the latter effect is small near the surface and reaches its maximum value at the level of the tropopause (STARR, 1951 a), so that we are faced with a surplus of angular momentum in the upper layers of the belt and a deficit in the lower layers. The situation in latitudes with surface easterlies is reversed; there we have an excess of momentum near the surface and a deficit at higher altitudes.

As can easily be seen by writing the angular momentum equation for a ring-shaped region limited by two latitude circles and two values of the height, there are three principal mechanisms available by which the angular momentum may be redistributed intramurally within a complete latitude belt (from the surface to the top of the atmosphere) so that the angular momentum budget for each layer in the latitude belt is also balanced:

1. A vertical transport by small-scale turbulence, for example, that brought about by cumulus activity. This process can certainly lead to a downward transport, which is what is needed in the region of the surface westerlies, but it is difficult to imagine that this process will provide an upward transport in the regions with surface easterlies.

2. A vertical transport by large-scale turbulence due to correlations in the zonal and vertical velocity components when measured on a synoptic scale. Momentum transport by this process need not be in the direction of decreasing momentum, and conceivably could be directed upwards in low and high latitudes and downwards in middle latitudes. Some measurements of this in middle latitudes have been made by WHITE and COOLEY (1952), and their results suggest that some of the downward transport in middle latitudes may be by this process.

[1] The results derived here are much in the spirit of those derived by ELIASSEN (1952); we have merely emphasized the meridional circulation brought about by the eddy heat transport, while Eliassen has analysed that due to axially symmetric non-adiabatic heat and cold sources.

3. A meridional circulation consisting of a net poleward motion in layers where there is a deficit of momentum (e.g. in the lower levels of middle latitudes) and an equatorward motion in the layers where there is an excess of momentum. PALMÉN and ALAKA have used this mechanism with some success in discussing the details of the momentum budget in low latitudes (1952).

The absence of correlations in u and v in our solution (due to the fact that U_1 and U_3 were assumed to be initially independent of latitude) does not allow us to say anything theoretically about the *total* transport of momentum into a given latitude belt. Furthermore, the crudeness of our two-layer model will not allow us to use it to study the vertical redistribution of momentum in great detail. However, it is possible to apply our results to the atmospheric layer below the 500-mb level, i.e. the lower half of the atmosphere. We shall see that the weak implicit meridional circulation (25), (26) (which in our theory is to be considered as a *result* of the presence of the baroclinic waves) provides local sources and sinks of relative momentum of the correct order of magnitude to help balance the local excesses and deficits of momentum at different altitudes which result from the observed horizontal eddy transport and exchange of momentum with the earth.

WIDGER (1949) has computed the geostrophic eddy flux of angular momentum per unit height during the month of January 1946 at the surface, 700-mb, and 500-mb levels. His observations also include the observed change in momentum during the month together with estimates of the loss (or gain) of momentum due to skin friction and the mountain effect (WHITE, 1949). Let us reckon H, the horizontal momentum transport by the uv correlations during January 1946 from the surface to the 500-mb level, as positive when directed northward. Let $\triangle$ be the change during January 1946 in the angular momentum of the volume limited by two latitude circles, the surface of the earth, and the 500-mb surface. Finally, we shall count E, the total amount of momentum gained from the surface of the earth by a latitude belt during the month, as positive when it represents a gain for the atmosphere. For each latitude belt we may then summarize the angular momentum requirements for the layer surface – 500 mb in the equation

$$\triangle = H_S - H_N + E + Q \qquad (29)$$

where the subscripts S and N refer to values at the southern and northern latitudes of the belt. The quantity Q then represents an additional "source" of momentum due to some or all of the three mechanisms described above.

Values of $H_S - H_N$, $\triangle$, E, and Q [computed from (29)] have been taken from Widger's data and are entered in Table I.[1] The Q values have then been converted into a value of $\partial U/\partial t$ by dividing them by the approximate mass of each ring and its mean distance from the axis of the earth. These values of $\partial U/\partial t$ are entered in the last column of Table I and may be thought of as the net relative acceleration required from the three processes listed above if the momentum budgets for these rings of air are to be satisfied as shown by (29).

Table I. Angular momentum budget for the layer 1,000—509 mb for the month of January 1946. [After WIDGER (1949)].

Lat. Belt	$H_S - H_N$	E	$\triangle$	Q	$\partial U/\partial t$ (m sec^{-1} day^{-1}
	(in units of 10^{29} g cm^2 sec^{-1})				
15—20	— 309	4770	2	— 4459	— 2.2
20—25	— 622	2470	51	— 1797	— 1.0
25—35	— 747	1832	272	— 813	— 0.2
35—45	491	— 4495	100	4104	1.6
45—55	1119	— 3187	— 573	1495	0.8
55—65	200	214	— 131	— 546	— 0.5
65—75	156	280	— 209	— 645	— 1.2

The possible importance of the baroclinic waves and their associated meridional circulations in giving the required sources and sinks of momentum to satisfy (29) can be seen by referring to fig. 5. In addition to the theoretical values of U_{3t} obtained from (27), this figure has indicated on it the values of $\partial U/\partial t$ in Table I. [To make this comparison possible $\xi = 0$ was placed at latitude 45N and $\xi = -\pi/2$ and $\pi/2$ at 15N and 75N, in agreement with the choice of $2w$ as equal to sixty degrees of latitude. Furthermore, A in

[1] The values of H and $\triangle$ have been revised slightly so as to apply to the layer surface – 500 mb rather than for the layer surface – 7.5 km as used by Widger.

(27) was taken as equal to $(15.4)^{-1}$ m^2 sec^{-3} to correspond more closely to winter conditions.] The momentum changes given by (27) are clearly of the correct order of magnitude and even have the approximately correct variation in latitude.[1]

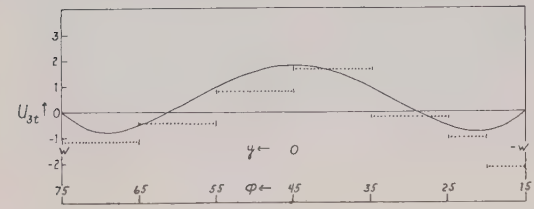

Fig. 5. $U_3\,t$ in m sec^{-1} day^{-1} when T_t^* is taken as 1 °C day^{-1}. The dotted horizontal line segments are the values of $\partial U/\partial t$ computed from Widger's data in table I.

The meridional circulation (25), (26), as shown in fig. 4, is of the same general type as that derived from the usual qualitative considerations based on the effect of skin friction on the *observed* surface wind distribution (e.g. the frictional drag on the middle latitude westerlies produces a poleward drift in the lower layers and, from mass continuity reasons, a return equatorward flow at upper levels). However, our argument has not proceeded from an observed distribution of surface wind, but has instead tried to show that *the quasi-geostrophic baroclinic waves are associated with weak meridional circulations which, in combination with the horizontal eddy flux of momentum, prescribes the main features of the observed surface zonal wind distribution.* Thus, for example, if we considered the initial state of our basic current to be such that U at the surface was everywhere zero (this does not affect the second-order effects of the unstable waves), the meridional circulation set up by the waves would create a system of surface winds with easterlies in high and low latitudes and westerlies in between.

[1] The boundary condition (5) places an artificial restraint on the theoretical values of U_t at the northern end of the region. This undesirable feature could be removed at the polar end by using spherical coordinates at the expense of some additional complication in the computations. The proper procedure at the equatorial end is less obvious since the quasi-geostrophic theory cannot be justified so readily for small values of the Coriolis parameter.

The role played by large-scale correlations in ϱuw (or in ωu) in providing a vertical transport of momentum in our model can be computed, but it is negligible in comparison to the effect of the meridional circulation (25), (26). On the other hand, the observations by White and Cooley (1952) seem to demonstrate that a downward transport of momentum of this type does exist in middle latitudes and that it is of the proper order of magnitude. It may be that the value of this correlation in a perturbation analysis is greatly influenced by the assumption that U_1 and U_3 are independent of latitude. Or it may be, as is perhaps indicated by Kuo's analysis of this effect in the baroclinic waves of infinite lateral extent, that the two-level model is too crude to include this effect explicitly but includes it implicitly in the form of a meridional circulation. In any case, it is clear that the simple two-level model we have used does contain a mechanism for the vertical redistribution of zonal momentum, and may therefore be used with some hope of success in the computational experiment described at the end of section 1.

9. Energy transformations in the unstable waves

In section 3 we have shown that the quasi-geostrophic equations (1), (2) and the boundary conditions (4) and (5) are consistent with the mechanical energy equation. It is perhaps of some interest to apply this fact to the system we have used in studying the unstable baroclinic perturbations.

Introducing the expression (3) for ω_2 into (10), we find that the energy equation may be rewritten

$$\frac{\partial}{\partial t}\int\int\left[q_1+q_3+\frac{\lambda^2}{2f^2}(\varphi_1-\varphi_3)^2\right]dx\,dy=0 \quad (30)$$

where the integration is over $-w \leqslant y \leqslant w$ $0 \leqslant x \leqslant L$ and we have used the fact that the integral of $\boldsymbol{v}\cdot\nabla h$ (h arbitrary) over this region vanishes when $\boldsymbol{v}$ is geostrophic. The term $1/2\,f^{-2}\lambda^2(\varphi_1-\varphi_3)^2$ clearly represents some type of potential energy for the system. The kinetic energy q_1+q_3 and the potential energy $1/2\,f^{-2}\lambda^2(\varphi_1-\varphi_3)^2$ may each be divided up into a part representing the energy of

the basic current and a part representing that of the perturbation. Thus (30) becomes

$$\left.\begin{aligned}\frac{1}{2\pi}\frac{\partial}{\partial t}\int_{-\pi/2}^{\pi/2}\Big\{\Big[U_1^2+U_3^2+f^{-2}\lambda^2(\Phi_1-\Phi_3)^2\Big]+\\ +\Big[\overline{u_1'^2+v_1'^2+u_3'^2+v_3'^2}+f^{-2}\lambda^2\overline{(\varphi_1'-\varphi_3')^2}\Big]\Big\}d\xi=0\end{aligned}\right\}\quad(31)$$

The rate of change of the basic current energies may be computed from (27) and (23). We find

$$\left.\begin{aligned}\frac{1}{2\pi}\frac{\partial}{\partial t}\int_{-\pi/2}^{\pi/2}(U_1^2+U_3^2)\,d\xi=\\ =-X\frac{2(2+\alpha)\tanh\sqrt{2\gamma}\,\pi/2}{\pi\sqrt{2\gamma}\,(2+\gamma)}\end{aligned}\right\}\quad(32)$$

$$\left.\begin{aligned}\frac{1}{2\pi}\frac{\partial}{\partial t}\int_{-\pi/2}^{\pi/2}\frac{\lambda^2}{f^2}(\Phi_1-\Phi_3)^2\,d\xi=\\ =-X(2+\alpha)\left[\frac{1}{2}-\frac{2\tanh\sqrt{2\gamma}\,\pi/2}{\pi\sqrt{2\gamma}\,(2+\gamma)}\right]\end{aligned}\right\}\quad(33)$$

where

$$X\equiv[AV\mu]/[f(2+\alpha)]$$

The time rate of change of the perturbation kinetic and potential energies are readily computed from (17):

$$\frac{1}{2\pi}\frac{\partial}{\partial t}\int_{-\pi/2}^{\pi/2}(\overline{u_1'^2}+\overline{v_1'^2}+\overline{u_3'^2}+\overline{v_3'^2})\,d\xi=X\alpha\quad(34)$$

$$\frac{1}{2\pi}\frac{\partial}{\partial t}\int_{-\pi/2}^{\pi/2}\frac{\lambda^2}{f^2}\overline{(\varphi_1'-\varphi_3')^2}\,d\xi=X\left(\frac{2-\alpha}{2}\right)\quad(35)$$

It is easily seen, by adding (32) – (35), that the energy equation is indeed satisfied.

In (32), the factor multiplying $X(2+\alpha)$ has the value .026. Since this term, representing a loss of kinetic energy by the basic current, is exactly balanced by the last term in (33), we may say that of the total increase in perturbation energy 95 per cent comes from the potential energy of the basic current, the other 5 per cent coming from the kinetic energy of the zonal motion. These figures are obtained when $\gamma=\lambda^2\mu^{-2}$ has the value 5.3. For smaller γ, e.g. smaller values of w or smaller values of f, the fraction of perturbation energy which comes from the kinetic energy of the basic current increases.

The rate of production of kinetic energy per unit area, given approximately by one half the value of (34), has a value of about 0.375×10^{-3} m^2 sec^{-3}, when A is taken equal to $(30.8)^{-1}$ m^2 sec^{-3}. If we multiply this by 10 tons (the approximate mass of the atmosphere per square meter) we get a value of about 3.75 joules sec^{-1} m^{-2} as the rate at which the disturbances are creating kinetic energy. This can be compared with BRUNT's estimate (1939) of about 5 joules sec^{-1} m^{-2} as the average rate of dissipation of kinetic energy in the atmosphere.

10. The vertical transport of entropy

Computations of the gain and loss of heat by radiation show that the upper half of the troposphere loses heat while the lower half gains heat by this process if we consider conditions averaged with respect to latitude. EADY (1949) has pointed out that the positive correlation between the vertical velocity and potential temperature in the unstable baroclinic waves must give a net upward transport of entropy which will act to balance this effect of radiation.

Our equations prescribe Φ_t at only two levels, and therefore define a temperature at only one level. Thus they cannot be used for a direct computation of the time rate of change of the mean entropy in the upper and lower halves of the atmosphere. However, if Θ_1^* and Θ_3^* are defined as the mean values of the potential temperature in the upper and lower halves of the atmosphere, the following formula holds for adiabatic motion:

$$\frac{\partial\Theta_1^*}{\partial t}=-\frac{2}{\pi p_0}\int_{\pi/2}^{\pi/2}\overline{\omega_2\Theta_2}\,d\xi$$

Θ_2 may then be expressed in terms of $(\varphi_1-\varphi_3)$ with the aid of the equation of state and the hydrostatic equation. For a disturbance of the type we have considered, with T_t^* taken as 0.5°C day^{-1}, we find that $\Theta\partial^*/\partial t$ is about

$0.25°C\ day^{-1}$. Therefore any complete theory of the existing distribution of temperature with height in the atmosphere must include this effect of the large-scale extratropical disturbances.

Since this effect of the disturbances is proportional to the square of their amplitude, this upward transport of entropy should be greater in the winter season than in the summer season. This should cause the lapse rate to be more stable in winter than in summer. Evidence that this is so can be readily seen in the meridional cross sections of Hess for the winter and summer seasons (Hess, 1948).

Acknowledgment

The writer wishes to acknowledge with thanks the opportunity afforded him by the Institute for Advanced Study, the Institut för Meteorologi at Stockholms Högskola, and the Astrofysisk Institutt at the University of Oslo to visit the last two institutes, where much of this paper was written.

REFERENCES

Bjerknes, V., and collaborators, 1933: *Physikalische Hydrodynamik*. Berlin, J. Springer.

Brunt, D., 1939: *Physical and dynamical meteorology*, 2nd ed. Cambridge, University Press.

Charney, J. G., 1947: The dynamics of long waves in a baroclinic westerly current. *J. Meteor.*, **4**, 135–162.

— 1948: On the scale of atmospheric motions. *Geofys. Publ.*, **17**, no. 2.

— and N. A. Phillips, 1952: Numerical integration of the quasi-geostrophic equations for barotropic and simple baroclinic flows. *J. Meteor.*, **10**, 71–99.

Defant, A., 1921: Die Bestimmung der Turbulenzgrössen der atmosphärischen Zirkulation aussertropischer Breiten. *S. B. Akad. Wiss. Wien*, Abt. IIa, 130, 383–403.

Eady, E. T., 1949: Long waves and cyclone waves. *Tellus*, **1**, no. 3, 33–52.

Eliassen, A., 1949: The quasi-static equations of motion with pressure as independent variable. *Geofys. Publ.*, **17**, no. 3.

— 1952: Slow thermally or frictionally controlled meridional circulations in a circular vortex. *Astrophys. Norv.*, **V**, no. 2, 19—60.

Hadley, G., 1735: Concerning the cause of the general trade winds. *Phil. Trans. Roy. Soc.* London, **39**.

Hess, S. L., 1948: Some new meridional cross sections through the atmosphere. *J. Meteor.*, **5**, 293–300.

Jeffreys, H., 1926: On the dynamics of geostrophic winds. *Quart. J. roy. meteor. Soc.*, **52**, 85–104.

Kuo, H. L., 1949: Dynamic instability of two-dimensional non-divergent flow in a barotropic atmosphere. *J. Meteor.*, **6**, 105–122.

Kuo, H. L., 1952: Three-dimensional disturbances in a baroclinic zonal current. *J. Meteor.*, **9**, 260–278.

Palmén, E., and M. A. Alaka, 1952: On the budget of angular momentum in the zone between equator and 30° N. *Tellus*, **4**, 324–331.

Palmén, E., and C. W. Newton, 1948: A study of the mean wind and temperature distribution in the vicinity of the polar front in winter. *J. Meteor.*, **5**, 220–226.

Rossby, C.-G., and collaborators, 1939: Relation between variations in the intensity of the zonal circulation of the atmosphere and the displacements of the semi-permanent centers of action. *J. mar. Res.*, **2**, 38–55.

Starr, V. P., 1948: An essay on the general circulation of the earth's atmosphere. *J. Meteor.*, **5**, 39–43.

— 1951 a: The physical basis for the general circulation. *Compendium of meteorology*. Boston, Amer. meteor. Soc., 541–550.

— 1951b: Application of energy principles to the general circulation. *Compendium of meteorology*. Boston, Amer. meteor. Soc., 568–574.

White, R. M., 1949: The role of mountains in the angular momentum balance of the atmosphere. *J. Meteor.*, **6**, 353–355.

— 1951: The meridional flux of sensible heat over the northern hemisphere. *Tellus*, **3**, 82–88.

— and D. S. Cooley, 1952: The large scale vertical eddy-stress in the free atmosphere. *Trans. Amer. geophys. Union*, **33**, 502–506.

Widger, W. K., 1949: A study of the flow of angular momentum in the atmosphere. *J. Meteor*, **6**, 291–299.

The Present Climatic Fluctuation and its Bearing on a Reconstruction of Pleistocene Climatic Conditions

By JOHN R. MATHER, The Johns Hopkins University Laboratory of Climatology
Seabrook, New Jersey

(Manuscript received October 15, 1953, Revised April 2, 1954)

Abstract

Study of the broad scale pressure, temperature, and precipitation changes which have occurred over the Northern Hemisphere during the last forty years gives considerable information concerning the nature and mechanism of a climatic change. If it is assumed that these small-scale changes resemble in certain aspects those that have occurred in the great glacial to interglacial changes of the Pleistocene period, conclusions concerning the broad scale meteorologic conditions of that period can be drawn. Evidence from synoptic meteorology is also used to reveal possible circulation changes accompanying the shift from a glacial to an interglacial period. Certain ideas obtained from these studies are further investigated by means of more detailed studies over North America.

Knowledge concerning the nature and mechanism of a climatic variation is not extensive. There is, however, general agreement (AHLMANN, 1953; KINCER, 1946; LANDSBERG, 1949) that during the last fifty years many of the regions of the Northern Hemisphere have experienced large-scale climatic fluctuations. Thus, the present climatic fluctuation offers meteorologists their first opportunity to study at close range the interaction of forces which are necessary to initiate and to carry to completion such a fluctuation in climate over a wide area. This is the first variation in climate that man has been able to measure and record and about which world-wide climatic data are available. Other variations of possibly greater magnitude have occurred in the past. From a knowledge of the present variation some insight into the past variations may be gained. Extensive and direct extrapolation from the present into the past is not, of course, advisable because of the number of variables involved. Present land-water distributions are not the same as in the geologic past, the elevations of the continents have changed, the extent and distribution of the ice sheets are different now from what they were in historic and prehistoric times; these and other differences preclude any large-scale extrapolation from the present data. However, when applied with caution, the method should produce some results. Certain factors, either within or outside of the earth's surface and atmosphere, will cause variations in the meteorologic parameters. The original cause of the variations may be obscure and never uncovered, but the results of those variations might follow some organized pattern whether they occur now or have occurred many years ago.

The importance of investigating the present climatic fluctuation lies not in the accumulation of actual data of temperature, rainfall, wind,

and pressure shifts, but in obtaining information concerning the change of one variable with respect to another and the areal distribution of such changes. This type of investigation will not permit the determination of the exact glacial period temperature, but it should tell whether the Aleutian and Icelandic winter low pressure areas moved eastward or westward, strengthened or weakened, during a glacial period. From this information, good estimates of the other meteorologic parameters may be made. In this manner the present fluctuation can reveal much concerning the nature of past fluctuations.

Most observers agree that the recent increase in mid- and northern latitude temperatures must result from a northward movement of the Icelandic low pressure area and a change in the direction of the atmospheric pressure gradient over the North Atlantic so as to increase the flow of warm air to the Arctic. Ångström (1939) shows that the warmer temperatures and small annual temperature variations noticed in high latitudes at present are a result of an increased circulation. Large temperature contrasts signify a reduced atmospheric circulation. He believes the atmospheric circulation itself, however, is probably fairly independent of the temperature conditions even though it is the circulation which is so influential in determining the temperature pattern. He suggests that in recent years the increased circulation would result in an increased number of cyclones over the North Atlantic although later studies by Petterssen (1949) do not seem to confirm this. Ångström feels that both the secular temperature fluctuations of the past century and the minor climatic changes of prehistoric times are due to variations in atmospheric circulation.

Eriksson (1943) investigated the warming of the North Atlantic region in more detail. He indicates that over the North Atlantic the mean winter pressure has decreased and the mean summer pressure has stayed the same or increased slightly. By plotting the deviations of the mean January and July barometric pressures during the periods 1915 to 1930 and 1930 to 1936 from the corresponding mean values for the years 1901 to 1930, he obtains lines of equal deviation and deviation gradients. On the basis of these gradients, a wind corresponding to the slope of the gradient can be constructed. This wind component for the region of the North Atlantic and Scandinavia was generally southerly. Thus, this component, superimposed on the normal wind, resulted in the more intense flow of heat toward the north during the period 1930 to 1936. In addition, Eriksson shows that the Icelandic low has moved far north of its previous position, changing the direction of the pressure gradient over the North Atlantic and allowing more warm air to flow into the Arctic.

Petterssen (1949) has investigated the zonal and meridional transport of air across latitudinal squares in the North Atlantic. He concludes that the climatic fluctuations of the past forty years must have been due to an increase in the gradient between the Icelandic low pressure area and the high pressure over the European continent. The increase in the strength of the high pressure area was the major factor responsible for this increased gradient. He concludes that the recent climatic fluctuation over Europe and the North Atlantic is characterized by a development from a high index (zonal flow) to a low index (meridional flow) circulation.

Willett (1949) in a discussion of long-period fluctuations in the general circulation shows that variations in the zonal index are associated with definite latitudinal shifts in the main branches of the general circulation as well as with longitudinal shifts. He further suggests that "the great Pleistocene climatic cycles between glacial and interglacial extremes have been essentially zonal in character, between low- and high-index extremes" (p. 43). Although this, at first, appears to be contrary to the findings of Petterssen the two views have been reconciled by recent studies by Rex (1950, 1951) and Wallén (1951). In investigations of the effect of atmospheric blocking action over western Europe, Rex points out that blocking anticyclones, which most frequently develop between longitude 0 – 10°W and extend northward, produce southerly flow over the North Atlantic region and northerly flow over eastern and central Europe. This circulation pattern is meridional rather than zonal in character. Rex has found that the number of blocking action situations has increased considerably in recent years.

As a result of detailed studies, Rex shows that the climatic conditions which have been experienced over the North Atlantic-Scandinavian region in recent years correspond to those that might be anticipated with an increase in the number of blocking anticyclones over the western Europe region.

Wallén (1951) in a study of the Kårsa glacier concludes that the climatic conditions which result from the occurrence of a blocking anticyclone are unfavorable for glacier development and advance. More importantly, he also suggests how it may be possible for strong zonal and meridional flow to exist simultaneously over the Northern Hemisphere.

"Since the atmospheric circulation has definitely increased in recent years, blocking-action must be a manifestation of this increased general circulation and causes an intensified exchange of air between southern and northern latitudes. It may very well be that the increased general circulation in other areas around the hemisphere has mainly shown up as an increased zonal flow as Willett has suggested. This should also be expected from Rex's conclusions that blocking-action is necessarily favoured by very strong westerly flow in the upstream area." (p. 153).

L. Rubinstein (1946) has mapped the distribution of the differences in mean annual temperature during the period 1929 to 1938 from the mean for the period 1881 to 1938 for northern latitudes. The largest positive anomalies were found in January and February and occurred over the Greenland-Spitsbergen region. Actually the whole Arctic region was included within the + 1° C anomaly line. From Rubinstein's maps, it may be seen that the divergence of the 1929 to 1938 mean annual temperature from the 1881 to 1938 mean was everywhere positive north of latitude 50° N. The divergence of the December temperatures for the same periods, however, showed positive values only over the Greenland-North Atlantic-Scandinavia region while negative values (or, hence, a decrease in temperature during the period 1929 to 1938) appeared over most of Canada, central Russia, and Siberia. The cause of this particular distribution was not well discussed by Rubinstein, although she believed it was connected with the strength of the atmospheric circulation.

I. Investigations of the Present Climatic Fluctuations

The method of using the past forty years of data to investigate the mechanics and areal distribution of the present climatic fluctuation as exemplified by Rubinstein may be carried farther. Fairly reliable and complete pressure, temperature, and precipitation data for a number of stations over the whole world have been collected together by the Smithsonian Institution in the World Weather Records (Clayton, 1947). Using these data, the recent changes in atmospheric pressure, temperature, and precipitation over the Northern Hemisphere can be determined. Since Rubinstein and others have shown that winter temperatures in the Arctic and sub-Arctic regions have risen markedly in the last few decades, it was thought that winter pressure and precipitation patterns might likewise show marked change over this same period. The month of January was selected as representative of wintertime conditions. It must be pointed out in all fairness that summer temperatures and the length of the ablation season, factors of far greater importance in controlling glacier action than mean winter or January temperature, have also undergone marked change in recent years. In order to gain a complete understanding of the nature of the recent climatic fluctuation, it would be necessary to apply a similar analysis to these data in order to determine the changes in the temperature, pressure, and precipitation patterns during the important summer period.

The selection of the time periods to use in the investigation was arbitrary and determined primarily on the basis of the periods used in the published data in order to save computation time. Thus, in the presentation of temperature and precipitation records, periods from 1901 to 1930 and from 1931 to 1940 were used, while in the investigation of atmospheric pressure, periods from 1899 to 1928 and from 1929 to 1938 were used. The two sets of periods appear to be quite comparable.

Later analysis showed that the selection of these time periods was somewhat unfortunate since the period from 1931 to 1940 (or 1929 – 1938) was in many respects unrepresentative of the general trend of conditions found

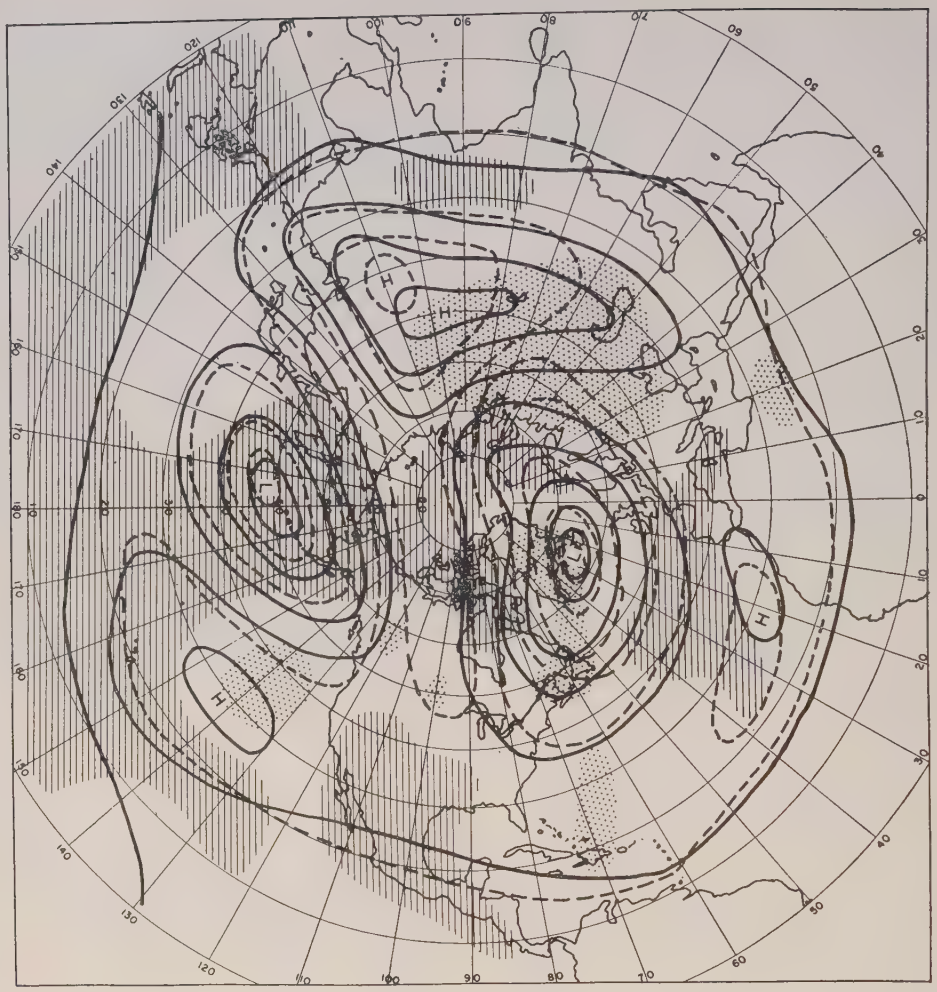

Figure 1. Mean January sea-level isobars for periods 1899—1928 (dashed lines) and 1929—1938 (solid lines). The departure of the mean sea-level barometric pressure January 1929 to 1938 from the 1899 to 1928 mean January pressure is shown by shading, the dot pattern indicating where pressure is considerably higher during 1929—1938 period and the slant line pattern showing where pressure is considerably lower during the 1929—1938 period.

during the period from 1900—1930. In the United States the period of the 1930's is remembered because of its extreme dryness. Over northern Europe as well as in other regions the period stood out as one of high temperatures and mild winters. The period, perhaps, marked the culmination of the warming trend which had been under way for nearly a century. In many respects the period of the 1930's was more one of climatic extremes than of continuation of the general trends. This must be remembered in any interpretation of the results.

The mean January sea level barometric pressure distributions for the periods 1899 to 1928 and 1929 to 1938 over the Northern Hemisphere are given in Figure 1. Pressures at every 10 degrees of latitude and longitude, which were reported in the World Weather Records, were used to obtain these distributions. Actual station pressures could not be used for most of them had not been corrected to sea level.

The most noticeable pressure changes which are found to occur in the shift from the 1899—1928 period of warming to the very warm

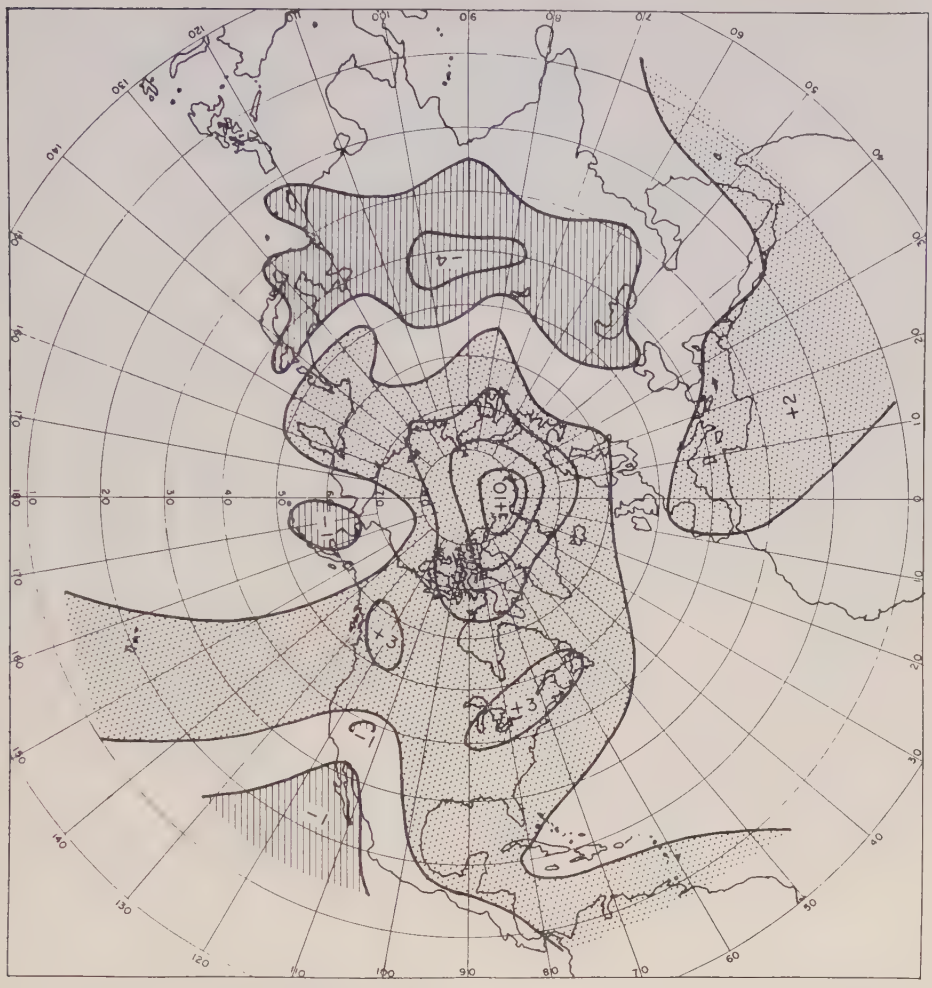

Figure 2. Departure of the mean January temperature (°F) during the period 1931—1940 from the mean January temperature from 1901—1930. Dot pattern indicates increased temperature during 1931 – 1940 period while slant line pattern indicates decreased temperature during that period.

1929—1938 period are associated with the location of the three major semi-permanent winter pressure systems of the Northern Hemisphere. The Siberian high pressure area which on the average is centered at about 110° E and 45 °N during the month of January from 1899 to 1928 moves northward and westward, so that during the same month from 1929 to 1938 it is centered at about 98° E and 50° N. This shift in pressure is accompanied by a weakening of the ridge of high pressure over northeastern Siberia and the Arctic Ocean. In opposition to the shift of the high pressure area, the Aleutian and Icelandic low pressure area sshift their positions more than five degrees of longitude to the east. The eastward movement of the Icelandic low and the westward movement of the Siberian high result in an intensification of the southerly flow of air over the North Atlantic and northwestern Europe.

Other pressure changes are more easily identified by means of the shaded regions in Figure 1, which show the average January pressure in mb from 1929 to 1938 minus the average January pressure from 1899 to 1928. They include the slight increase in the pressure gradient over the eastern Pacific which would

aid in the transport of warm air northward and the increase in the intensity and the small northward shift of the eastern Pacific sub-tropical high pressure area. This shift and the weakening of the ridge of high pressure over the western Arctic allow for a slight northward movement of the paths of the migratory storms of mid- and high latitudes, especially over western and central United States.

Figure 2 shows the difference in the mean January temperatures in degrees F, during the period 1931 to 1940 from the corresponding values from 1901 to 1930 over the Northern Hemisphere. Over northern and eastern Canada the data in the World Weather Records were supplemented with data from the Canadian Weather Records.

Many of the pressure changes noted on Figure 1 are reflected in the distribution of temperature changes over the Northern Hemisphere. The westward shift of the Siberian high pressure area is accompanied by a decrease in temperature through central Europe and Russia. The increased southerly flow over the North Atlantic-western Europe region resulting from the shifts in the Siberian high and Icelandic low and the weakening of the tongue of high pressure over the Arctic and resulting northward shift of the major pressure systems is accompanied by an increase in temperature over the entire Arctic area. The center of this temperature rise appears to be in the Greenland-Spitsbergen region where a rise of over 10° F during the 1931 to 1940 period is found. The area of greatest temperature rise continues to the south over the Western Hemisphere with centers of +3° F in Canada and at least a 1° F temperature rise through eastern United States and the Caribbean area. The strengthening of the eastern Pacific sub-tropical high pressure area during the period from 1929—1938 is related to the below normal temperatures found over the southwestern part of the United States. Many of the changes indicated over the ocean areas, Siberia, and North Africa, however, may be questioned because of the paucity of data in these regions.

The mean January precipitation at a number of stations over the Northern Hemisphere during the period 1931 to 1940 expressed as a percentage of the mean January amount from 1901 to 1930 has also been obtained from the data of the World Weather Records. Figure 3 shows the areal distribution of the precipitation change from one period to the other. Since precipitation is usually more variable than temperature, the uniform large-scale pattern noted in Figure 2 should not be expected here.

Significant feature on the map of precipitation are as follows: 1) the smaller amount of precipitation over North Africa, southeast Asia, and the Great Basin region of the United States during the 1931—1940 period; 2) the larger amount of precipitation during the same period over mid- to high latitudes. This shift in the distribution of precipitation indicates that the major storm paths had probably moved farther northward during the period of the 1930's. Over the United States, the 1901—1930 period appears to have been more moist over the Great Basin region than the 1931—1940 period, while little change in precipitation was experienced over the eastern part of the country. This indicates that a strict north to south shift of the storm tracks all across the country did not take place, but that local shifts of different magnitudes probably occurred.

It can be seen from Figure 2 that the period 1931 to 1940 experienced much warmer temperatures over the formerly glaciated regions of the Northern Hemisphere than did the 1901 to 1930 period. This is significant in any attempt to make use of the present climatic fluctuation to explain the larger- scale glacial-interglacial climatic fluctuations of the Pleistocene period, because it corresponds to the one difference between glacial and interglacial periods that must have existed. Many different theories concerning the origin and climate of the glacial periods have been proposed. Agreement on many of the broad aspects of the weather of the Pleistocene has not yet been achieved. Nevertheless, there is general agreement that the temperature of the air over the glaciated regions of Europe and North America was lower during the glacial periods than it is at present or was during an interglacial period when no ice sheets existed in the region. The change from a glacial to an interglacial period must have been marked by a warming of the air temperature over the formerly glaciated regions no matter what theory of glaciation is accepted.

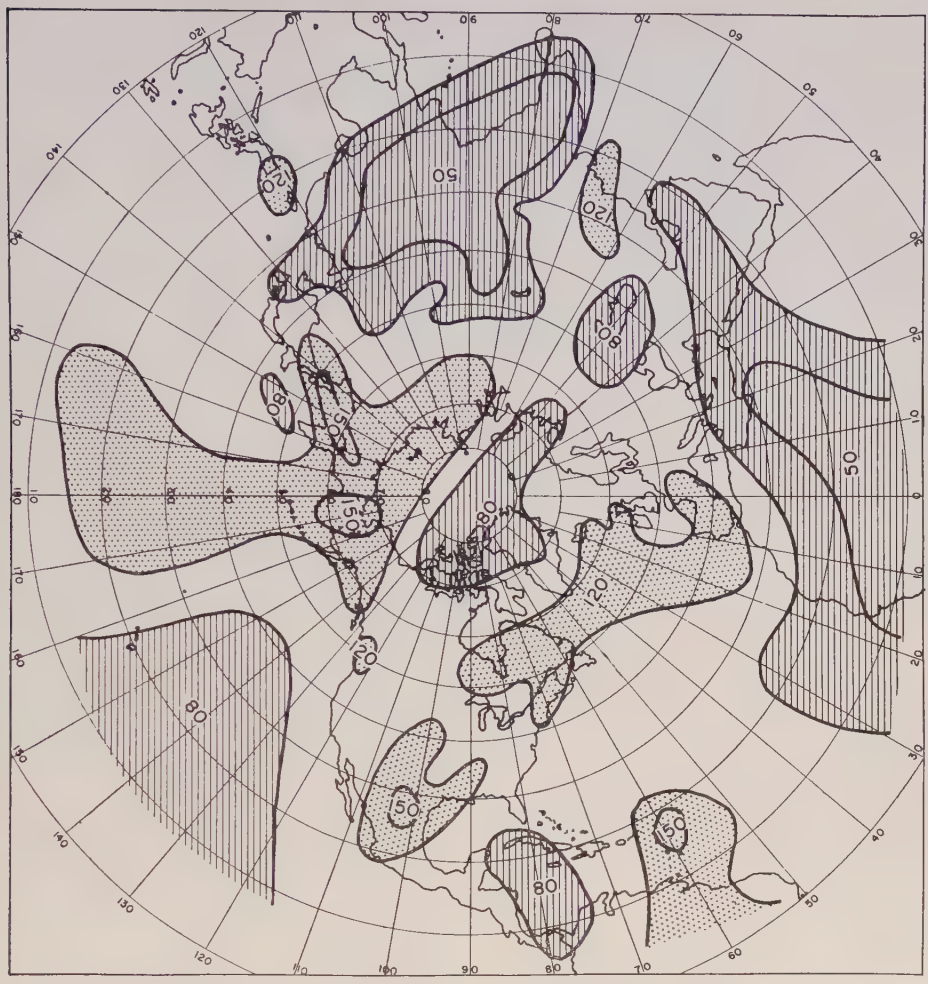

Figure 3. Mean January precipitation during period 1931—1940 expressed as a percentage of the 1901—1930 mean January precipitation. Dot pattern indicates 1931—1940 January precipitation more than 120 percent of that during 1901—1930 period while slant line pattern indicates mean January precipitation 1931—1940 less than 80 percent of January mean during 1901—1930 period.

The use of information from the month of January 1901—1930 and 1931 – 1940 in any attempt to learn more of the nature of a climatic fluctuation and to infer from this knowledge something of the conditions during the great Pleistocene glacial and interglacial periods is highly speculative. One major concern is the representativeness of the periods selected. The question must be asked whether the period of warming from 1901 to 1930 might be at all representative of a cool period when compared with the 1931—1940 period of exceptional warmth over the formerly glaciated regions. It must also be wondered whether the changes found on Figure 1 are related to the fact that only the month of January has been considered in the investigation or whether they are representative of changes which might be noticeable in seasonal or annual summaries of data.

In order to help decide some of these questions the locations of the three major pressure systems were recalculated using, instead of mean January pressures, the mean annual pressures for two years which experienced below normal and two years with above

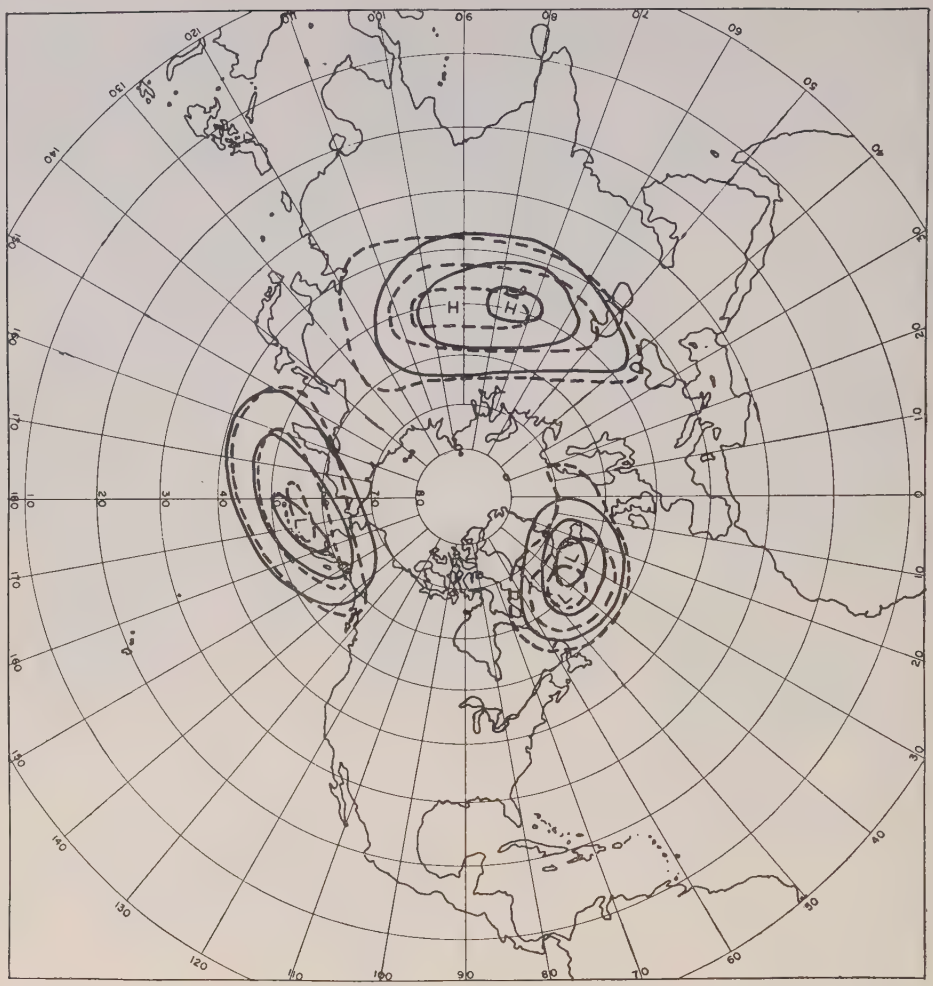

Figure 4. Mean annual sea-level isobars for 1933 and 1935 (dashed lines) and 1934 and 1937 (solid lines) showing positions of three major semi-permanent pressure centers. Years 1933 and 1935 experienced generally below normal temperatures over formerly glaciated regions of Northern Hemisphere while years 1934 and 1937 experienced generally above normal temperatures.

normal temperatures in the formerly glaciated regions of the Northern Hemisphere. The average mean annual pressure distributions for the two cold and two warm years are given in Figure 4. It can be seen that even on an annual basis the three major pressure systems undergo movement—the low pressure areas to the east and the high pressure areas to the west—during the shift from below normal to above normal temperature conditions. Thus, the distributions shown on Figure 1 appear to be real and related in some way to the temperature shifts.

If the distributions of pressure, temperature, and precipitation shown on Figures 1—3 are considered together, a number of generalizations concerning the variations in meteorologic parameters during such a period of climatic amelioration may be made. These are summed up in Table 1. Although the categories used in the table are quite general and many local exceptions may be found, some reliance may be placed on the conclusions because of the homogeneity of most of the pattern. One important fact noted in the table is the difference between the Greenland region

Table 1. Geographic Distribution of Changes in Meteorologic Parameters during January from 1901—1930 to 1931—1940 Period.

Region	*Pressure*	*Temperature*	*Precipitation*
Northern Alaska.....	Lower	Warmer	Wetter
Southern Alaska.....	Lower	Warmer	Wetter
Greenland.....	Higher	Warmer	Drier
Canada.....	Higher	Warmer	Wetter
Western United States	Lower	Colder	Drier
Eastern United States	Lower	Warmer	Wetter
Western Europe.....	Lower	Warmer	Wetter
Southwest Asia	Higher	Colder	Drier
Southern Asia.....	Lower	Colder	Drier
Southeast Asia	Lower	Colder	Drier
Central Asia.....	Higher	Colder	Drier
Northern Siberia.....	Higher	Warmer	Wetter
Central and Eastern Pacific	Lower	Warmer	Drier

of the Arctic and the Alaskan-North Siberian region. The former area, along with the central and eastern Pacific region, are the only two areas listed in the table which experience a shift to warmer and drier conditions during the 1931—1940 period. In all other regions noted, the climate becomes either colder and drier or warmer and wetter. The question may well be asked whether these pairs of temperature and precipitation conditions are found together over the whole hemisphere or just over special parts of it. From a consideration of Figures 1—3 it would appear that these conditions are confined almost entirely to the land areas. Generally, over the oceans of the Northern Hemisphere, warm and dry and cold and wet conditions are paired together; hence, there appears to be a definite difference in the reaction of the land and water areas to the climatic fluctuation of the past forty years. This difference might be of some significance since it is known that changes in solar radiation, either in intensity or wave length, would not produce similar climatic changes over the land and water areas of the earth. Thus, the distribution of the various changes in the meteorologic parameters may well hold a key to the possible cause of the recent climatic fluctuation. The sub-tropical Atlantic Ocean area and the North African region do not appear to conform to the foregoing pattern of temperature and precipitation, but this may be a result of the almost complete lack of data in those regions.

The difference between the Greenland and the Alaska-North Siberia Arctic areas becomes apparent at once from the foregoing considerations. Of the areas listed, the Greenland and the central Pacific areas are the most oceanic and so should experience either colder and wetter or warmer and drier conditions during the much warmer 1931—1940 period. The other areas listed including the Alaska-North Siberia region are more continental in character and, hence, should be subject to warmer and wetter or colder and drier conditions during this same period. Since all four pairs of conditions are found in the same hemisphere at the same time during the very warm 1930's there is every reason to believe they might also occur together during the less warm 1901—1930 period.

If it can be reasoned that the 1931—1940 period is by nature more interglacial in character than the 1901—1930 period then it might be argued that in the glacial periods of the Pleistocene some of the continental areas of the Northern Hemisphere experienced conditions warmer and wetter than at present while other land regions were colder and drier than at present. This would seem to agree with the glacial climates inferred by most writers, although many do not specify such possibilities. Too often, glacial periods are merely termed cold and dry. One is led to suppose that this applies to all parts of the world and not just to restricted areas. In any discussion of paleo-climates not only must the time period be specified but also the region of the world must be clearly defined before meaningful information can be presented.

In order to examine the previously mentioned suggestion of Willett (1949) that circulation conditions during the great Pleistocene glacial and interglacial periods were essentially zonal in character, between low and high index extremes, mean sea-level pressure maps for both situations were prepared from the large amount of data assembled by Willett, Bodurtha, and Others (1949) for the period 1932—1939. The results are shown in Figure 5. The changes in the pressure distributions shown on this figure agree in certain respects with the changes shown on Figure 1. It can be seen that the Aleutian and Icelandic low pressure areas are far to the southwest of their normal positions during

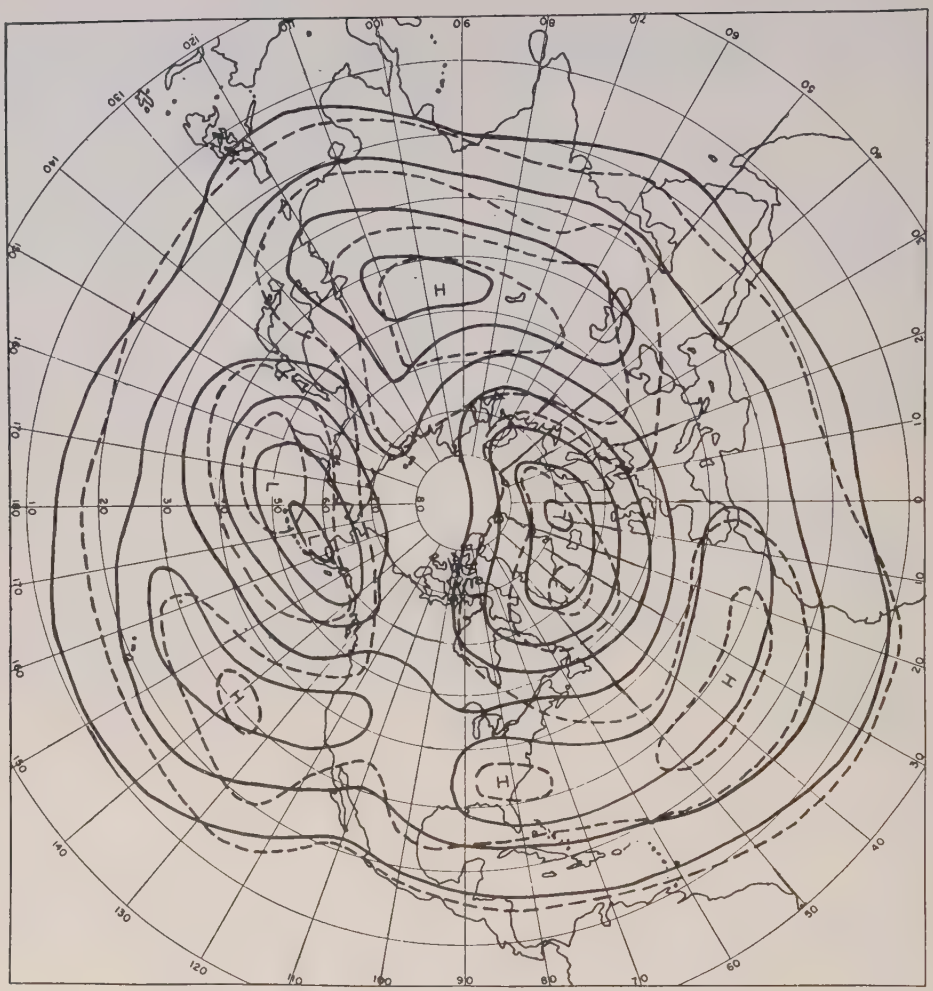

Figure 5. Average sea-level isobars for all cases of low midlatitude zonal westerlies (M.Z.W. $\leq$ 1.5 m/sec.) (dashed lines) and for all cases of high midlatitude zonal westerlies (M.Z.W. $\geq$ 3.5 m/sec) (solid lines), during period 1932—1939. Adapted from WILLERT, BODURTHA, and others (1949).

the periods of low zonal index. In addition, during these periods a large high pressure area exists over the Siberian region with a ridge of high pressure extending over the Arctic and the northwestern part of the Western Hemisphere. With this distribution, the storm tracks would follow a more southerly path around the globe. During the high zonal index periods the Aleutian and Icelandic low pressure areas shift their positions somewhat to the north and to the east of their most favored positions during the periods of low zonal index. In addition, the Siberian high weakens and moves slightly to the east.

In the previous investigation of the present climatic fluctuation it was shown that during the shift from the 1901—1930 period to the very warm 1931—1940 period the Aleutian and Icelandic low pressure areas do move to the east but that the Siberian high pressure area undergoes a westward movement. It appears, therefore, that the cause of the shifts noted in the study of the past forty years is more than a result of a shift to a high zonal circulation. This is not surprising since it is believed that the recent period of rapid warming must be associated with increased meridional heat transfer at least over the North Atlantic and

western Europe region as pointed out by Petterssen (1949). The maps, however, do bear out the previously mentioned suggestions of Wallén (1951) that certain of the recent circulation changes might indicate an increased zonal flow while as a result of greater North Atlantic blocking action an increased meridional flow might simultaneously occur over the North Atlantic and western Europe region. The movement of the Icelandic and Aleutian low pressure areas are similar on Figures 1 and 5 in the shift to the very warm 1931—1940 period and the high zonal index situation respectively so that the shifts noted on Figure 1 might be related to zonal index shifts. On the other hand the Siberian high is found to the west of its normal position during the warm 1930's while it moves eastward during the high index situations. Because of the decrease in the distance between the Iceland and Siberian pressure centers during the 1930's an increased southwest—northeast gradient is established over western Europe and the Atlantic. These pressure shifts shown on Figure 1 but not on Figure 5 indicate an increased meridional rather than zonal flow in that region.

II. Previous Attempts to Map the Atmospheric Circulation of the Pleistocene

In addition to general statements concerning Pleistocene climatic conditions, several investigators have attempted to reconstruct circulation maps for different periods of the Pleistocene from various lines of evidence. One of the most rational of these reconstructions was published several decades ago by Sir George Simpson (1934).

In constructing a hypothetical wintertime glacial-period circulation map, Simpson begins with the present day January circulation map. He points out that over the continental areas the presence of the large ice sheets should make little difference for, at present, snow covers the continents in January to well south of the Pleistocene glacial borders. Simpson also expects little change in the circulation pattern over the Pacific Ocean area since the effect of the large continental ice sheets would be relatively negligible. The main difference between the present day circulation maps and the hypothetical Pleistocene conditions would occur in the North Atlantic. At the present time, a low pressure area is found just south of the coasts of Greenland and Iceland, at about latitude 60° N in the region of most extreme temperature contrast between the cold ice-covered land areas and the warm ocean areas. During the glacial periods, the northern part of the North Atlantic would be covered with ice, so that the temperature difference between the land and the adjacent ice-covered ocean areas would be relatively small. The region of most extreme temperature variation would no longer be in the northern part of the ocean but farther south near the border of the sea ice where the contrast between ice and open water would intensify the temperature contrasts. The Icelandic low pressure therefore would move southward to agree with this new region of most intense temperature contrast. Its new position, according to Simpson, would be between 40° and 50° N. latitude in the eastern and central part of the Atlantic.

It is interesting to note how well the changes in pressure distribution shown on Figure 1 (dashed lines) agree with the theoretical changes suggested by Simpson in arriving at his hypothetical Pleistocene glacial period circulation. The general agreement would suggest that Simpson's distribution of pressure systems during the glacial period winter is basically sound and might only be improved with the slight westward movement of the low pressure area located over the eastern and central Atlantic Ocean. This westward shift of the low pressure area can be justified on the basis that the main region of instability and temperature contrast between the cold air masses over the land and the warm air masses will, during glacial times, occur off the Nova Scotia-Labrador coast and, hence, result in a westward displacement of the low pressure area. When this is done, with a slight increase in the pressure over the polar areas, resulting from possibly colder temperatures than Simpson would postulate under his glacial theory of increased solar radiation, Simpson's map (1934, Fig. 6, p. 437) of the glacial period circulation appears to be a sound and logical reconstruction of possible Pleistocene glacial period circulation conditions.

It is difficult to obtain a true present day picture of the possible Pleistocene interglacial conditions because some ice always exists at the present time over the Polar regions. The lack of this ice cover during interglacial times, although not eliminating the region as a source of cold air, would weaken the intensity of the cold air mass formed over it and reduce the hemispherical air mass contrasts. The resulting atmospheric circulation should be less intense and the storminess reduced. The circulation patterns given in the figures can only indicate the direction of the changes that would be noted on the pressure maps.

III. Studies of the Present Climatic Fluctuation over North America

a) *Storm Tracks*

Since variations in the average paths followed by storms as they move across the country influence the character of the weather considerably in those regions experiencing mostly cyclonic precipitation, a consideration of the paths of cyclones offers a method of partial explanation of climatic conditions. The general movement of the storm tracks over the Northern Hemisphere during both glacial and interglacial times has already been mentioned. It has been suggested that in local areas the storm tracks were farther south during the glacial ages than they are at present or were during interglacial periods while in other areas little change in the position of the storm tracks might be noticed. Since general southward and northward shifting of the storm tracks cannot be accepted for glacial and interglacial times, but only shifts in local areas, it is necessary to investigate the relation which exists between storm tracks and other meteorologic variables in an effort to obtain more information concerning the past distribution of the paths of the low pressure areas.

Figure 4 showed that in the shift from a cold to a warm period the pressure over the Aleutian region changed with the low pressure center moving to the eastward some five or ten degrees of longitude. It was accepted, at the time, that an easterly position of this low pressure area in winter was more characteristic of above normal temperatures over northern latitudes than was a westerly position.

The paths of the low pressure areas over the North American continent at times when the Aleutian low pressure area is far east and west of its normal position may be investigated to see how well they agree with what has already been postulated. During December 1912 and 1914, the Aleutian low pressure area was far east and west respectively of its normal position. Figure 6, adopted from BOWIE and WEIGHTMAN (1917), shows the paths of the low pressure areas as they moved across the country during those two different periods. On the basis of preceding reasoning, a westerly position of the Aleutian low pressure area is possibly a glacial-like characteristic while an easterly position of the low is more interglacial-like.

The paths of the low pressure areas show a decided shift from one period to the other. When the low pressure over the Aleutian region is far east of its normal position, the migratory low pressure areas are almost entirely restricted to Canada. Some southward movement east of the Rockies does occur. Several of the low pressure centers originate in the Great Basin region of western United States but recurve immediately to the northeast, and all the low pressure areas pass off the east coast in the vicinity of the St. Lawrence Valley. In contrast, with the Aleutian low pressure area west of its normal position the paths of the low pressure areas moving across the country shift southward. Many of the low pressure areas enter the western part of the United States, through California, and pass southeastward over the Great Basin region, recurving to the northeast over Texas or the Gulf of Mexico, and pass off the east coast in the southern part of the country. A few low pressure areas still pass across the country in Canada.

The shifts in the storm tracks shown on Figure 6 appear to bear out some of our previous suggestions concerning glacial and interglacial conditions. It must be remembered that only two individual months have been investigated so far. Results may be slightly modified on the basis of further investigations.

b) *Statistical Relationship Among Meteorologic Parameters Over North America*

Many meteorologic examples can be found which show that the occurrence of below

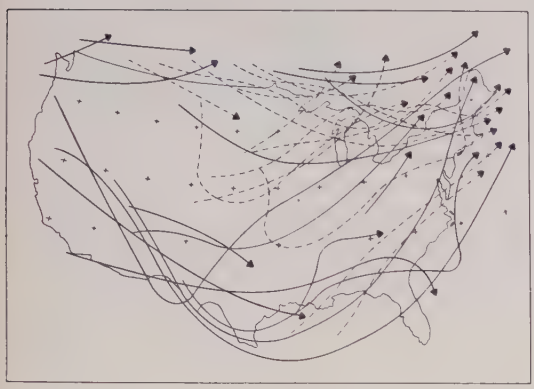

Figure 6. Tracks of low pressure areas across the United States during months of December 1914 (solid lines) and December 1912 (dashed lines). Aleutian low was west of its normal position (possibly more glacial in character) in December 1914 while it was far east of its normal position (possibly more interglacial in character) in December 1912. Adapted from BOWIE and WEIGHTMAN (1917).

normal temperatures over the plains of central and western Canada is associated with above normal precipitation in the Great Basin region of western United States. The reason for this is found in the existence of an upper air trough of low pressure which is formed over the central and western part of the continent under such conditions. This trough results in unstable conditions favorable for precipitation in the vicinity of the southern part of the trough, or over the Great Basin region in the United States. This combination of meteorologic conditions is significant, for a correlation between moist conditions in the southwestern part of the United States and below normal temperatures over the northern and western parts of the United States and Canada would well satisfy present day climatic evidence of the Pleistocene glacial-pluvial period correlation.

In order to obtain a more quantitative idea of the relation between certain of the meteorologic parameters over the Western Hemisphere, several correlation studies have been performed. The period covered by the investigations was from 1926 to 1950 and the mean monthly pressure, temperature, and precipitation data for the months of December, January, and February were used. The specific relations determined were as follows: 1) the relation between the pressure at Dutch Harbor and the amount of precipitation over Utah; 2) the relation between the pressure over Dutch Harbor and the temperature in the Alberta-Saskatchewan region of Canada; and 3) the relation between the amount of precipitation over Utah and the temperature in the Alberta-Saskatchewan region of Canada. The mean monthly pressure at Dutch Harbor was used to record the position of the Aleutian low pressure area. If the pressure at Dutch Harbor is low, the Aleutian low pressure area is generally to the east of its normal position, while if the pressure at Dutch Harbor is higher than normal, the Aleutian low pressure area will normally be found to the west of its average position. The investigation of the precipitation over Utah and the temperature of the Alberta-Saskatchewan region of central and western Canada is clear in the light of the previous discussion of the upper air trough and resulting precipitation pattern.

The correlation coefficient found in each case is listed below, the sign indicating the nature of the relation.

	Correlation coefficient
Pressure Dutch Harbor vs. Precipitation over Utah	.42
Pressure Ducth Harbor vs. Temperature Alberta-Saskatchewan	—.50
Temperature Alberta-Saskatchewan vs. Precipitation over Utah	—.67

From the above, it is seen that low amounts of precipitation over Utah and high temperatures over western Canada may be partially related to an easterly position of the Aleutian low pressure area. Since such a position of the Aleutian low pressure area is thought to be an interglacial characteristic, the fact that this position may be associated with warm Canadian temperatures and low rainfall in the Southwest is entirely consistent with present day observed facts and our hypothesis about Pleistocene interglacial conditions. The converse of the above relation would indicate that a westerly position of the Aleutian low pressure area would be associated with more moist conditions over the southwestern part of the country and below normal temperatures over Canada. These are all hypothetical glacial characteristics.

IV. Summary and Conclusions

From a study of the present climatic fluctuation, it has been found that during the 1931—1940 period as compared with the 1901—1930 period the three major pressure systems present in the hemisphere, the Siberian high and the Aleutian and Icelandic low pressure areas have generally moved five to ten degrees of longitude, the high pressure to the west and the low pressure areas to the east. At the same time the land regions of the Northern Hemisphere have experienced either warmer and wetter or cooler and drier conditions. Similar conditions would, of course, also be found over the land during the 1901—1930 period as compared with the 1931—1940 period. Over the ocean areas, it appears that conditions colder and wetter or warmer and drier than normal might have been experienced during both periods. These changes are significant for two reasons. First, they show that the hemisphere as a whole might not have experienced the same change of meteorologic conditions. If it is possible to reason from these present fluctuations to the great Pleistocene climatic shifts then it would appear that each local region might have experienced its own climatic variation. Thus, it would not be possible to say whether the glacial periods were warmer or colder than at present, or wetter or drier, for the answer would be "Yes" to each depending on the region of the globe selected. Second, the frequent occurrence of definite pairs of temperature and precipitation conditions together over the continents and over the oceans indicates that the cause of the recent climatic fluctuation has been of such a nature to affect the land and ocean areas differently. This may give a clue to the nature of the cause of the larger scale Pleistocene glacial and interglacial periods. In addition to these conclusions, there is a reorientation of the pressure gradients and other pressure centers of the hemisphere, suggesting that during the warm 1931—1940 period and, hence, perhaps in an interglacial period, the various storms and fronts are somewhat north of their normal positions.

Some of the ideas obtained from the previous general studies were investigated on the basis of more detailed studies over North America. It was shown that the eastward and northward movement of the Aleutian low pressure area was definitely associated with a northward movement of the paths of storms over the North American continent. Eastward and northward movement of the Aleutian low had previously been seen to be an interglacial-type characteristic. Statistical studies of the relation between moist periods over the Great Basin region and the temperature in Canada and the position of the Aleutian low pressure area showed that there was a partial relation between these meteorologic parameters. An eastward position of the Aleutian low and above normal temperatures in the glaciated regions of Canada were both associated with dry conditions in western United States.

In any study of paleoclimatology it is important to realize that the weather patterns which existed in the past periods were, for the most, similar to those found today. If this is understood, much erroneous thinking about the great ice ages or the "periods of refrigeration" as they are sometimes called by way of emphasis, may be corrected. The Pleistocene glacial and interglacial periods should be thought of as periods of climatic fluctuation of a slightly larger order and longer extent than the present one but possessing many of the characteristics of the present change.

Acknowledgements

The author wishes to express his sincerest thanks to Drs. C. W. Thornthwaite and G. F. Carter of The Johns Hopkins University for the many discussions and valuable advice they gave during the progress of these investigations. He also wishes to thank Dr. A. Ångström and Dr. C. C. Wallén both of the Swedish Meteorological and Hydrological Institute, Mr. N. Rosenan of the Israel Meteorological Service, and Dr. E. L. Deacon of the Commonwealth Scientific and Industrial Research Organization, Australia, for their kindness in reading the manuscript and offering many helpful suggestions.

REFERENCES

Ahlmann, H. W., 1953: Glacier Variations and Climatic Fluctuations. *Amer. Geogr. Soc., Bowman Memorial Lectures*, Series Three, 51 pp.

Ångström, Anders, 1939: The Change of the Temperature Climate in the Present Time. *Geogr. Annaler*, **21**, pp. 119—131.

Bowie, E. H. and Weightman, R. H., 1917: Types of Anticyclones of the United States and Their Average Movements. *Mon. Wea. Rev.*, Supp. No. 4, 25 pp., 7 figs., 73 ch.

Clayton, H. H., 1947: World Weather Records, 1931—1940. *Smithsonian Inst., Misc. Coll.*, **105**, 646 pp. (Also *79*, 1927; *90*, 1934).

Eriksson, Backa E., 1943: Till Kanvredomen om den Nutida Klimatandringen inom Omradena Kring Nordligaste Atlanten. *Geogr. Annaler*, **25**, pp. 170–201.

Kincer, J. B., 1946: Our Changing Climate. *Amer. Geophys. Union, Tr.*, **27**, pp. 342—347.

Landsberg, H., 1949: Climatic Trends in the Series of Temperature Observations at New Haven, Connecticut. *Geogr. Annaler*, **31**, pp. 125—132.

Petterssen, S., 1949: Changes in the General Circulation Associated with the Recent Climatic Variation. *Geogr. Annaler*, **31**, pp. 212—221.

Rex, D. F., 1950: Blocking Action in the Middle Troposphere and its Effect upon Regional Climate. (a) Part I: An Aerological Study of Blocking Action. *Tellus*, **2**, 3, pp. 196—211. (b) Part II: The Climatology of Blocking Action. *Tellus*, **2**, 4, pp. 275—301.

— 1951: The Effect of Atlantic Blocking Action upon European Climate. *Tellus*, **3**, 2, pp. 100—112.

Rubinstein, L., 1946: K Probleme Izminenija Klimata. *Sci. Res. Dept. Ser.*, Hydr.-Met. Service, U.S.S.R., Moscow, pp. 1—84. (English rev., Ahlmann, 1948, *Geogr. Jour.*, **112**, pp. 175—178).

Simpson, G. C., 1934: World Climate During the Quaternary Period. *Roy. Met. Soc., Quart. Jour.*, **60**, pp. 425—478.

Wallén, C. C., 1951: Influences Affecting Glacier Extension in Northern Sweden. *U.G.G.I., Assoc. Internationale d'Hydrologie Scientifique*, Bruxelles, **1**, pp. 145—153.

Willett, H. C., 1949: Long Period Fluctuations of the General Circulation of the Atmosphere. *Jour. Met.*, **6**, pp. 34—50.

— Bodurtha, F. T., and others, 1949: *Final Report of the Weather Bureau-Massachusetts Institute of Technology Extended Forecasting Project for the Fiscal Year July 1, 1948—June 30, 1949*. Cambridge, Massachusetts, Massachusetts Institute of Technology, 109 pp.

NOTE

Report on an informal conference in atmospheric chemistry held at the Meteorological Institute, University of Stockholm, May 24—26, 1954

By E. ERIKSSON

Institute of Meteorology, University of Stockholm

In October 1952 a small conference was held at the Institute of Meteorology of the University of Stockholm to discuss research problems in cloud physics. At that time a first attempt was made to focus the attention of meteorologists on the important role played by the general atmospheric circulation in the transport and redistribution of certain chemical elements which are of interest to cloud physicists but also, though for somewhat different reasons, to such diverse groups as students of agronomy, of atmospheric pollution and of general geochemistry. At that time, and to illustrate a desirable method of representation, charts were presented which showed the geographic distribution over Sweden of the amounts of fixed nitrogen brought to the soil annually through precipitation. These charts had been constructed by Dr. A. Ångström and Mr. L. Högberg of the Swedish Meteorological and Hydrological Office from data analyzed at the Royal Agricultural College of Ultuna under the supervision of Dr. H. Egnér.

Since then it has become increasingly evident that a thorough description of the synoptic, or climatological distribution of a number of chemical elements brought to the soil by precipitation must be undertaken *before* a satisfactory, quantitative interpretation of the geochemical cycles of these elements can be given. In many cases we know little or nothing about the strength of the sources and sinks for these elements. Under those circumstances it is probable that a thorough description of the *geophysical circulation patterns* of the different elements might help us to understand their *geochemical cycles*.

To foster such synoptic, or climatological studies in atmospheric chemistry a second small conference in atmospheric chemistry was held at the University of Stockholm during the period May 24 – 26, 1954. The synoptic aim of this second conference was to assess our present knowledge of atmospheric chemistry in a few lectures and discussion sessions, and to review certain programs for research formulated since the previous conference.

The present note is published in the hope that the observational and research plans presented at the 1954 meeting, through the co-operation of geophysicists in other parts of the world, may be extended to cover a much larger part of the earth's surface than could be included in our original plans.

The conference was attended by the following invited guests:

Prof. K. Buch, Oceanographic Institute, Helsingfors, Finland.

Dr. Ch. Junge, Cambridge Research Center, U. S. Air Force, Cambridge, Mass., U. S. A.
Dr. N. Jerlov, Oceanographic Institute, University of Gothenburg, Sweden.
Dr. H. Egnér, Royal Agricultural College, Ultuna, Sweden.
Dr. O. Arrhenius, Grödinge, Sweden.
Prof. F. Wickman, Geological Section, Natural History Museum, Stockholm, Sweden.
Mr. A. Emanuelsson, Swedish Sugar Factories Research Institute, Hilleshög, Sweden.

The following members of the staff of the Institute of Meteorology took part in the meetings:

Prof. C.-G. Rossby
Mr. E. Barrett
Mr. E. Eriksson
Mr. N. Koroleff
Mr. S. Fonselius

Mr. W. A. Mordy, Chief Meteorologist of the Pineapple Research Institute in Honolulu, Hawaii, who visited the Institute prior to the conference, took an active part in the preparatory discussions.

The conference was opened by Professor Rossby, who in his introductory comments pointed out that atmospheric chemistry is a part of geochemistry and as such concerns itself with a study of the role of the atmosphere in the circulation of various chemical substances. For this study conventional meteorological observations are indispensable but an additional and equally important prerequisite is the organization and operation of a large, preferably permanent, network of chemical stations capable of yielding synoptic or climatological data on the geographic distribution of the various chemical elements as observed directly in the air or in precipitation. Until such a network has been established and synoptic or climatological distribution charts for various chemical elements have been prepared, our ideas concerning the nature of the chemical circulation processes must remain highly speculative. On the other hand, such charts might help us to formulate appropriate special field or laboratory investigations designated to clarify the specific nature of the cycles of individual elements.

The role of the atmosphere in the circulation of most, though not all, chemical elements is mainly one of transfer and redistribution. For a complete description of the atmospheric part of the cycles of these elements one must, in addition, know the locations and intensities of their sources and sinks. The sea is a well-recognized source as well as a sink for most of the compounds in the atmosphere, but although the physico-chemical equilibrium conditions at the sea surface are supposed to be fairly well known, little information is available about the rate at which this equilibrium is reached. To determine these rates co-operation with oceanographers is necessary.

Professor K. Buch gave some details on the carbon dioxide cycle, especially the exchange between the sea and the atmosphere. The carbon dioxide tension in the sea is a function of several factors, of which the most important is the temperature. Due to the temperature difference in the sea between the equator and the polar regions it can be expected that carbon dioxide should be given off to the atmosphere in equatorial regions and be absorbed by sea water in polar regions. Another factor is the upwelling at deep water along the west coasts of the continents in middle and low latitudes. This deep water has a high carbon dioxide tension and when heated, it releases some of its carbon dioxide to the atmosphere, especially in equatorial regions. That absorption of carbon dioxide takes place in polar regions has been very strongly indicated by air analyses carried out by Professor Buch in Spitzbergen. Air masses which have travelled a great distance over the cold water masses are poor in carbon dioxide and have nearly adjusted themselves to the carbon dioxide tension of the sea. The rate of the absorption is, however, not known.

Professor Buch also commented on the influence of the combustion of fossil products on the carbon dioxide content in the atmosphere, a point first raised by Callendar in England in 1940. If none of this carbon dioxide has been taken up by the sea there would have been a ten percent increase in the carbon dioxide in the atmosphere. Whether or not this increase has taken place has not yet been definitely established. There are strong indications that such is the case but a systematic research program in the future could give a more definite answer. Professor Buch also reviewed Callendar's discussion on the influence of this increase in carbon dioxide on the heat balance of the earth, the carbon

dioxide being a rather important constituent for absorption of outgoing infrared radiation. He also mentioned that the increase of fossil carbon would cause a decrease of the ratio of radiocarbon C^{14} to common carbon C^{12}, the fossils having lost all their C^{14} during the past. Therefore in very recent plant organic matter one would expect a lower C^{14} radioactivity than the average found in "recent" organic matter (of age 50 – 100 years). If this is true it would indicate an increase of CO_2 in the atmosphere due to combustion of fossil carbon.

The problem of the heat balance of the earth was reviewed by Mr. Barrett, who gave an account of the rather complicated methods which must be used in computing the radiation economy of the earth. Estimates made by Callendar, and recent, as yet unpublished computations by L. Kaplan and Plass suggest that an increase of the atmospheric CO_2-content by ten percent might bring about, or at least contribute a significant portion of, the observed change in climatic conditions during the last half century which has manifested itself for instance in the recession of glaciers.

Mr. Eriksson gave some geochemical aspects of carbon dioxide with special reference to the net yearly circulation. There are at present some quantitative estimates about the various processes contributing to this circulation. From these it is seen that the total yearly assimilation amounts to about one tenth of the total carbon dioxide in the atmosphere. Probably ninety percent of this, however, takes place in the sea where the atmosphere is not directly involved. It was also shown that the yearly contribution by combustion of fossil carbon is very substantial, amounting to more than a third of the annual assimilation by terrestrial plants. The assimilation is probably very nearly balanced by respiration and so there should be an accumulation of CO_2 in the atmosphere due to the combustion of fossils. About ten percent of this is, however, removed by runoff from land to sea, but how much of the rest is taken up by the sea is unknown and is one of the basic questions to be solved. If equilibrium could be established within a year between the atmosphere and the sea practically the whole excess production would be removed, but as this is certainly not the case the actual amount going to the sea has to be estimated by some other means. There are two main lines of approach to this problem. One is to estimate the yearly flux of carbon dioxide from the equator towards the poles, and from the magnitude of this stationary process to estimate the effective volume of the sea exposed to the atmosphere yearly. Another way of approach is to map the age of the ocean water at different depths and positions by the C^{14} method. This method was discussed by Dr. Jerlov, who also gave a description of the geographical distribution of carbon dioxide in the oceans and of the deep water current systems. As the current pattern is very complex and the motion of the deep waters is very slow, such an age mapping would be very valuable. Since the work involved is rather time-consuming such a project cannot be carried out in one year, without considerable cost, but would preferably have to be extended over a number of years. The sporadic age determinations done so far were discussed by Dr. Jerlov. They give rather high values for the age of some deep water samples but they are, however, too few in number to be conclusive.

The second day was devoted mainly to reviews and discussions of the composition of atmospheric precipitation. Dr. Ch. Junge reported on some of his recent determinations of the chemical composition of aerosols. He went on to describe a magnificent undertaking for which he had worked out the plans under the auspices of the U. S. Air Force Cambridge Research Center. The purpose of this project is to collect, for chemical analysis, samples of precipitation from a large net of stations covering continental U.S.A. and most of the North Atlantic, including some points on the west coast of Ireland and Scotland. The whole net includes about 90 stations and analyses are to be made monthly on the accumulated monthly precipitation amounts. As the chemical content of precipitation may at least partially reflect the chemical composition of the atmosphere it is hoped to get a climatological picture of the distribution of chemical compounds in the atmosphere in this region as well as to obtain knowledge about the importance of land and sea as sources and sinks for these compounds. The substances to be traced are ammonium, nitrate, sulfate, chloride, calcium, sodium and magnesium and from a few places some additional elements.

The composition of atmospheric precipitation has been studied for some years in Sweden where a network of sampling points was used. This work was mainly carried out to assess the importance to agriculture of chemical constituents in precipitation. For this reason the agricultural areas are best represented in the network but it was also intended to give some climatological information. Dr. Egnér and Mr. Eriksson are responsible for the first net and all analyses have been made under the supervision of Dr. Egnér who later modified the net somewhat and also included an arrangement for taking air samples. Dr. Egnér presented some of the results from this work which show interesting and highly significant latitudinal as well as longitudinal variations.[1] He also discussed some results of air analyses of samples taken in the equatorial regions of the Pacific by Dr. G. Arrhenius. One of the most interesting features of these latter analyses is that they show a remarkably high ammonia content. It has long been accepted that the sea is a sink for atmospheric ammonia but it is apparent, after examination of some recent data on rainwater from Hawaii, that this question has to be more thoroughly investigated.

Mr. Eriksson gave some geochemical data on nitrogen compounds in the atmosphere and in the sea and discussed the yearly net circulation of nitrogen compounds. The nitrogen compounds of interest are ammonia, nitrates and nitrous oxide. The last mentioned, which has only recently been studied, is apparently a very important link in the chain of nitrogen compounds in the biosphere.

It is evident from the data on the yearly circulation that both ammonia and nitrate are brought from the atmosphere to the sea in appreciable amounts. As there is no geologic evidence that the sea and the sediments are being enriched by nitrogen compounds to the extent which could be expected from the yearly income to the sea from the atmosphere through precipitation, it must be assumed that these nitrogen compounds are in some way or another brought back to the atmosphere and carried in over the land. From the estimated production of nitrous oxide by soils it is also necessary for balance to get additional nitrogen compounds to the soil apart from those in precipitation. Also, the physico-chemical properties of soils as compared to sea water favour a transport of *gaseous* ammonia from the sea water to the soil. Therefore it can be expected that the excess of nitrogen coming annually to the sea is given off as ammonia. Further investigations, however, are needed on that point. It should be mentioned in this connection that ammonia can occur in the atmosphere both as gas, in which case equilibrium conditions between this gaseous ammonia and that dissolved in water are well known, and as ammonium ion in various compounds. That the last is true has been convincingly shown by Dr. Junge in his research on aerosols.

Following the lectures, discussions took place concerning the various program of research in atmospheric chemistry which had been worked out before the conference. First the carbon dioxide program was considered. In the general discussion of air analysis for CO_2 it was concluded that the program must serve three separate purposes. One is to establish the geochemical distribution of CO_2 over a certain area, one is to study the modifications of the air with respect to CO_2 as it is carried from the oceans in over land areas and the last is to study secular trends. For the last purpose places with slight climatic variations and remote from any kind of atmospheric disturbances which may give rise to local changes are most suitable. Probably the most ideal place would be somewhere in the middle of the Sahara desert, and it was recommended to plan for such a station in the future. Another possible place would be Hawaii if samples were taken above the trade-wind inversion (which seems to be feasible). Below the inversion level the damping influence of the sea water is probably too strong to permit detection of secular trends.

For the geochemical distribution of CO_2 two projects were outlined. One, concerning Scandinavia, was initiated by Prof. Buch at a visit to the Institute in January 1954. A program worked out by Mr. Eriksson was presented according to which air samples would be taken at a few selected places and be analysed in Stockholm or, in the case of stations in Finland, by Prof. Buch. As to the number of samples per month and the time intervals

[1] The reader is referred to a paper by A. Emanuelsson et al., in this issue of Tellus, which contains a discussion of the geographic distribution of various chemical elements brought to the surface of the earth by precipitation.

between sampling, Prof. Buch suggested that from a geochemical point of view samples should be taken at regular intervals, preferably on the 1 st, 10 th and 20 th of each month. Furthermore, if some interesting weather situations appeared over Scandinavia additional samples ought to be taken on telegraphic order. This would then allow a study of modifications which can take place in air masses as they are travelling over continental regions. It was agreed upon that the procedure proposed by Prof. Buch should be followed. It was also recommended that, in connection with the regular sampling scheme, trajectories for the air masses should be worked out in order to determine their origin.

The sampling technique was also discussed. As worked out originally by Prof. Buch, air samples are taken by pumping air through common gas burettes. These burets are then sent to the place where analyses are carried out. Since the sampling time is a matter of few minutes, short time fluctuations (if they exist) can influence the results. This will be studied in some detail this summer. It was also recommended to use a suitable registering instrument to estimate short time fluctuations at the places in question. By registering these fluctuations during a month at each station, it would be possible to detect sources of random error in the sampling technique. The ideal arrangement would of course be to have such a registering instrument at each station and get continuous records from all, but the cost of this arrangement is prohibitive.

The second project on CO_2 determinations was worked out by Mr. Eriksson in collaboration with Mr. Mordy during the latter's visit at this Institute. This project concerns the North Pacific region, and according to this plan air samples should be taken at six places around the North Pacific current and be analysed for CO_2. The project is still in the preliminary planning stage, but it was suggested that suitable locations might be found in Hawaii, in the Philippines and in Japan. Fairbanks, Seattle and some place south of San Francisco were named as possible sites for the remaining three stations. Two alternatives were considered, one of which is to get scientists at these locations interested in the project so that the analyses could be made on the spot, while the other is to have the air samples analysed centrally. Arrangements will be made by Mr. Mordy, who will also be responsible for the meteorological part of the work. It is hoped that the information provided by these analyses will permit an estimate of the flux of CO_2 from the equator toward the poles. The sampling times might conveniently be the same as for the Scandinavian net.

The discussion then turned to the precipitation analysis programs. Two such programs were presented, the one by Dr. Junge mentioned earlier and one by Mr. Eriksson and Dr. Egnér. According to the second program the existing network of stations in Sweden would be modified so as to give a more uniform distribution of sampling points over Sweden. Furthermore three or four places would have to be added in Norway, two in Denmark, three or four in Finland; lastly a station on Vestmannaeyjar in Iceland should be considered. This network is more dense than that visualized by Dr. Junge but covers an important area and one which is ideally suited for a detailed study of the chemical modifications on maritime air masses as they move in over land. It was suggested that Dr. Junge's net which included three stations on the west coast of the British Isles should be extended through the establishment of three stations on the British east coast. These stations might then send samples also to the Scandinavian analysis centre at the Agricultural College in Ultuna, the analysis there being done under the supervision of Dr. Egnér. Through the introduction of these three stations and by using data from Dr. Junge's stations on the west coast of the British Isles it would be possible to make fairly detailed geoclimatological maps of the whole region from the British Isles across Scandinavia. The inclusion of the British Isles is quite important as this area doubtless represents an important source region for atmospheric constituents.

Since Dr. Junge's net is less dense, climatological maps covering his region cannot be so detailed. On the other hand, he can extend his region into the British Isles and Scandinavia through the selection of suitable stations.

It was also agreed that all data obtained should be distributed semiannually to all participating institutions (also in the CO_2 projects), that Dr. Junge should prepare climatological maps for the whole region and

that this Institute should make similar but more detailed charts for the British Isles – Scandinavian region.

In order to obtain a check on the two different projects it was recommended that both should have one sampling station in common.

The technical details were then discussed. It was found that although there were minor differences in the equipment they were both equally satisfactory. In the Scandinavian project, however, provisions for taking air samples are made with relatively low extra cost. Dr. Junge suggested that he might be able to make similar provisions, at least at some of his stations.

The period during which the sample is to be continuously taken was fixed at one month.

It was also discussed whether provisions should be made for avoiding settling dust in the sampling funnels during intervals between rains. Such provisions would doubtless raise the cost of maintenance of the equipment. It was agreed upon that preliminary investigations should be made to assess the importance of this source of error. Lastly, it was mentioned that at some points in Scandinavia special equipment should be used for sampling individual rains. The sampling should preferably be done on telegraphic order. In this way valuable information can be obtained about the time variation of the chemical content in, for instance, frontal rains. Of course, air trajectories would have to be worked out on these occasions.